UNIVERSITEIT VAN PRETORIA
UNIVERSITY OF PRETORIA
YUNIBESITHI YA PRETORIA

An investigation of the possible anticancer activity of seven novel bi(amido) gold(I) complexes derived from a purine or azole base

Wilna Potgieter

Submitted in the partial fulfilment of the requirements for the degree of

MSc. with specialisation in Pharmacology

April 2009

The Faculty of Medicine
Department of Pharmacology
University of Pretoria
Pretoria

Promotor: Prof C.E. Medlen

This dissertation is dedicated to

DS & MRS WA POTGIETER, MR E BOUWER

"[23]Whatever you do, work heartily, as for the Lord and not for men"… "[24]You are serving the Lord Christ." Colossians 3:23-24 (English Standard Version)

ACKNOWLEDGEMENTS

- I wish to express my gratitude and appreciation to my supervisor, Prof Connie E. Medlen for her patience, support and inspiration throughout my postgraduate studies.
- I would like to thank Dr Richard Bowen for the support, time and effort that he dedicated to my project.
- Thank you to Prof Raubenheimer and Dr Ulrike Horvath of the Department of Chemistry, University of Stellenbosch, for the design and synthesis of the novel experimental compounds that were used in this study.
- I wish to thank Lizelle Fletcher and her team at the Department of Biostatistics, University of Pretoria for their assistance with the statistical analysis of the data.
- I wish to extend my gratitude to Mintek for the financial support for this study.
- A special thank you to Margo Nell and Dr Gisela Joone of the Department of Pharmacology, University of Pretoria for culturing all the cells used in this study; and for their patience and support throughout the study.
- Thank you to Dr Duncan Cromarty of the Department of Pharmacology, University of Pretoria for his support and contribution during the study.
- I would like to thank Dr Roland Auer and the UPBRC staff for their help in conducting the *in vivo* experiments in this study.
- I wish to extend my gratitude and appreciation to my family and my fiancé for being my pillars of strength and support. Thank you for your patience and for granting me the opportunity to continue with postgraduate studies.

TABLE OF CONTENTS

CHAPTER 3: CYTOTOXICITY ASSAYS

CHAPTER 4: ASSESSMENT OF DNA DAMAGE VIA APTOSIS OR NECROSIS

CHAPTER 5: MITOCHONDRIAL MEMBRANE POTENTIAL

CHAPTER 6: DETERMINATION OF EFFECTS ON CELL CYCLE DIVISION

CHAPTER 7: ASSESSMENT OF *IN VIVO* ACUTE TOXICITY

CHAPTER 8: SUMMARY & CONCLUSION

REFERENCES

APPENDIX A

GLOSSARY OF ABBREVIATIONS

µmol/kg	Micro mole per kilogram
µl	Micro litre
µM	Micro Molar
°C	Degree Celsius
%	Percentage
AIDS	Acquired immunodeficiency syndrome
Alk P	Alkaline phosphatase
ALT	Alanine transaminase
APAF-1	Apoptotic protease activating factor 1
AST	Aspartate aminotransferase
ATCC	American Tissue Culture Collection
Cdk	Cyclin dependant kinase
Ci	Initial concentration
Co	Concentration remaining in octanol
Cw	Concentration remaining in the aqueous phase
DMEM	Dulbecco's Modified Eagle Medium
DMSO	Dimethyl sulfoxide
DNA	Deoxyribonucleic acid
E2F	Activating transcription factor
ECACC	European Collection of Cell Cultures
E.g.	For example
EMEM	Eagle's Minimal Essential Medium
Etc.	Etcetera
EtOH	Ethanol
FADD	Fas-associated death domain protein

FCS	Foetal calf serum
FITC	Fluorescein isothiocyanate
G1	First gap/growth (phase)
G2	Second gap/growth (phase)
GGT	Gamma glutamyl transpeptidase
Hb	Haemoglobin
HEPES	(4-(2-hydroxyethyl)-1-piperazineethanesulfonic acid)
HIV	Human immunodeficiency virus
HT	Haematocrit
IAP	inhibitor of apoptosis
IC_{50}	Inhibitory concentration that results in 50% cell death
i.e.	That is
IVC	individually ventilated cage
JAK	Janus kinase
JC-1	5,5',6,6'-tetrachloro-1,1',3,3' tetraethylbenzimidazolylcarbocyanine iodide
M	Mitosis
M	Molar
MCH	Mean corpuscular haemoglobin
MCHC	Mean corpuscular haemoglobin concentration
MCV	Mean corpuscular volume
mg	Milligram
min	Minutes
ml	Millilitres
mM	Milli molar
MMP	Mitochondrial membrane potential

MTD	Maximum tolerated dose
MTT	(3-{4, 5-dimethylthiazol-2-yl}-2, 5-diphenyltetrazolium bromide)
NA	Nucleoside analogue
nm	Nanometer
no.	Number
PBS	Phosphate buffered saline
PC	Partition coefficient
pH	Percentage hydrogen
PHA	Phytohaemagglutinine
PI	Propidium Iodide
Rb	Retinoblastoma
RCC	Red blood cell count
RDW	Red cell distributive width
RF	Resistance factor
RPMI	Roswell Park Memorial Institute Medium
RNA	Ribonucleic acid
Rpm	Revolutions per minute
r_S	Spearman's correlation coefficient
S	Synthesis
SA	South Africa
SEM	Standard error of mean
SD	Standard deviation of mean
Smac	Second mitochondria-derived activator of caspase
STAT	Signal transducer and activator of transcription
ULN	Upper limit of normal
UPBRC	University of Pretoria Biomedical Research Centre

Vs.	Versus
WCC	White blood cell count
WHO	World Health Organization

SUMMARY

Gold(I)phosphines, nucleoside analogues, and azole derivatives have been identified as promising anticancer compounds. The clinical use of these individual compounds is, however, limited due to non-selectivity associated with adverse effects and developed resistance. This study investigated seven novel gold compounds that contain either a nucleoside analogue or an azole, bound via a gold nitrogen bond, which have been designed and synthesized by Dr. Horvath under the supervision of Prof. Raubenheimer from the University of Stellenbosch. The novel compounds are divided into purine-containing/nucleoside analogue compounds (UH 86.2, UH 75.1, UH 58.1, UH 145.1) and azole-containing compounds (UH 107.1, UH 126.1, UH 127.1). The anticancer effects of these novel compounds were compared with that of previously described anticancer compounds $[Au(dppe)_2]Cl$ and cisplatin.

The octanol/water partition coefficients (PC) of the compounds were measured in order to determine whether a correlation between the lipophilicity of the structures and the cytotoxic potency and selectivity exists. This might provide further insight for structural alterations of the compounds in order to improve their anticancer activity. The results from octanol/water PC determinations, revealed that the purine-containing compounds (UH 86.2, UH 75.1, UH 58.1, and UH 145.1), as well as the azole-containing compound, UH 127.1, exhibited hydrophilic properties, while the azole-containing compounds, UH 107.1 and UH 126.1 are lipophilic. In contrast to results by Berners-Price *et al*. (1999), that reported a direct proportionality between lipophilicity and cytotoxicity, for the current study, involving HeLa cells, CoLo cells, normal resting and PHA stimulated lymphocytes, no correlation was observed. For the Jurkat cell line, however, an increase in lipophilicity for the series of compounds studied was accompanied by an increase in cytotoxicity. The reason for the exception is not yet fully understood.

The *in vitro* tumour specificity of each compound was established with cytotoxicity assays on various cancer cell lines and normal cell cultures. The cancer cell lines included human cervical cancer (HeLa) cells, human colon cancer (CoLo) cells, and human lymphocytic leukaemia (Jurkat) cells. The normal cell cultures included human

resting lymphocytes and human phytohemaglutin (PHA) stimulated lymphocytes. From this data, the four most promising novel compounds were identified. Additional tests were performed by adding these four compounds to cancer cells including human breast cancer (MCF-7) cells, and cisplatin sensitive and resistant human ovarian cancer (A2780 and A2780cis) cells as well as normal chicken embryo fibroblasts. The tumour specificity of each compound was determined from the results obtained via the cytotoxicity assays. The compound is more selective the higher the tumour specificity. Cisplatin exhibited the highest tumour specificity, and $[Au(dppe)_2]Cl$, the lowest. The two most promising novel compounds were identified as UH 126.1 and UH 127.1, which was evidenced by their high tumour specificities. Further experiments were conducted with these two azole-containing compounds by using Jurkat cells.

The possible mechanism by which the novel compounds induce cytotoxicity was investigated with flow cytometric analysis. The effects of the compounds on the cell death pathway, the mitochondrial membrane potential and the cell cycle were determined. These results indicated that the novel compounds, UH 126.1 and UH 127.1 initiate the apoptotic cell death pathway rather than the necrotic cell death pathway. According to results, UH 126.1 and UH 127.1 influenced the status of the mitochondrial membrane potential (MMP) non-selectively and only at high concentrations. Although involvement of mitochondria in the mechanism of action cannot be excluded, results indicated that it is most likely not the primary target. After investigating the effects of the two novel azole-containing compounds on the cell cycle in Jurkat cells, it was detected that these compounds induce cell accumulation in the G1 phase of the cell cycle. It was concluded that UH 126.1 and UH 127.1 might interfere with the cell cycle indirectly, possibly by inhibition of cyclin-dependent kinases and/or other enzymes necessary for DNA replication.

In an acute *in vivo* toxicity test during this study, results revealed drug induced adverse effects (such as significant weight loss, piloerection and diarrhoea), in the mice that received 3 and 6µmol/kg of both UH 126.1 and UH 127.1. Evidence also revealed signs of nephrotoxicity and hepatotoxicity. Due to minimal adverse effects observed in the

groups that received UH 126.1 and UH 127.1 at the concentration of 1,5µmol/kg, this is the suggested maximum tolerated dose (MTD) for these compounds. Further dose-range studies with UH 126.1 and UH 127.1 are, however, needed in order to evaluate clinical efficacy.

CHAPTER ONE

1.1 INTRODUCTION

Cancer is defined by the World Health Organization (WHO) as a generic term for a group of more than 100 diseases that can affect any part of the body. Other terms used, include malignant tumours and neoplasms. The major cause of death from cancer is due to metastasis. Metastasis is the rapid multiplication and growth of malignant cells, which then invade adjoining body parts and other organs (WHO).

Cancer is a leading cause of death worldwide. From a total of 58 million deaths worldwide in 2005, cancer accounts for 7.6 million (or 13%) of all deaths, according to the WHO.

The most effective cancer treatment remains chemotherapy. Platinum containing compounds such as cisplatin, carboplatin and oxaliplatin are widely used in the clinic (Wang and Lippard 2005). However, the occurrence of drug-resistant tumour cells and the non-selectivity of these cancer drugs cause severe adverse effects (such as emesis, nephro-, oto-, and neurotoxicity, asthenia and gastrointestinal toxicity), which limit their use (Boulikas 2004). The use of platinum containing compounds in various cancers has led to the investigation of alternative metal-based drugs as potential anticancer compounds (Barnard *et al*. 1995; Guo *et al*. 1999; Kopf-Maier 1994; Sadler et al.1998).

A variety of gold-containing compounds are promising anticancer drugs (Tiekink 2002). Although these compounds display anticancer activity, their toxicity to normal tissues is too high for clinical use (Sadler and Guo 1998; Smith *et al.* 1989). In this study, gold that has been combined with either a nucleoside analogue or an azole, are evaluated as anti-tumour agents. Seven novel neutral, two-coordinated linear gold compounds that contain either a nucleoside analogue or an azole base have been designed and synthesized by Dr. Horvath under the supervision of Prof. Raubenheimer from the University of Stellenbosch.

This study is significant because gold-containing compounds, nucleoside analogues as well as azole derivatives have displayed anticancer activity as reported in previous studies (Berners-Price *et al*. 1986; Mirabelli *et al*. 1986; Meira et *al*. 2005; Penso *et al*. 2002; Zemlicka 2000). The merge of gold with either a nucleoside analogue or an azole offers the advantage of combination chemotherapy in a single compound and might compare favourable to existing drugs that are used clinically.

1.2 LITERATURE REVIEW

1.2.1 Gold as anticancer compound

The term chrysotherapy refers to the use of gold compounds in medicine. The investigation of anticancer gold-containing compounds was instigated after observing lower malignancy rates in patients undergoing chrysotherapy for rheumatoid arthritis (Fries 1985). Furthermore, similarities were found between the square-planar complexes found in platinum(II) and gold(III) compounds (Sadler 1976).

Out of many gold complexes that have been investigated, the gold(I)phosphine derivatives show the most promise as anticancer compounds (McKeage *et al*. 2002). Auranofin (a linear tetra-acetylthioglucose gold(I)phosphine complex) and gold(I)phosphines such as triethylphosphine gold(I)chloride (Et_3PauCl), bis[1,2-bis(diphenylphosphino)ethane]gold(I)chloride ($[Au(dppe)_2]Cl$), and their derivatives have displayed significant cytotoxicity and *in vivo* anti-tumour activity (Berners-Price *et al*. 1986; Mirabelli *et al*. 1986). Auranofin displayed anti-tumour activity in mice inoculated with P388 leukaemia, Et_3PauC exhibited cytotoxicity *in vitro* in isolated rat hepatocytes, and $[Au(dppe)_2]Cl$ displayed reproducible and significant anti-tumour activity *in vitro* and in different murine tumour models *in vivo* (Berners-Price *et al*. 1986; Mirabelli *et al*. 1986). Au(I) complexes of bidentate pyridyl phosphines have shown significant *in vitro* and *in vivo* anti-tumour activity that is determined by their lipophilic status (Berners-Price *et al*. 1999). The exact mechanism by which the gold(I)phosphines induce anti-tumour activity is unclear, but it is known that they are directly cytotoxic and many appear to have anti-mitochondrial activity as well as the formation of DNA strand breaks and DNA protein cross-links (Berners-Price *et al.* 1986; Mirabelli *et al*. 1986;

Rush *et al.* 1987; Smith *et al*. 1989) Pre-clinical development of $[Au(dppe)_2]Cl$ was abandoned after the identification of severe hepatotoxicity, cardiotoxicity and pulmonary toxicity in beagle dogs (Berners-Price *et al*. 1999; Hoke *et al*. 1989).

Although previously tested gold compounds display definite anti-tumour activity, these effects are limited when compared to standard chemotherapeutic agents *in vivo* and is not suitable for clinical use (Hoke *et al*. 1989; Rush *et al.* 1987).

1.2.1.1 Mechanism of gold(1)phosphines involved in inducing cytotoxicity

The exact mechanism by which the gold(I)phosphine compounds induce cytotoxicity is not yet fully understood. Previous studies have indicated the occurrence of DNA-protein cross-links and DNA strand breaks (Berners-Price *et al*. 1986). It is, however, proposed that mitochondria are the primary target of both the neutral, linear gold(I)phosphine compounds (Hoke *et al.* 1989; Rush *et al.* 1987), as well as the cationic, tetrahedral gold(I)phosphines (Mirabelli *et al*. 1986; Smith *et al*. 1989). The major source of energy in all normal eukaryotic cells, originate from the mitochondria (Acton *et al*. 2004). Physical characteristics **(Figure 1.1, page 5)** of mitochondria include an inner and outer mitochondrial membrane, an intermembrane space and a matrix, which is encapsulated by the inner membrane (Olson and Kornbluth 2001). Within the matrix, mitochondria are responsible for (i) ATP production through oxidative phosphorylation and the citric acid cycle, (ii) the regulation of calcium homeostasis and (iii) activation of certain key steps in the cascade of intracellular events that end in programmed cell death (apoptosis) (Acton *et al*. 2004; Modica-Napolitano and Singh 2002). The mitochondrial genome is contained within the matrix.

The impermeable inner membrane forms cristae for an increased surface area and establishes the electrochemical gradient that drives ATP synthesis, a reaction that is catalysed by ATP synthetase (Fantin *et al*. 2002). Tumour cells possess a higher mitochondrial membrane potential than normal epithelial cells (Bernardi *et al*. 1999; Fantin *et al*. 2002).

The gold(I) lipophilic cations accumulate in the mitochondrial membranes in response to an increased mitochondrial membrane potential observed in transformed cells, which causes a subsequent negative inner membrane charge. The mitochondrial membrane concentrates the drug within the mitochondria (Davis *et al*. 1985), followed by a loss of proton gradient and subsequent dissipation of the membrane potential. This results in cell death i.e. apoptosis (Modica-Napolitano and Singh 2002). When a compound accumulates in the mitochondria, cytochrome c is released followed by the activation of the executioner caspases (caspases 3,6,7) after which the final apoptotic events follow: proteins involved in cytoskeletal functions are degraded which causes cell shrinkage and the collapse of the nucleus and the cell itself (Hill *et al*. 2003; Huppertz *et al*. 1999).

The neutral, two-coordinate linear compound, Et_3PAuCl, affects the mitochondria via complex mechanisms including i) inhibition of the electron transport chain, ii) interactions with mitochondrial thiols (Rush *et al.* 1987), iii) increased mitochondrial inner membrane permeability, iv) collapse of mitochondrial membrane potential and release of calcium, v) mitochondrial swelling and vi) ATP depletion (Hoke *et al.* 1989).

It is possible that the novel neutral, two-coordinate linear gold-containing compounds might also involve the mitochondria in exerting their cytotoxic activity. There is evidence that two-coordinate linear complexes, such as $[(AuCl)_2dppe]$ rearrange in the presence of thiols to form lipophilic cations. Hence, the pharmacologically active species, for this class of compounds, are lipophilic cations.

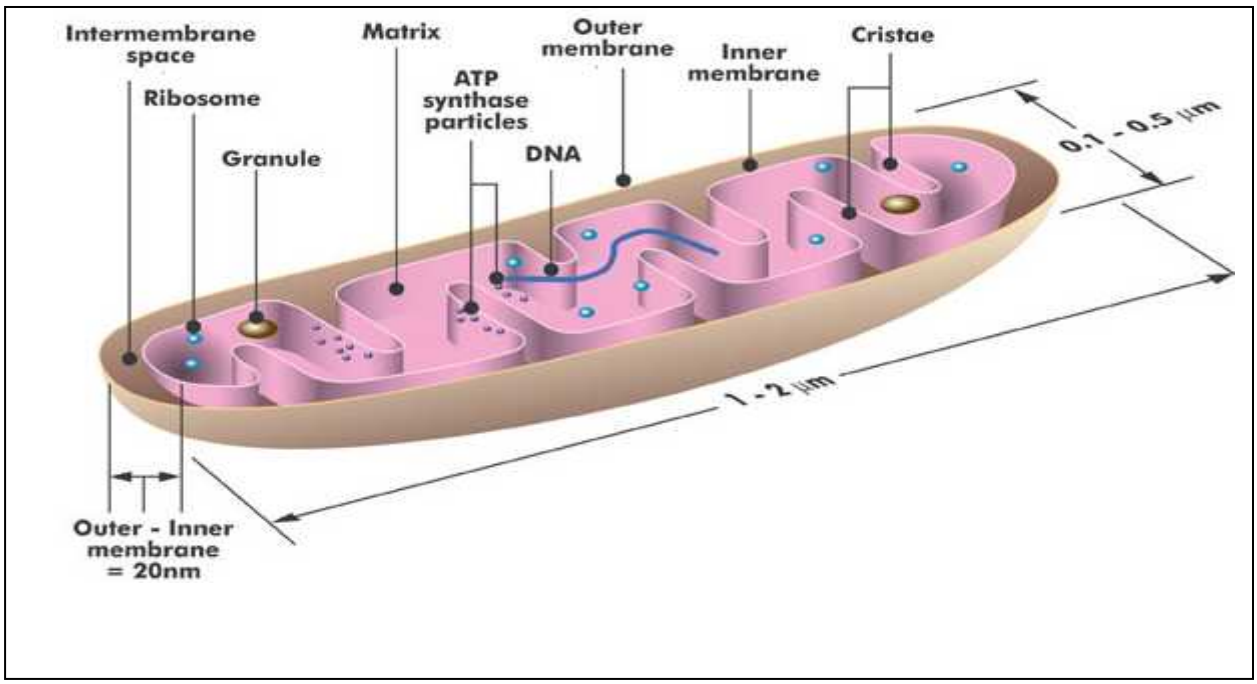

Figure 1.1. Schematic diagram of a mitochondrion. Adapted from Frey and Mannella (2000)

1.2.2 Nucleoside analogues as anticancer compounds

The building blocks of DNA and RNA are deoxyribonucleotides and ribonucleotides, which consist of a nitrogen structured base, a nucleoside, and a phosphate group (Van Rompay *et al*. 2003). A nucleoside is a pentose sugar (deoxyribose or ribose) with a purine or pyrimidine base. The purines, adenine and guanine, and the pyrimidines, thymidine and cytosine, are well known. Currently, nucleoside analogues (NAs) are used as antiviral treatment in HIV and AIDS as part of combination therapy (Zemlicka 2000). In addition to their antiviral properties, NAs show promise as anti-tumour compounds. Anticancer deoxyribonucleoside analogues that are currently in clinical use are: Cladribine, Fludarabine, Cytarabine, Gemcitabine, (Zemlicka 2000), 6-mercaptopurine and 6-thioguanine (Elgemeie 2003).

Major problems in the treatment of cancer and viral diseases with NAs are: acquirement of resistance, side effects such as dose limiting cytotoxicity, poor drug bioavailability, metabolic deactivation, and bone marrow suppression (Elgemeie 2003; Galmarini *et al*.

2002). NAs induce apoptosis via incorporation into the nuclear DNA. It is suggested that the combination of NAs with gold(I) compounds might be beneficial in eliminating resistance and delayed cytotoxicity (Solary *et al.* 2003; Zhu 2000).

1.2.2.1 Mechanism of NAs involved in inducing cytotoxicity

Incorrect DNA replication and synthesis are involved in the aging process and in the development of diseases such as cancer. It has been suggested that NAs (which contain purine or pyrimidine bases) exert their anti-tumour properties via interference with DNA synthesis (Van Rompay *et al*. 2003) and may also involve mitochondria in the induction of apoptosis. After being phosphorylated to their triphosphate form, NAs can then be incorporated into DNA and RNA (Elgmeie 2003; Van Rompay *et al*. 2003).
The analogues act as DNA chain terminators after being incorporated into DNA instead of the normal nucleoside, due to lacking the 3V-OH group (Van Rompay *et al*. 2003). This interference with DNA synthesis is of clinical importance when developing novel anticancer and anti-viral compounds.

1.2.3 Azoles as anticancer compounds

Azoles are heterocyclic aromatic compounds consisting of carbon and nitrogen atoms in varying positions. Depending on the number and position of the nitrogen atoms, azoles are classified as either being a pyrrole (containing one N atom), an imidazole (containing two N atoms at position 1 and 3), a pyrazole (containing two N atoms at position 1 and 2), a triazole (containing three N atoms) (Maertens 2004), or a tetrazole (containing four N atoms).

Azole derivatives are well known for their anti-fungal effects (Rodriguez *et al*. 1995). Various azole derivatives have also shown potent anticancer activity *in vitro* (Bradshaw *et al*. 1998a; Bradshaw *et al*. 1998b; Kashiyama *et al*. 1999; Meira *et al*. 2002; Penso *et al*. 2005; Shi *et al*. 1996) and *in vivo* in mice inoculated with human melanoma cells (Penso and Beitner 2002). Well known anticancer azole derivatives that are currently

being used in the clinic are Vorozole, Letrozole, Anastrozole, Ketoconazole and Liarozole (Rodriguez and Acosta 1995; Salih 2008). Due to the occurrence of drug resistance by cancer cells and side effects such as severe gastrointestinal side effects, hepatotoxicity, myelosuppression, neutropenia and nausea, further research and development of novel azole derivatives and combination chemotherapy compounds should continue (Magedov *et al*. 2007; Rodriguez and Acosta 1995). Previously, an azole-platinum combination compound displayed anticancer activity comparable to that of cisplatin *in vitro*, but were only slightly more active against cisplatin-resistant cancer cells (Spiegel *et al*. 2007). Through combining gold with azole derivatives, it was thought that this problem might be overcome.

1.2.3.1 Mechanism of azoles in inducing cytotoxicity

Several studies have designated the inhibition of glycolysis as mechanism of action for some azole derivatives (Hegemann *et al*. 1993; Meira *et al*. 2005; Mignen *et al*. 2005). The reasoning behind this is that tumour cells are reliant on glycolysis for ATP production, which makes it a promising drug target (McKeage *et al*. 2002).

It is, however, believed that most azole derivatives primarily induce cytotoxicity via interference with the cell cycle. Survival of multicellular organisms depends on the "cell division cycle" or "cell cycle". The cell cycle can be divided into two phases namely interphase and mitosis (Fairbanks and Andersen 1999). During interphase, cells can remain in a quiescent or resting phase (G0) for days to weeks before entering the first gap/growth (G1) phase (Perchellet *et al*. 2005). Cell growth takes place in the (G1) phase and enables the cell to confirm that the conditions for cell replication are optimal before committing to DNA replication. DNA duplication is a very important event in the cell cycle and takes place during the synthesis (S) phase where after cells continue to grow during the second gap/growth (G2) phase (**Figure 1.2, page 8**). The G2 phase is followed by mitosis, which consists of orderly cell division into two daughter cells over various stages namely interphase, prophase, metaphase, anaphase and telophase (De Souza and Osmani 2007).

In order for a cell to proceed to a following phase in the cell cycle, the cell is evaluated at certain checkpoints. At these checkpoints, it is confirmed whether the cell can proceed or whether it should abort further division due to the detection of cell damage. The checkpoint between the G1 and S phase requires the interaction of cyclins and cyclin-dependent kinases (cdks) (Perchellet *et al*. 2005). The kinase proteins are at the centre of events that control the cell cycle and are thus possible targets for cancer therapy (Dansey and Sausville 2003). It has been proposed that some azole derivatives interfere with DNA synthesis via either targeting kinases (Perhellet *et al*. 2005), or by forming DNA adducts (Trapani *et al*. 2003), which will lead to DNA cleavage (Kim *et al*. 2007; Thurston 2007) resulting in induction of the apoptotic cascade.

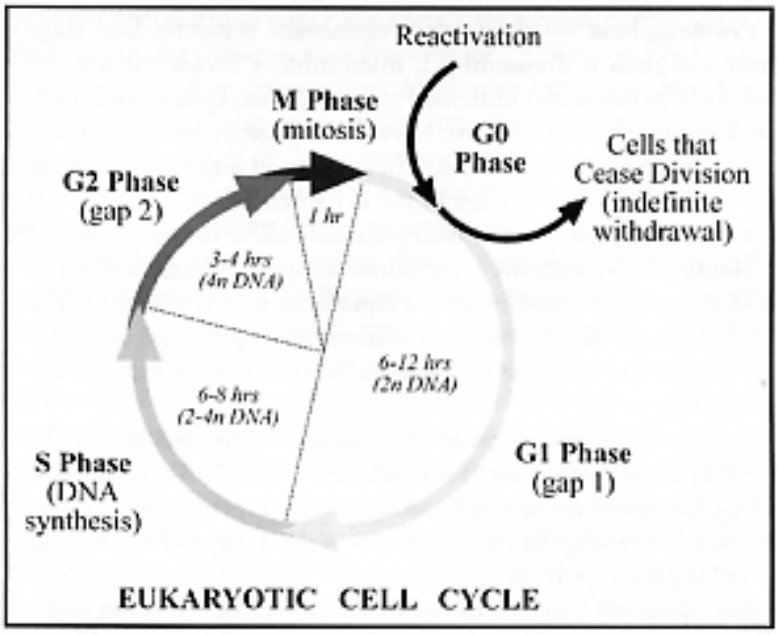

Figure 1.2. The eukaryotic cell cycle. Adapted from Lewin 1995.

1.3 EXPERIMENTAL COMPOUNDS

The seven novel gold compounds that contain either a NA or an azole base have been designed and synthesized by Dr. Horvath under the supervision of Prof. Raubenheimer from the University of Stellenbosch.

$[Au(dppe)_2]Cl$ (**Figure 1.3, page 10**) and cisplatin (**Figure 1.4, page 10**) were used as positive control compounds due to their well-documented toxicity and mechanisms of action. All the novel structures are similar to the control compound, $[Au(dppe)_2]Cl$ in that they contain gold (Au) atoms coordinated by aryl substituted phosphines, with aryl group substitution appearing to be particularly important for anticancer activity (Price and Sadler 1988). The novel compounds described here, differ from $[Au(dppe)_2]Cl$ in that they are neutral, two-coordinated linear complexes, whereas $[Au(dppe)_2]Cl$ is a cationic, tetrahedral four-coordinated complex. It has been suggested, however, that the cationic four-coordinated complexes are the pharmacological active species of two-coordinated bridged di-gold complexes, such as the novel compounds investigated in this study (Berners-Price *et al*. 1988). Another structural alteration is that the novel compounds contain either an azole or NA (purine) bound via a gold-nitrogen bond, which completes the coordination sphere.

The compounds containing NAs (purines) are UH 86.2, UH 75.1, UH 58.1, and UH 145.1. The compounds containing azoles are: UH 107.1 (imidazole derivative), UH 126.1 (pyrazole derivative), and UH 127.1 (triazole derivative) (**Figures 1.5 –1.11, pages 10-11**).

The compounds were designed to combine the properties of anticancer gold(I) phosphines as well as NAs or azoles in order to improve the selectivity of these compounds and to overcome resistance.

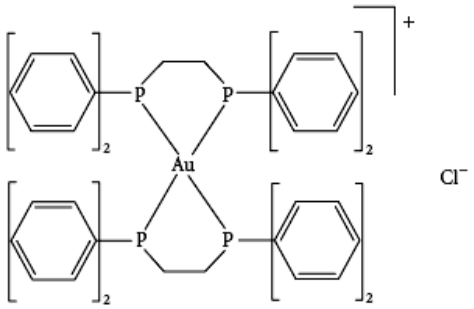

Figure 1.3 Structure of [Au(dppe)$_2$]Cl

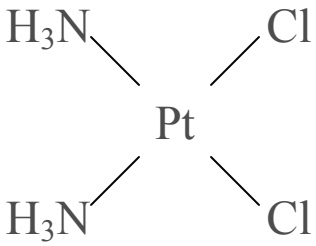

Figure 1.4 Structure of cisplatin

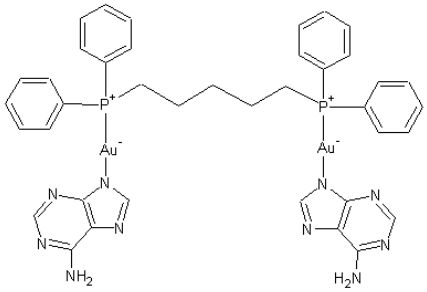

Figure 1.5 Structure of UH 86.2

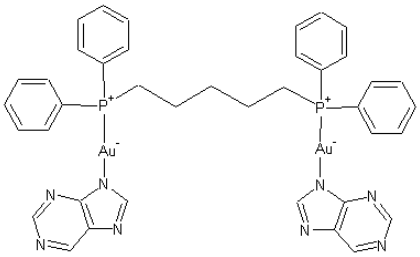

Figure 1.6 Structure of UH 75.1

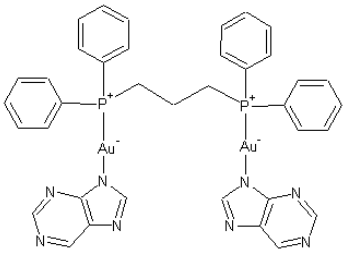

Figure 1.7 Structure of UH 58.1

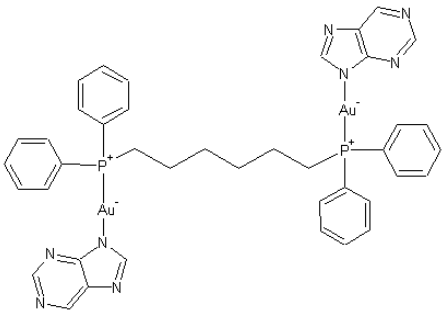

Figure 1.8 Structure of UH 145.1

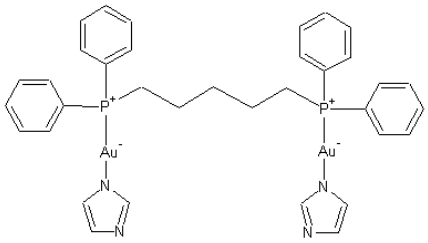

Figure 1.9 Structure of UH 107.1

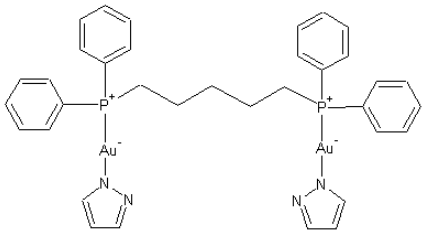

Figure 1.10 Structure of UH 126.1

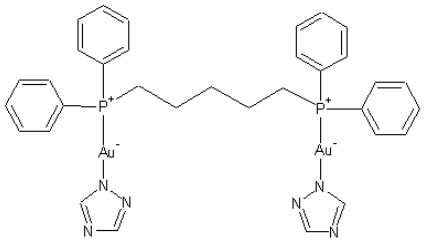

Figure 1.11 Structure of UH 127.1

1.4 RATIONALE FOR THIS STUDY

It has been proven that gold-containing compounds, NAs and azole based compounds display anticancer activity as individual compounds. The occurrence of non-selective *in vivo* toxicity and resistance of tumour cells to these drugs still remain problematic. It has previously been shown that by varying the lipophilicity of gold-containing phosphine complexes, that selectivity and/or potency can be varied. A similar approach has been undertaken here, where novel compounds of varying lipophilicities have been prepared to establish (i) whether the novel compounds induce selective cytotoxicity in cancer cells, (ii) which mechanism might possibly be involved in inducing cytotoxicity and (iii) whether the compounds are toxic *in vivo*.

1.5 AIM

The aim of this study was (i) to determine the tumour specificity of seven novel compounds, (ii) to examine cross-resistance on a cisplatin resistant cell line, (iii) to determine a possible mechanism of action by which the compound induce cytotoxicity and (iv) to determine the *in vivo* toxicity of the two most promising compounds in a mouse model.

1.6 HYPOTHESIS

The novel compounds will have a high tumour specificity and will be less toxic than $[Au(dppe)_2]Cl$ in mice, owing to the extended coordination of gold to the additionally anti-tumour active nitrogen-containing heterocycles included in this study.

1.7 OBJECTIVES

1. To identify the four most promising novel compounds by comparing the cytotoxicity of all the experimental compounds on cancer cell lines and normal cell cultures:
   - Cancer cell lines: human cervical cancer (HeLa), human colon cancer (CoLo), and lymphocytic leukaemia (Jurkat) cells
   - Normal cells: human resting lymphocytes and phytohemaglutinin (PHA) stimulated lymphocytes
2. To determine the tumour specificity of the selected four compounds when using an extended range of normal and cancer cell cultures:
   - Cancer cell lines: human breast cancer (MCF-7), human ovarian cancer sensitive to cisplatin (A2780) as well as resistant to cisplatin (A2780cis)
   - Normal cells: chicken embryo fibroblasts
3. To identify the two most promising compounds based on the *in vitro* tumour specificities for further investigation.
4. To determine whether there is a correlation between the lipophilicity and cytotoxic activities of the test compounds
5. To determine the induced cell death pathway on Jurkat cells with a flow cytometric method.

6. To determine whether the selected compounds have an effect on the mitochondrial membrane potentials of primary stimulated human lymphocyte cultures and of Jurkat cells (lymphocytic leukaemia cell line).
7. To determine the effect of the selected compounds on the cell cycle progression of Jurkat cells
8. To determine the *in vivo* toxicity of the two most promising compounds in a mouse model.

CHAPTER TWO

DETERMINATION OF THE OCTANOL/WATER PARTITION COEFFICIENT

2.1 INTRODUCTION

The non-selectivity of cancer drugs in differentiating between tumour cells and normal tissues leads to severe host toxicity. Lipophilic cations, a relatively new class of anticancer drugs, displayed selective targeting of mitochondria with hyperpolarized membranes in cancer cells (Berners-Price *et al*. 1999). Strong anticancer activity has been detected for these cationic lipophilic compounds, however, *in vivo* toxicity remained too high for clinical use (Hoke *et al*. 1989, McKeage *et al*. 2002). The lipophilic character of lipophilic cations, such as $[Au(dppe)_2]Cl$, determines the rapid cellular uptake of these compounds through the degree of protein binding. Pertaining to these gold-containing charged (i.e. cationic) structures, a decrease in lipophilicity indicates greater selectivity where an increase in lipophilicity increases the potency of the drug (Berners-Price *et al*. 1999). Although the novel compounds have neutral, linear two-coordinated structures, an objective of this study is to investigate whether a correlation exists between the lipophilicity and cytotoxic activities of the novel compounds. It has also been suggested that, in the presence of thiols, the charged four-coordinated species are the pharmacological active species of two-coordinated phosphine bridged di-gold species, such as the compounds investigated in this study (Berners-Price *et al*. 1988).

After several structurally diverse lipophilic cations have displayed cytotoxicity in tumour models (Denny *et al*. 1979; Rideout *et al*. 1989), it was concluded that aromatic substituents appear to be important for this anticancer activity (Berners-Price and Sadler 1988). In this study the phenyl substituents were retained in the newly synthesized seven novel gold(I) derivatives. Azole or nucleoside derivatives bound via a gold-nitrogen bond were chosen to complete the coordination sphere. It was hypothesized that, with the addition of azole or nucleoside analogue (NA) derivatives, the novel compounds would be more hydrophilic than $[Au(dppe)_2]Cl$ (Pandit 2006).

The hydrophilic-lipophilic balance is expressed as an octanol/water partition coefficient (PC) in this study (Rideout *et al*. 1989). The octanol/water PC of a compound is defined as the concentration of the compound in the aqueous phase. It is known that $[Au(dppe)_2]Cl$ is an extremely lipophilic compound (Berners-Price *et al.* 1999). The aim was to develop gold-containing compounds that are more hydrophilic than $[Au(dppe)_2]Cl$ to increase selectivity but lipophilic enough to retain cytotoxic potency.

2.2 AIM

The aim of this experiment was to determine and compare the octanol/water PCs of the seven novel compounds, $[Au(dppe)_2]Cl$ and cisplatin.

2.3 MATERIALS

Experimental compounds

Novel experimental compounds were provided by Dr. U Horvath from the Department of Chemistry, University of Stellenbosch: UH 86.2, UH 75.1, UH 58.1, UH 145.1, UH 107.1, UH 126.1, and UH 127.1. The control compound, $[Au(dppe)_2]Cl$, was provided by Messai Mamo from Department of Chemistry, University of Witwatersrand. Cisplatin was purchased from Sigma Aldrich, Johannesburg, SA.

2.4 METHOD

1. A volume of octanol-saturated water and water-saturated octanol was prepared by shaking required volumes of octanol and de-ionized water for 5min.
2. Octanol and aqueous phases separated overnight in a separation funnel.
3. The octanol and water fractions were collected separately.
   - Octanol = water-saturated octanol
   - Water = octanol-saturated water
4. A 20µM octanol solution (5ml) of the novel gold compounds, $[Au(dppe)_2]Cl$ and cisplatin was prepared.

5. These solutions were added to a 1 ml quartz cuvette and analysed separately by UV spectroscopy using a Secoman UV spectrophotometer (Anthelly Advanced model).
6. An absorbance maximum for each compound at a wavelength between 251nm and 298nm was obtained.
7. This absorbance corresponded to a Ci value (initial concentration) for each solution.
8. The drug/octanol solutions were returned to the corresponding 20µM solutions.
9. A volume of 5ml water was then added to the drug/octanol solutions and a final volume of 10ml was obtained.
10. The 10ml solutions were shaken for 15 minutes to separate the octanol and aqueous phases.
11. The solutions were centrifuged for 10min at 1000rpm (300g). The aqueous extract thus separated completely from the octanol extract.
12. The aqueous solution was dispensed into a 1 ml quartz cuvette and analysed with a UV spectrophotometer in order to determine an absorbance maximum at the wavelength identified from the Ci determination.
13. This absorbance corresponded to a Cw value (unknown concentration of the compound in the aqueous phase) for each solution.
14. The concentration of each complex remaining in the octanol layer, Co, was determined by Ci-Cw.

2.5 EXPRESSION OF RESULTS

Statistical evaluation was done by a Kruskal-Wallis non-parametric test in order to compare the lipophilicity of the different groups of compounds with each other (**refer to Appendix A, number 1.1, a-b, page 130**). All calculations were done with BMDP Statistical Software© (**refer to Appendix A, number 1.1, c, page 130**). The difference was considered statistically significant at $p \leq 0.05$.

The concentration of each complex in the aqueous layer (Cw), and in the octanol layer (Ci), was determined. The concentration of each complex remaining in the octanol layer,

Co, was determined by Ci-Cw. The final octanol/water PC values were calculated with the formula:

$$\mathbf{PC=Co/Cw}$$

Results are expressed as the mean log PC values ± standard error of the mean (SEM) of the final PC value.

2.6 RESULTS

It is known that $[Au(dppe)_2]Cl$ is an extremely lipophilic compound (Berners-Price *et al*. 1999) and was, therefore, seen as the lipophilic standard. The octanol/water PC was determined for each compound with the shake-flask method and the average octanol/water PC values and the mean log octanol/water PC values are summarized in **Table 2.1, page 18**. A mean log PC value equal to one, represents a compound that has equal affinities for lipid and water. A mean log PC value less than one implies that the compound is hydrophilic, whereas a mean log PC value higher than one implies that the compound is lipophilic (Pandit 2006).

$[Au(dppe)_2]Cl$ is the most lipophilic compound of the tested compounds with an octanol/water PC of 1.62. Cisplatin is indicated as a hydrophilic compound with an octanol/water PC of 0.33. The purine-containing compounds (UH 86.2, UH 75.1, UH 58.1, UH 145.1) and the azole containing compound, UH 127.1, display hydrophilic properties, with octanol/water PCs of 0.70, 0.53, 0.66, 0.71 and 0.81 respectively. The azole-containing compounds, UH 107.1 and UH 126.1, are indicated as lipophilic compounds with octanol/water PCs of 1.16 and 1.25 respectively.

When analysed in groups, a significant difference in lipophilicity ($p \leq 0.05$) is seen when comparing the purine-containing compounds to both $[Au(dppe)_2]Cl$ and the azole-containing compounds (**Table 2.1, page 18)**. Further, a significant difference ($p \leq 0.05$) is observed between the the azole-containing and cisplatin compounds (**Table 2.1, page 18)**.

Table 2.1. The average octanol/water partition coefficient values and the mean log octanol/water partition coefficient values ± SEM of all the experimental compounds

Octanol/water partition coefficient values and mean log octanol/water partition coefficient				
Group name	**Experimental compounds**	**Average octanol/water partition coefficient value [1]**	**Mean log octanol/water partition coefficient ± SEM [1]**	**Lined values indicate significant difference between groups**
Purine-containing compounds	UH 86.2	5.01	0.70 ± 0.03	* #
	UH 75.1	3.39	0.53 ± 0.06	
	UH 58.1	4.57	0.66 ± 0.11	
	UH 145.1	5.13	0.71 ± 0.24	
Azole-containing compounds	UH 107.1	14.45	1.16 ± 0.07	¤ §
	UH 126.1	17.78	1.25 ± 0.06	
	UH127.1	6.46	0.81 ± 0.02	
[Au(dppe)$_2$]Cl as lipophilic standard	[Au(dppe)$_2$]Cl	41.69	1.62 ± 0.06	¤
Cisplatin as hydrophilic standard	Cisplatin	2.14	0.33 ± 0.13	*

* $p \leq 0.05$ when compared to [Au(dppe)$_2$]Cl

¤ $p \leq 0.05$ when compared to cisplatin

\# $p \leq 0.05$ when compared to the azole-containing compounds (UH 107.1, UH 126.1 and UH 127.1)

§ $p \leq 0.05$ when compared to the purine-containing compounds (UH 86.2, UH 75.1, UH 58.1 and UH 145.1)

1. Average of three experiments

2.7 DISCUSSION

The structures of the novel compounds were based on previously described bridged di-gold bisphosphine complexes of type ion $[(AuCl)_2dppe]$, where dppe is a bisphosphine, which have shown to transform, in the presence of biological media, into the anti-tumour cationic complexes of type $[Au(dppe)_2]Cl$. Alterations were made in order to potentially manipulate the lipophilicity of the novel compounds. In this study the phenyl substituents that are important for anticancer activity (Berners-Price and Sadler 1988), were retained in the newly synthesized seven novel gold(I) derivatives. Additionally, azole or purine derivatives bound via a gold-nitrogen bond were chosen to complete the coordination sphere, since azole and purine bases have also shown previously to exhibit anti-tumour activity.

HPLC (high performance liquid chromatography) analysis has been used to confirm the lipophilicity of $[Au(dppe)_2]Cl$, with a mean log PC of 1.41 having been obtained (McKeage *et al*. 2000). A similar water/octanol PC value of 1.62 ± 0.06 was obtained in this study by using a different method (the shake-flask method). The obtained results also correlate with the findings of Berners-Price *et al*. (1999), which concluded that $[Au(dppe)_2]Cl$ is a lipophilic compound.

Ohwada *et al*. (2002) classifies azoles as lipophilic compounds that consist of heterocyclic rings that display non-polar functionalities. Although the free azole bases are insoluble in water, they are soluble in other organic solvents such as ethanol. In this study, the azole-containing compounds, UH 107.1 and UH 126.1, displayed similar octanol/water PC values to each other (1.16 ± 0.07 and 1.25 ± 0.06 respectively). In contrast to this, the azole-containing compound, UH 127.1, was indicated as being hydrophilic with a mean log PC value of 0.81 ± 0.02. Results obtained in this study indicate that UH 107.1 and UH 126.1 display lipophilic properties, although they are slightly less lipophilic than $[Au(dppe)_2]Cl$. The novel compound, UH 127.1, is the least lipophilic azole-containing compound. The apparent hydrophilicity of this compound is

most likely attributed to the additional N atom within the azole ring system (Pandit 2006).

According to the literature, the lipophilicity of purine compounds is generally low (Shirasaka *et al*. 1990). This is echoed by the results obtained during this study, where similar octanol/water partition coefficient values (approximately 0.53 – 0.71) are seen for the purine-containing compounds. These compounds displayed lower mean log octanol/water PCs when compared to both $[Au(dppe)_2]Cl$ and the azole-containing compounds. The hydrophilic purine- containing compounds are still less hydrophilic than cisplatin (which has the lowest mean log octanol/water PC value of 0.33 ± 0.13).

As expected, cisplatin was found to display hydrophilic characteristics by exhibiting a low mean log octanol/water partition coefficient value, which correlates with previous findings (Burger *et al*. 2002).

It can be concluded that the purine-containing compounds as well as the azole-containing compound, UH 127.1, display hydrophilic properties. In contrast to this, the azole-containing compounds, UH 107.1 and UH 126.1, are lipophilic. When comparing the lipophilicity of the compounds with their cytotoxic activities (**refer to Chapter 3, page 31**), it can be determined whether a correlation exists between these two variables.

CHAPTER THREE

CYTOTOXICITY ASSAYS

3.1 INTRODUCTON

In vitro toxicity can be a predictor of the *in vivo* activity. Although a high level of cytotoxicity does not always predict a high degree of anti-tumour activity *in vivo*, a low level of cytotoxicity does correlate with marginal or no activity *in vivo* (McKeage *et al*. 2002). A correlation has also been seen between the *in vitro* cytotoxic potency of the compounds and their maximum tolerated doses *in vivo* (McKeage *et al*. 2002). By comparing the cytotoxicity of the novel compounds on a range of cancer cell lines as well as normal cell cultures, the *in vitro* tumour specificity of each compound can be determined. The tumour specificity will indicate the selectivity of the compounds and might be a predictor of the *in vivo* activity.

Previous studies have used a variety of cancer cell lines to test for *in vitro* activity. Carcinoma cells from the cervix, breast, ovary, and colon have proved to be successful models for determining cytotoxic potency (Caldwell *et al*. 1999; Chen 1988; Schoonen *et al*. 2005; Tiekink 2002). T-cell leukaemia cells and both cisplatin sensitive and cisplatin resistant ovarian cancer cell lines are widely used for the evaluation of novel compounds (Tiekink 2002). These cell lines have also been selected to use in this study. Normal cells that will be used are: chicken embryo fibroblasts, human resting lymphocytes and PHA (phytohemaglutinin) stimulated lymphocytes. PHA stimulated lymphocytes are known to have a higher mitochondrial membrane potential when compared to resting lymphocytes (Chen 1988).

Cell proliferation can be determined with the quantitative, colorimetric MTT assay. Only within viable cells, the yellow tetrazolium salt, MTT ([3-(4,5-dimethylthiazol-2-yl)-2,5-diphenyltetrazolium bromide]), is metabolised by mitochondrial succinic dehydrogenase activity to form a water-soluble violet formazan reaction product (Freimoser *et al*. 1999). Cytotoxicity is indicated with a decrease of cell viability, indicated by a decrease in the intensity of the violet formazan product when measured spectrophotometrically.

In order to determine selectivity, the *in vitro* tumour specificity is determined for each compound by comparing induced cytotoxicity in cancer cell lines versus normal cells. Tumour specificity is an indicator of selectivity. An increase in tumour specificity indicates greater selectivity.

3.2 AIMS

The aims of this experiment were:

1. To identify the four most promising novel compounds by comparing the tumour specificities of all the experimental compounds on cancer and normal cell cultures:
    (i) Cancer cell lines: human cervical cancer (HeLa), human colon cancer (CoLo), and lymphocytic leukaemia (Jurkat) cells
    (ii) Normal cells: human resting lymphocytes and phytohemaglutinin (PHA) stimulated lymphocytes
2. To determine the tumour specificities of the selected four compounds when using an extended range of normal and cancer cell cultures, in order to determine the two most promising novel compounds for further *in vitro* and *in vivo* tests:
    (i) Cancer cell lines: human breast cancer (MCF-7), human ovarian cancer sensitive to cisplatin (A2780) as well as resistant to cisplatin (A2780cis)
    (ii) Normal cells: chicken embryo fibroblasts
3. To determine if cross-resistance exists between cisplatin and the selected four novel gold derivatives using two human ovarian cancer cell lines: A2780 (human ovarian cancer) and A2780cis (cisplatin resistant human ovarian cancer).
4. To determine whether a correlation exists between the octanol/water partition coefficients and the cytotoxic potencies of the tested compounds (UH 75.1, UH86.2, UH 58.1, UH 145.1, UH 107.1, UH 126.1, UH 127.1, $[Au(dppe)_2]Cl$ and cisplatin) against various cancer cell lines (HeLa cells, CoLo cells, Jurkat cells) and normal cell cultures (human resting lymphocytes and PHA stimulated lymphocytes).

3.3 MATERIALS

3.3.1 Media and reagents

Ammonium chloride solution

Prepared by dissolving 8,3g Ammonium chloride (NH_4Cl), 1g Sodium bicarbonate ($NaHCO_3$), (both purchased from Merck, JHB, SA) and 74mg EDTA (Sigma-Aldrich, JHB, SA) in 1000ml of distilled water. The solution was then filter sterilized using a 0.22 µm cameo filter and refrigerated at 4ºC until use.

Cell counting fluid

A volume of 1ml of a 0.1% crystal violet solution and 2ml glacial acetic acid was dissolved in 97ml of distilled water. The solution was mixed well and refrigerated at 4ºC until use.

Dulbecco's Modified Eagle Medium (DMEM)

DMEM powder (Sigma-Aldrich, JHB, SA) was dissolved in sterile water with the aid of a sterile stirrer. The pH of the solution was adjusted to 4.0 with 1M HCl to ensure complete solubilisation. Thereafter 2mg of $NaHCO_3$ was added to each litre of the medium. The pH was readjusted to 7.1 through the addition of either 1M HCl or 1M sodium hydroxide (NaOH). The medium was filter-sterilized through a 0.22µm filter and divided into 500ml aliquots. A volume of 55ml was removed from the 500ml aliquot and the remaining solution was supplemented with 5ml of a 1% penicillin/streptomycin solution and 50ml sterile HI FCS. The medium was stored at 4ºC.

Essential Modified Eagle's Medium (EMEM)

EMEM powder (Sigma-Aldrich, JHB, SA) was dissolved in sterile water with the aid of a sterile stirrer. The pH of the solution was adjusted to 4.0 with 1M HCl to ensure complete solubilisation. Thereafter, 2mg of $NaHCO_3$ was added to each litre of the medium. The pH was readjusted to 7.1 through the addition of either 1M HCl or 1M sodium hydroxide (NaOH). The medium was filter-sterilized through a 0.22µm filter and divided into 500ml aliquots. A volume of 55ml was removed from the 500ml aliquot

and the remaining solution was supplemented with 5ml of a 1% penicillin/streptomycin solution (Adcock-Ingram, JHB, SA) and 50ml sterile heat inactivated foetal calf serum (HI FCS), (Adcock Ingram, JHB, SA). The medium was stored at 4ºC.

Experimental compounds

A 10mM stock solution was prepared by dissolving the appropriate mass of each compound (UH 86.2, UH 75.1, UH 58.1, UH 145.1, UH 107.1, UH 126.1, UH 127.1, $[Au(dppe)_2]Cl$ and cisplatin) in dimethyl sulphydroxide (DMSO) (obtained from Merck, Darmstadt, Germany). A 50µl volume of each compound was aliquoted in eppendorf vials and stored at -70°C. Dilutions were prepared in the appropriate supplemented medium.

Heparin

A mass of 30g heparin (Sigma-Aldrich, JHB, SA) was dissolved into 90ml of distilled water. The solution was filter sterilized using a 0.22 µm cameo filter and refrigerated at 4ºC until use.

MTT solution

A mass of 200mg MTT was dissolved in 40ml PBS solution. After solubilising, the light sensitive solution was filter sterilized using a 0.22 µm cameo filter and stored (covered in tin foil) at 4ºC until use.

Phosphate buffered saline (PBS)

A mass of 0.923g of FTA hemagglutinin buffer powder (The Scientific Group, JHB, SA) was dissolved in 100ml of distilled water. The pH was adjusted to 7.2.

Phytohemagglutinin (PHA) solution

A volume of 5ml of distilled water was added to the freeze-dried PHA bottle content (Bioweb (PTY) Ltd., JHB, SA). Aliquots of 0.2ml were dispensed under sterile conditions and stored at -20°C.

Roswell Park Memorial Institute Medium (RPMI) 1640

RPMI 1640 powder (Sigma-Aldrich, JHB, SA) was dissolved in sterile water with the aid of a sterile stirrer. The pH of the solution was adjusted to 4 with 1N HCl to ensure complete solubilisation. Thereafter, 2mg of $NaHCO_3$ was added to each litre of the medium. The pH was readjusted to 7.1 through the addition of either 1N HCl or 1N NaOH. The medium was filter-sterilized through a 0.22µm filter and divided into 500ml aliquots. A volume of 55ml was removed from the 500ml aliquot and the remaining solution was supplemented with 5ml of a 1% penicillin/streptomycin solution and 50ml sterile HI FCS. The medium was stored at 4ºC until use.

3.3.2 Cell cultures

3.3.2.1 Description of carcinoma cell lines

A2780 cisplatin sensitive cells

Human ovarian cancer cells (ECACC no. 93112519) were maintained in Roswell Park Memorial Institute medium (RPMI 1640) medium with 10% bovine FCS.

A2780cis cisplatin resistant cells

Human ovarian cancer cells (ECACC no. 93112517) were maintained in RPMI 1640 medium with 10% bovine FCS.

CoLo 320 DM cells

Human colon cancer cells (ATCC no. CCL-220) were maintained in RPMI 1640 with 10% bovine FCS.

HeLa cells

Human cervical cancer cells (ATCC no. CCL-2) were maintained in Eagles minimum essential medium (EMEM) containing 2mM L-glutamine, 0.1 mM non-essential amino acids, 1.0 mM sodium pyruvate and 5% bovine foetal calf serum (FCS).

Jurkat cells

Human T –lymphocyte leukaemia cells (ATCC no. TIB-152) were maintained in RPMI 1640 medium with 10% bovine FCS.

MCF-7 cells

Human breast cancer cells (ATCC no. HTB 22) were maintained in Dulbecco's minimum essential medium (DMEM) containing 2mM L-glutamine, 0.1 mM non-essential amino acids, 1.0 mM sodium pyruvate and 5% bovine FCS.

All the cells cultures are maintained in their appropriate growth medium at 37°C with 5% CO_2. They were sub-cultured as needed and cell suspensions of appropriate concentrations were made prior to the experimental procedure (**see section 3.4.3, page 27**).

3.3.2.2 Description of normal cells (primary cultures)

Chicken embryo fibroblasts

Cells were derived from chicken embryos. Procedures for isolation of lymphocytes are discussed in **Appendix B**, **number 1, page 140.**

Human lymphocytes

Cells were derived from preservative free heparinized peripheral human blood. Procedures for isolation of lymphocytes are discussed in **Appendix B, number 2, page 141.**

3.4 METHODS

3.4.1 Passaging the cells

1. The culture medium was discarded from a 75cm^2 flask and 5ml of Trypsin Versene (obtained from the National Institute for Communicable Diseases, Johannesburg, SA) was added in order to rinse the cells.

2. The Trypsin Versene was then discarded and a further 15ml of Trypsin Versene was added to the cells.
3. The flask was placed in the incubator where the cells were incubated for 20 minutes at 37°C in a 5% CO_2 atmosphere until the cells were detached from the flask.
4. Five millilitres of medium supplemented with foetal calf serum (FCS) were added to the cells in order to neutralize the action of the Trypsin Versene.
5. The latter suspension was then aspirated to a 15ml centrifuge tube and centrifuged at 1000 rpm for 5 minutes.
6. The supernatant was discarded after which 1ml medium supplemented with foetal calf serum (FCS) were added to the cell pellet and aspirated to form a suspension.

3.4.2 Counting the cells

1. A volume of 50µl of the cell suspension was added to 450µl white cell counting fluid.
2. This suspension was then added to a glass slide (haemocytometer) and cells were counted using a Reichert-Jung Microstar 110 microscope at a magnification of 40 times.
3. The cells were re-suspended to obtain the relevant cell concentration for each assay.

3.4.3 Experimental procedure

1. 96-well plates (obtained from AEC-Amersham P/L, Johannesburg, South Africa) were prepared by adding 80µl (60µl in the case of lymphocytes) of appropriate medium to each well followed by the addition of 100µl cell suspension as prepared previously (**see section 3.4.1, page 26**).
2. The cell suspensions were incubated at 37°C in a 5% CO_2 atmosphere for a period of 1 hour before the addition of 20µl of the experimental drugs at varying concentrations to each of the experimental wells. Lymphocytes to be stimulated, received 20µl PHA 5 minutes after the addition of the drug.
3. The untreated control groups received 20µl of the appropriate growth medium.
4. The final volume in each of the wells was 200µl.

5. Cell cultures were incubated for 7 days (3 days in the case of lymphocytes)
6. After the incubation period, 20µl of a MTT solution was added to the cells in each well [MTT was used at a concentration of 5mg/ml phosphate buffered saline (PBS), and PBS was used at a concentration of 9.23g/L purified water (MTT obtained from Sigma- Aldrich, Johannesburg, SA and PBS obtained from The Scientific group SA)].
7. Cell cultures were incubated for 4hrs at 37°C in a CO_2 incubator and then centrifuged at 200rpm (800g) for 10 minutes.
8. The supernatant was removed without disturbing the cell pellet and then washed by adding 150 µl PBS to the cells in each well.
9. The cells were left to dry where after 100 µl DMSO was added to the cells in each well to solubulise the formazan crystals. These crystals were formed when enzymes, that are only present in viable cells, reduced the yellow coloured MTT to purple coloured formazan.
10. Culture plates were put on a shaker for 1-2 hours.
11. A spectrophotometric plate reader was used to measure the absorbance of the DMSO/formazan solution at a wavelength of 570nm and a reference wavelength of 630nm.
12. The percentage survival of cells was determined.

3.5 EXPRESSION OF RESULTS

An average of three independent experiments was done. Each experiment included triplicate readings per concentration per experiment. Results were expressed as percentage of cell growth (i.e. % viability) compared to the untreated control ± standard error of mean (SEM). This was calculated with the formula:

% Viability = Mean Absorbance of Sample / Mean Absorbance of Control x 100

The obtained percentages of viability for the control and each of the experimental compounds were inserted in GRAPHPAD Prism 4 software© (**refer to Appendix A, number 2.1, c, page 132**). The IC_{50} (the concentration of the experimental compound

that induces 50% decrease in cell growth) was calculated with a cubic spline dose response curve, which extrapolated to the concentration at which 50% of cells survived. The curve was created with GRAPHPAD Prism 4 software© (**refer to Appendix A, number 2.1, c, page 132**). Statistical evaluation was done by a Wilcoxon signed-rank test at a confidence interval of 95% (**refer to Appendix A, 2.1, a-c, pages 131-132**). The difference was considered statistically significant at $p \leq 0.05$.

The *in vitro* tumour specificity of each compound was calculated with the formula:

Tumour specificity = Σ [IC_{50} (normal cells)] / Σ [IC_{50} (cancer cells)]

The resistance factor of the novel compounds was calculated with the formula:

Resistance factor (RF) = IC_{50} (A2780cis cells) / IC_{50} (A2780 cells)

The correlation between the octanol/water partition coefficients (PCs) and cytotoxic potencies of the tested compounds against various cancer cell lines and normal cell cultures, was calculated with the Spearman rank correlation coefficient test at a confidence interval of 95% by GRAPHPAD Prism 4 software© (**refer to Appendix A, number 2.2, a-c, pages 132-133**).

3.6 RESULTS

Cytotoxicity assays were conducted in order to determine the *in vitro* tumour specificities of the novel anticancer compounds with comparisons being made against the control compounds $[Au(dppe)_2]Cl$ and cisplatin. In order to answer the first aim, which relates to the identification of the four most promising compounds, through evaluation of tumour specificities, the cytotoxic potencies of all the experimental compounds were determined by using the HeLa, CoLo and Jurkat cancer cell lines and normal resting and PHA stimulated human lymphocytes. These results, recorded as the percentage of cell growth compared to the untreated control for the corresponding cell lines (± SEM), are presented graphically in **Figures 3.1- 3.9, pages 33-34 (**for HeLa cells**), 3.10-3.18, pages 35-36 (**for

CoLo cells**), 3.19-3.27, pages 37-38 (**for Jurkat cells**), 3.28-3.36, pages 39-40 (**for normal resting lymphocytes**),** and **3.37-3.45, pages 41-42 (**for normal PHA stimulated lymphocytes). Using this data, IC_{50} values were determined by extrapolating to the concentration at which 50% of cells survived. Furthermore, using the formula, $\Sigma[IC_{50}$ (normal cells)] / $\Sigma[IC_{50}$ (cancer cells)], the IC_{50} values for normal (resting and PHA stimulated human lymphocytes) and cancer cells (HeLa, CoLo and Jurkat cancer cell lines) were used to determine the *in vitro* tumour specificity. The IC_{50} values and tumour specificities of all the experimental compounds on the various cell cultures are summarized in **Table 3.1, page 43**. The obtained *in vitro* tumour specificities of the control compounds, $[Au(dppe)_2]Cl$ and cisplatin, are 1.4 and 30.5 at this point of the experiment respectively. The four novel compounds that exhibited the highest tumour specificities in comparison with the other novel compounds at this point, are UH 75.1, UH 107.1, UH 126.1 and UH 127.1, with tumour specificities of 5.6, 7.4, 26.5 and 24.1 respectively. The results indicated that these compounds are the four most promising experimental compounds. It is noteworthy that the tumour specificities of all four compounds are greater than that of $[Au(dppe)_2]Cl$. The tumour specificities of UH 126.1 and UH 127.1 are markedly higher than that of the other novel compounds and are close to the value obtained for cisplatin.

In order to answer the second aim, which relates to the final identification of the two most promising compounds, through evaluation of tumour specificities, the cytotoxic potencies of the four most promising experimental compounds, UH 75.1, UH 107.1, UH 126.1 and UH 127.1 were determined by additionally using the MCF-7, A2780 and A2780cis cancer lines and normal chicken embryo fibroblasts (**refer to section 3.2.1 and 3.2.2 of this Chapter, page 22**). These results, recorded as the percentage of cell growth compared to the untreated control for the corresponding cell lines (± SEM), are presented graphically in **Figures 3.46-3.51, page 44 (**for MCF-7 cells**), 3.52-3.57, page 45 (**for A2780 cells**), 3.58-3.63, page 46 (**for A2780cis cells**),** and **3.64-3.69, page 47 (**for chicken embryo fibroblasts**)** respectively. Using this data, IC_{50} values were determined by extrapolating to the concentration at which 50% of cells survived. Furthermore, using the

formula, Σ [IC_{50} (normal cells)] / Σ [IC_{50} (cancer cells)], the IC_{50} values for normal (resting and PHA stimulated human lymphocytes and chicken embryo fibroblasts) and cancer cells (HeLa, CoLo, Jurkat, MCF-7, A2780 and A2780cis cancer cell lines) were used to determine the final *in vitro* tumour specificities of the four most promising experimental compounds. In this part of the study, the cytotoxic effects of $[Au(dppe)_2]Cl$, cisplatin, UH 75.1, UH 107.1, UH 126.1 and UH 127.1 on all the tested cancer cell lines and normal cell cultures were evaluated. The IC_{50} values and tumour specificities of the selected four compounds on the various cell cultures are summarized in **Table 3.2, page 48**. The addition of the MCF-7, A2780 and A2780cis cancer cell lines and normal chicken embryo fibroblast to the previously tested cell cultures, resulted in altered tumour specificities of the tested compounds when compared to those obtained in the first aim of this experiment (**refer to Table 3.1, page 43)**. The final *in vitro* tumour specificities for $[Au(dppe)_2]Cl$ and cisplatin are 0.9 and 17.3 respectively. The results obtained at this point indicated that UH 126.1 and UH 127.1 are the two most promising novel compounds due to their high tumour specificities (9.4 and 8.7) in comparison with that of UH 75.1 (3.7) and UH 107.1 (4.5) (**Table 3.2, page 48**).

The third aim was to determine whether cross-resistance exists between cisplatin and the selected four most promising compounds. This was determined through evaluation of the resistance factors (RFs), which were calculated from the cytotoxic potencies of cisplatin, UH 75.1, UH 107.1, UH 126.1 and UH 127.1 against A2780 (cisplatin sensitive) and A2780cis (cisplatin resistant) cancer cell lines. IC_{50} values were determined by extrapolating to the concentration at which 50% of cells survived. The RFs were calculated by using the formula, IC_{50} (A2780cis cells) / IC_{50} (A2780 cells). The IC_{50} values and RFs of the compounds for the A2780 and A2780cis cell lines are summarized in **Table 3.3, page 49**. An increase in the RF indicates an increase in resistance. With RFs of 12.19, 13.80, 16.07, 12.50 and 6.47 for UH 75.1, UH 107.1, UH 126.1, UH 127.1 and $[Au(dppe)_2]Cl$ respectively it is evident that that cross-resistance does exist between cisplatin (RF=3.016) and these compounds. These results suggest that A2780cis cells are more resistant to the novel compounds than to cisplatin.

The fourth aim relates to the relationship between the octanol/water PCs and the cytotoxic potencies of all the tested compounds (UH 75.1, UH 86.2, UH 58.1, UH 145.1, UH 107.1, UH 126.1, UH 127.1, $[Au(dppe)_2]Cl$) against various human cancer cell lines (HeLa cells, CoLo cells, Jurkat cells) and normal cell cultures (human resting and PHA stimulated lymphocytes). IC_{50} values were determined by extrapolating to the concentration at which 50% of cells survived (**refer to Table 3.1, page 43**). The octanol/water PCs were calculated previously (**refer to Chapter 2, Table 2.1, page 18)**. Using this data, the Spearman correlation coefficient (r_S), was calculated with specialized software (GRAPHPAD Prism 4 software©) by inserting the octanol/water PCs as the independent variable (x-axis) and the IC_{50} values as the dependant variable (y-axis). An r_S value of "+1" represents a perfect positive correlation (both variables increase/decrease proportionately), an r_S value of "0" indicates that no correlation is present, and an r_S value of "–1" represents a perfect negative correlation (one variable increases as the other decreases or *vice versa*). The respective r_S values are summarised in **Table 3.4, page 50**. According to the results of this study, no significant correlations were seen between the octanol/water PCs and cytotoxic potencies of the compounds against HeLa cells, CoLo cells, normal resting and PHA stimulated lymphocytes. In contrast to this, a significant negative correlation between the octanol/water PC and cytotoxicity against Jurkat cells were displayed. Pertaining to this cancer cell line, it was detected that an increase in the lipophilicity of the compounds was associated with a decrease in IC_{50} values (i.e. an increase in cytotoxic potency).

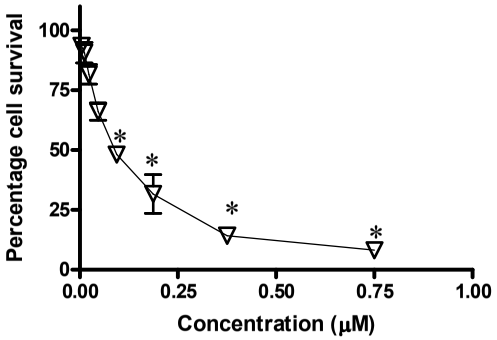

Figure 3.1 Effects of UH 86.2 on the growth of HeLa[1]

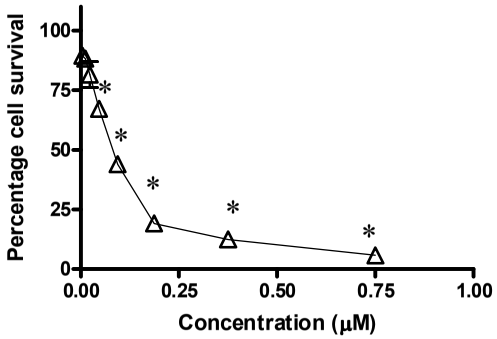

Figure 3.2 Effects of UH 75.1 on the growth of HeLa[1]

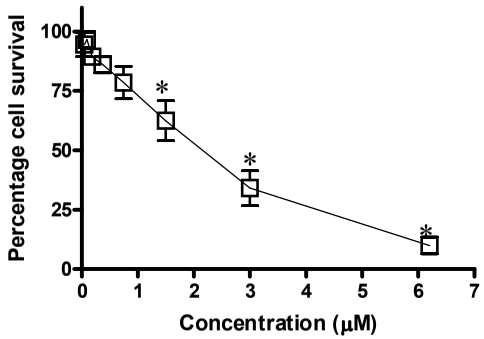

Figure 3.3 Effects of UH 58.1 on the growth of HeLa[1]

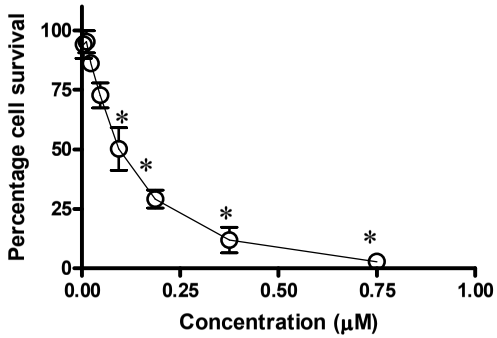

Figure 3.4 Effects of UH 145.1 on the growth of HeLa[1]

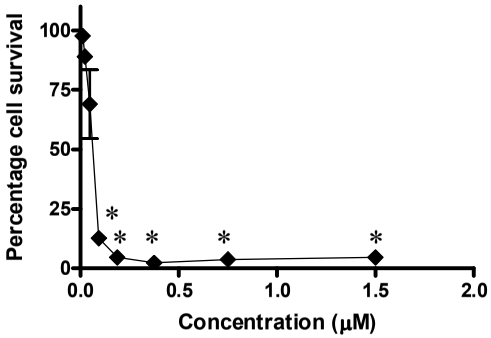

Figure 3.5 Effects of UH 107.1 on the growth of HeLa[1]

* $p \leq 0.05$ when compared to the untreated control

1. Each endpoint represents the mean of three different experiments ± standard error of mean (SEM)

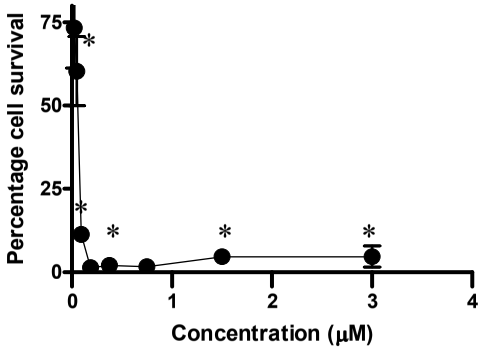

Figure 3.6 Effects of UH 126.1 on the growth of HeLa[1]

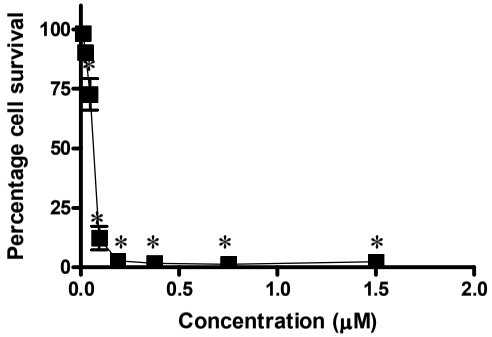

Figure 3.7 Effects of UH 127.1 on the growth of HeLa[1]

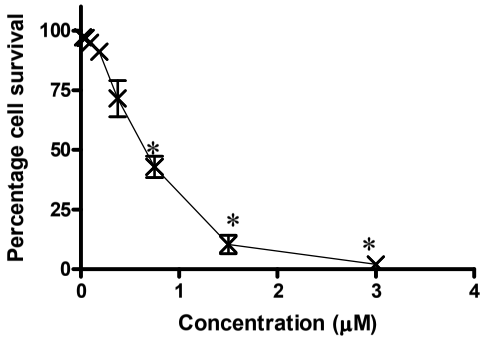

Figure 3.8 Effects of UH $[Au(dppe)_2]Cl$ on the growth of HeLa[1]

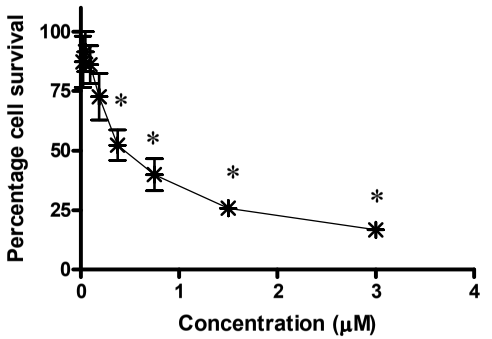

Figure 3.9 Effects of UH cisplatin on the growth of HeLa[1]

* $p \leq 0.05$ when compared to the untreated control

1. Each endpoint represents the mean of three different experiments ± standard error of mean (SEM)

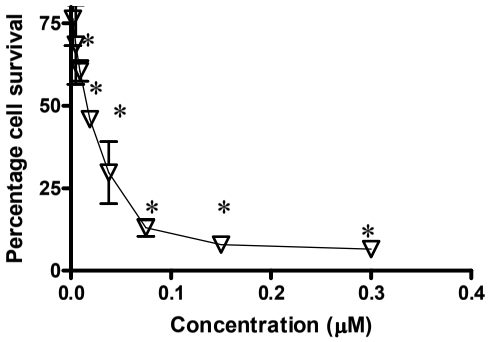

Figure 3.10 Effects of UH 86.2 on the growth of CoLo[1]

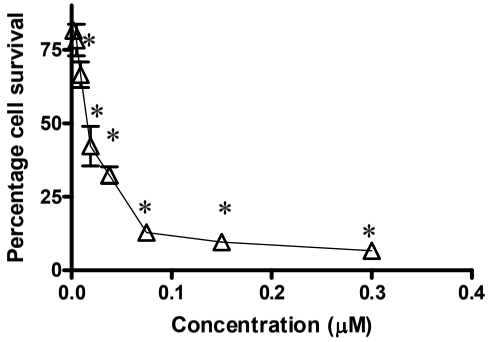

Figure 3.11 Effects of UH 75.1 on the growth of CoLo [1]

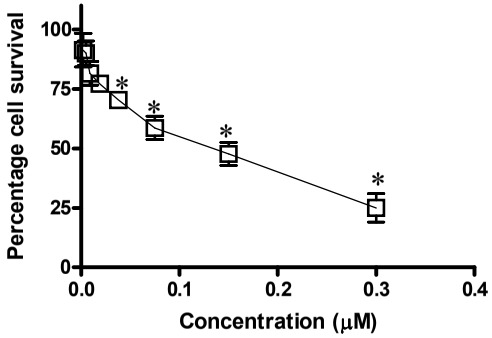

Figure 3.12 Effects of UH 58.1 on the growth of CoLo [1]

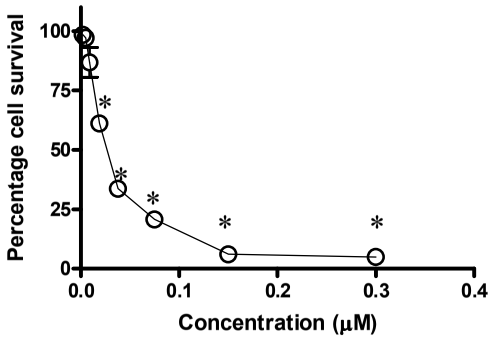

Figure 3.13 Effects of UH 145.1 on the growth of CoLo [1]

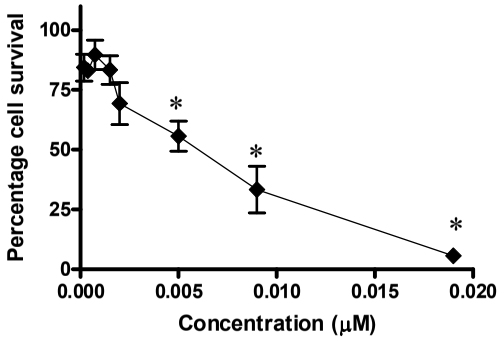

Figure 3.14 Effects of UH 107.1 on the growth of CoLo [1]

* $p \leq 0.05$ when compared to the untreated control

1. Each endpoint represents the mean of three different experiments ± standard error of mean (SEM)

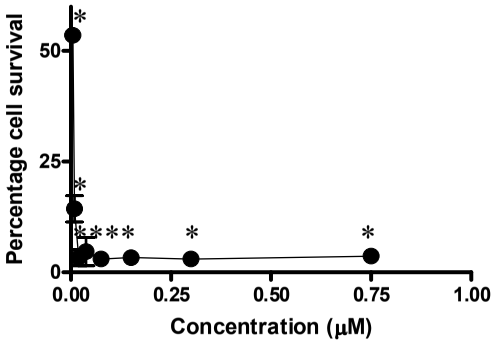

Figure 3.15 Effects of UH 126.1 on the growth of CoLo[1]

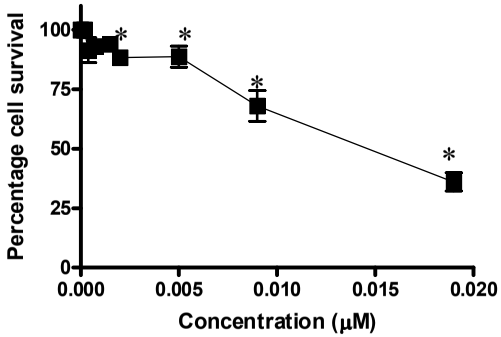

Figure 3.16 Effects of UH 127.1 on the growth of CoLo[1]

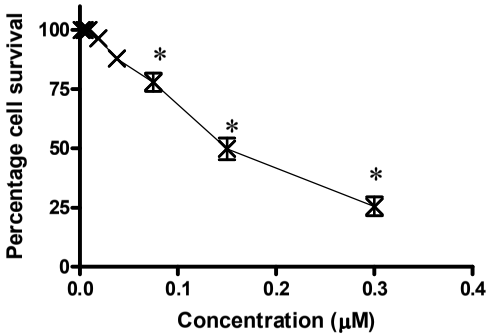

Figure 3.17 Effects of $[Au(dppe)_2]Cl$ on the growth of CoLo[1]

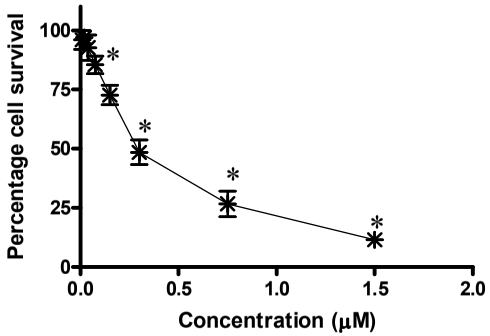

Figure 3.18 Effects of cisplatin on the growth of CoLo[1]

* $p \leq 0.05$ when compared to the untreated control

1. Each endpoint represents the mean of three different experiments ± standard error of mean (SEM)

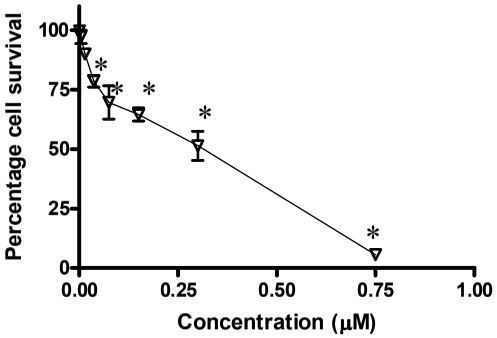

Figure 3.19 Effects of UH 86.2 on the growth of Jurkat[1]

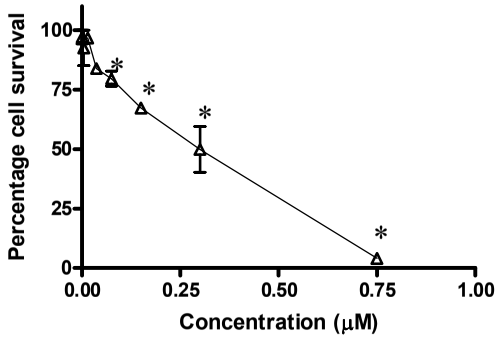

Figure 3.20 Effects of UH 75.1 on the growth of Jurkat [1]

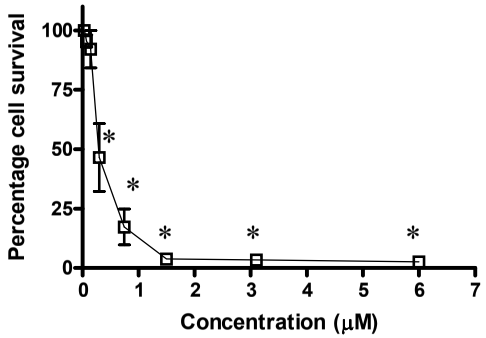

Figure 3.21 Effects of UH 58.1 on the growth of Jurkat [1]

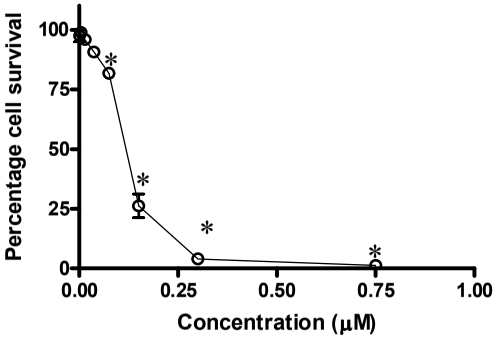

Figure 3.22 Effects of UH 145.1 on the growth of Jurkat [1]

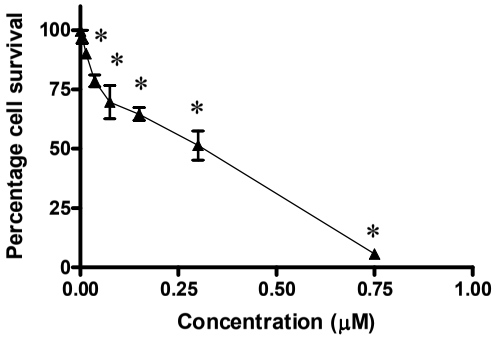

Figure 3.23 Effects of UH 107.1 on the growth of Jurkat [1]

* $p \leq 0.05$ when compared to the untreated control

1. Each endpoint represents the mean of three different experiments ± standard error of mean (SEM)

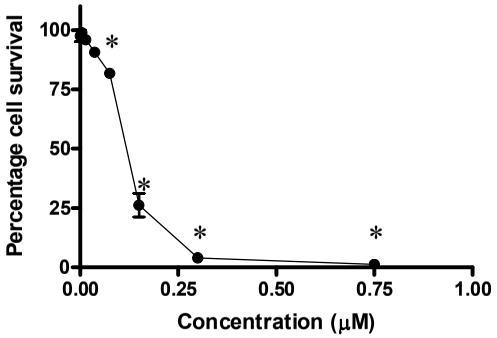

Figure 3.24 Effects of UH 126.1 on the growth of Jurkat[1]

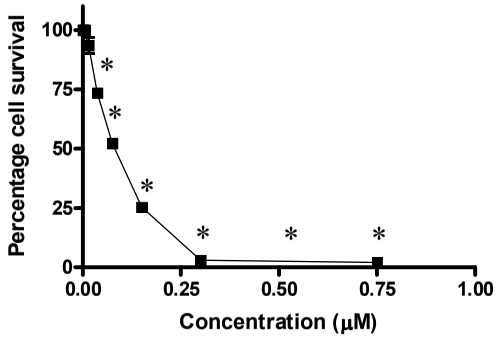

Figure 3.25 Effects of UH 127.1 on the growth of Jurkat[1]

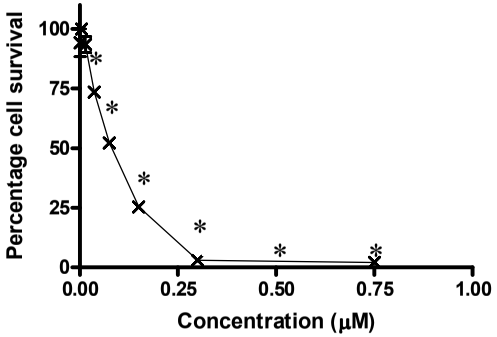

Figure 3.26 Effects of $[Au(dppe)_2]Cl$ on the growth of Jurkat[1]

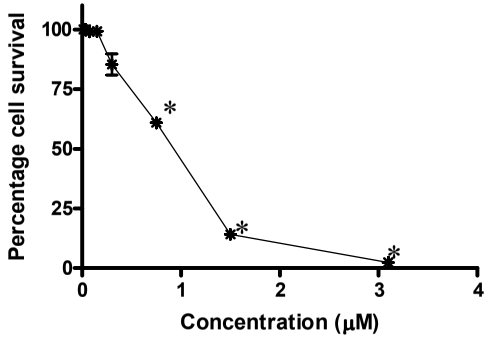

Figure 3.27 Effects of cisplatin on the growth of Jurkat[1]

* $p \leq 0.05$ when compared to the untreated control

1. Each endpoint represents the mean of three different experiments ± standard error of mean (SEM)

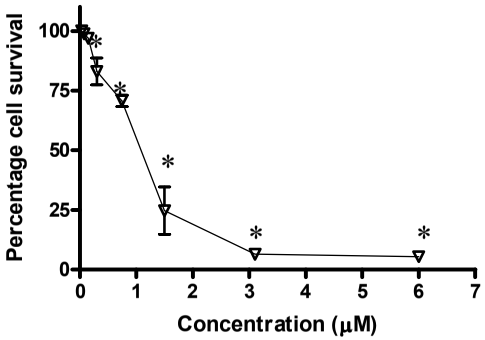

Figure 3.28 Effects of UH 86.2 on the growth of resting lymphocytes [1]

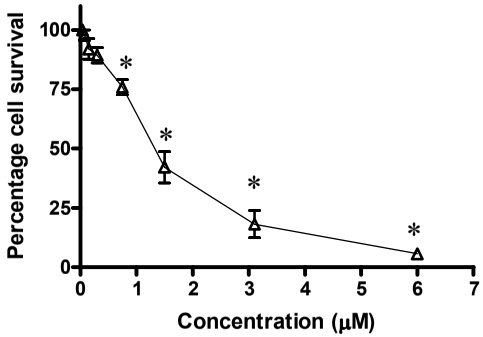

Figure 3.29 Effects of UH 75.1 on the growth of resting lymphocytes [1]

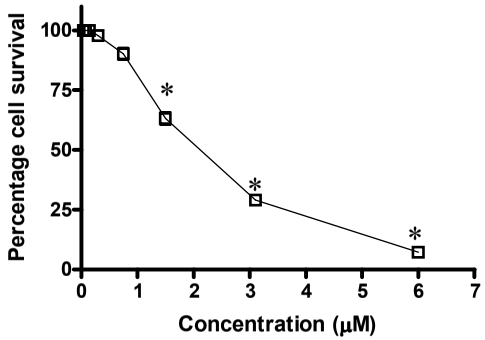

Figure 3.30 Effects of UH 58.1 on the growth of resting lymphocytes [1]

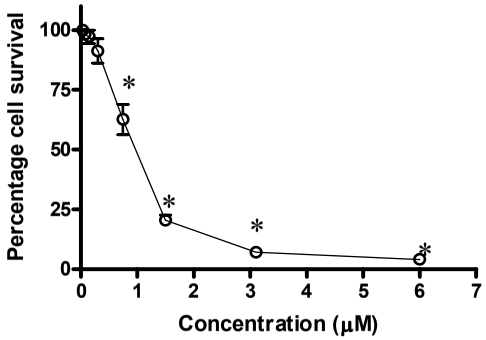

Figure 3.31 Effects of UH 145.1 on the growth of resting lymphocytes [1]

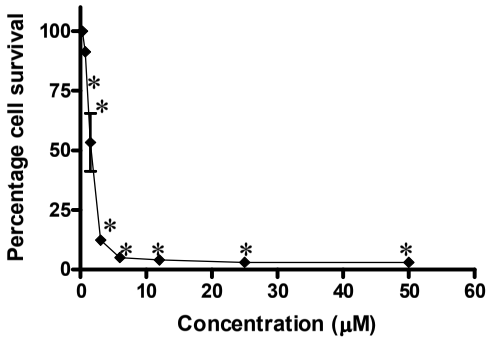

Figure 3.32 Effects of UH 107.1 on the growth of resting lymphocytes [1]

* $p \leq 0.05$ when compared to the untreated control

1. Each endpoint represents the mean of three different experiments ± standard error of mean (SEM)

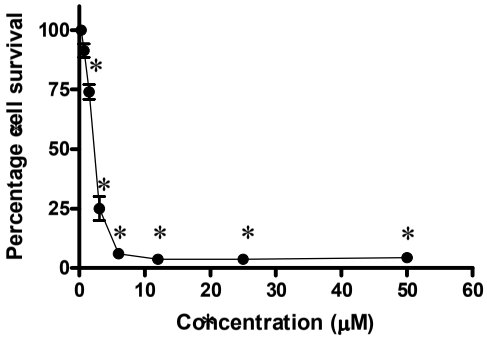

Figure 3.33 Effects of UH 126.1 on the growth of resting lymphocytes [1]

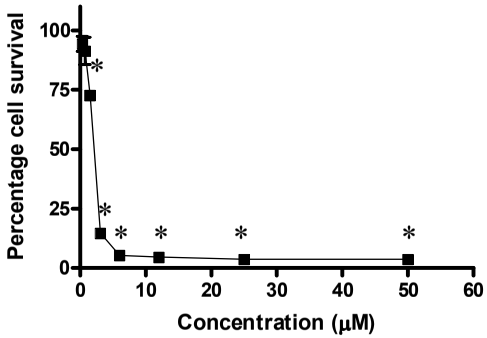

Figure 3.34 Effects of UH 127.1 on the growth of resting lymphocytes [1]

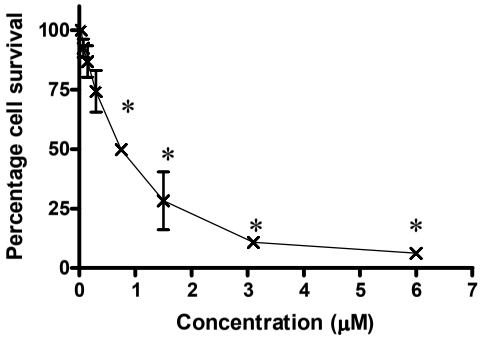

Figure 3.35 Effects of $[Au(dppe)_2]Cl$ on the growth of resting lymphocytes [1]

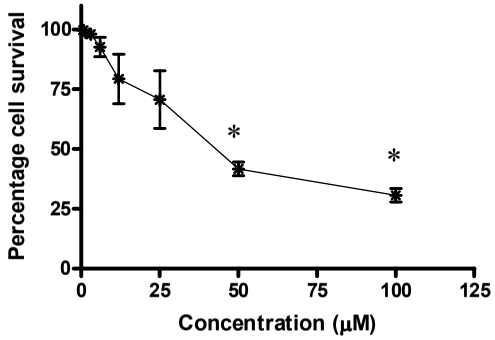

Figure 3.36 Effects of cisplatin on the growth of resting lymphocytes [1]

* $p \leq 0.05$ when compared to the untreated control

1. Each endpoint represents the mean of three different experiments ± standard error of mean (SEM)

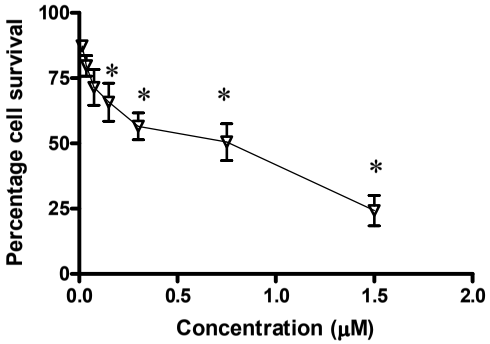

Figure 3.37 Effects of UH 86.2 on the growth of PHA stimulated lymphocytes [1]

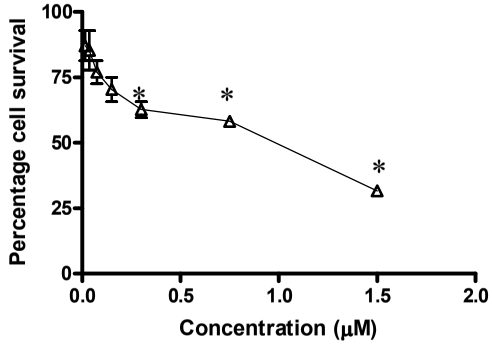

Figure 3.38 Effects of UH 75.1 on the growth of PHA stimulated lymphocytes [1]

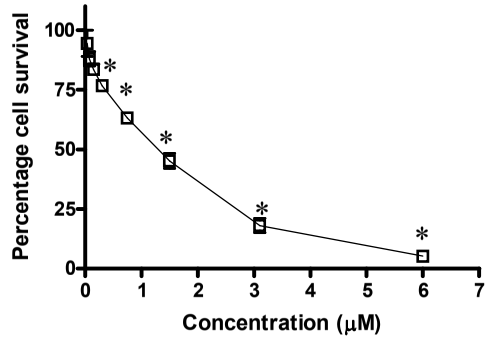

Figure 3.39 Effects of UH 58.1 on the growth of PHA stimulated lymphocytes [1]

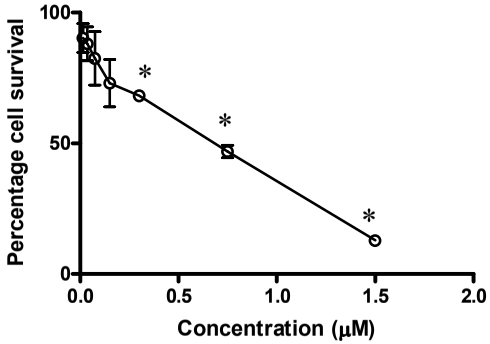

Figure 3.40 Effects of UH 145.1 on the growth of PHA stimulated lymphocytes [1]

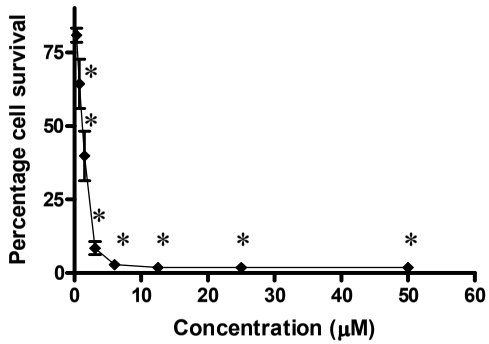

Figure 3.41 Effects of UH 107.1 on the growth of PHA stimulated lymphocytes [1]

* $p \leq 0.05$ when compared to the untreated control

1. Each endpoint represents the mean of three different experiments ± standard error of mean (SEM)

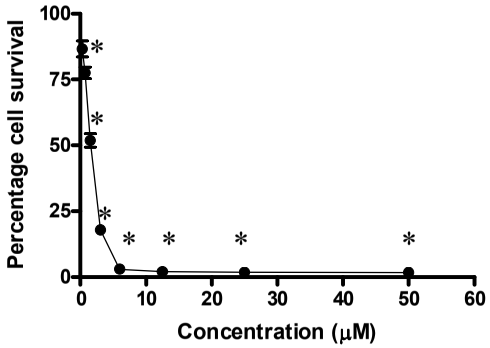

Figure 3.42 Effects of UH 126.1 on the growth of PHA stimulated lymphocytes [1]

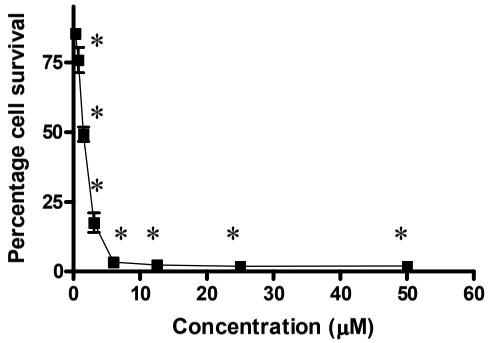

Figure 3.43 Effects of UH 127.1 on the growth of PHA stimulated lymphocytes [1]

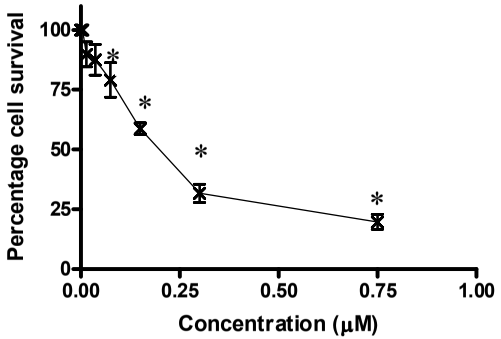

Figure 3.44 Effects of $[Au(dppe)_2]Cl$ on the growth of PHA stimulated lymphocytes [1]

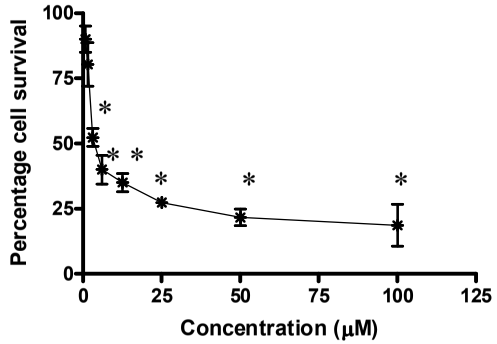

Figure 3.45 Effects of cisplatin on the growth of PHA stimulated lymphocytes [1]

* $p \leq 0.05$ when compared to the untreated control

1. Each endpoint represents the mean of three different experiments ± standard error of mean (SEM)

Table 3.1. Mean drug concentration (μM) causing 50% cell death (IC_{50}) and the calculated tumour specificities of various cell lines and cell cultures after treatment with seven novel compounds, $[Au(dppe)_2]Cl$ and cisplatin

Cells	HeLa	Jurkat	CoLo	Human Lymphocytes (resting)	Human Lymphocytes (PHA stimulated)	Tumour specificity
Compounds	**IC_{50} (μM) ± SEM of cells after treatment with each of the experimental compounds[1]**					
UH 75.1	0.081 ± 0.000	0.344 ± 0.115	0.016 ± 0.003	1.390 ± 0.178	1.097 ± 0.12	**5.6**
UH 86.2	0.092 ± 0.010	0.376 ± 0.100	0.015 ± 0.001	1.172 ± 0.047	0.715 ± 0.295	**3.9**
UH 58.1	2.178 ± 0.398	0.322 ± 0.055	0.138 ± 0.037	1.936 ± 0.123	1.330 ± 0.122	**1.2**
UH 145.1	0.098 ± 0.020	0.219 ± 0.000	0.025 ± 0.001	0.846 ± 0.066	0.594 ± 0.035	**4.2**
UH 107.1	0.063 ± 0.010	0.325 ± 0.060	0.005 ± 0.002	1.708 ± 0.218	1.204 ± 0.244	**7.4**
UH 126.1	0.050 ± 0.011	0.119 ± 0.010	0.005 ± 0.000	3.052 ± 0.885	1.559 ± 0.076	**26.5**
UH 127.1	0.065 ± 0.005	0.075 ± 0.030	0.007 ± 0.000	2.095 ± 0.010	1.454 ± 0.085	**24.1**
$[Au(dppe)_2]Cl$	0.603 ± 0.084	0.081 ± 0.003	0.156 ± 0.013	1.007 ± 0.300	0.192 ± 0.006	**1.4**
Cisplatin	0.413 ± 0.098	0.962 ± 0.061	0.312 ± 0.037	39.775 ± 4.888	11.650 ± 0.245	**30.5**

1. Average of three independent experiments

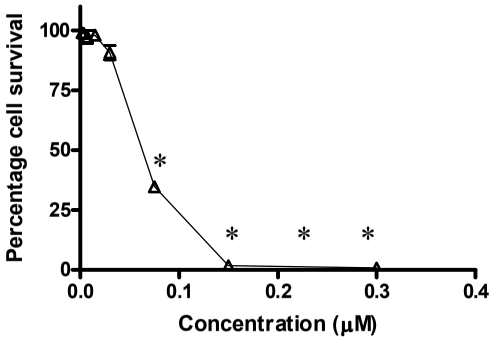

Figure 3.46 Effects of UH 75.1 on the growth of MCF-7[1]

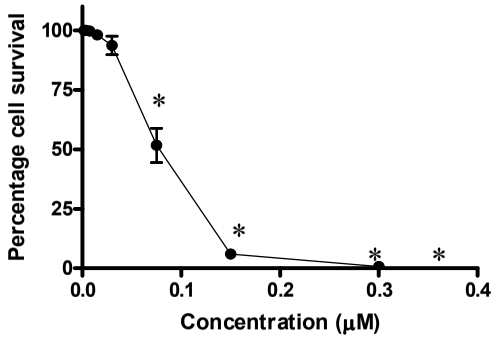

Figure 3.47 Effects of UH 107.1 on the growth of MCF-7[1]

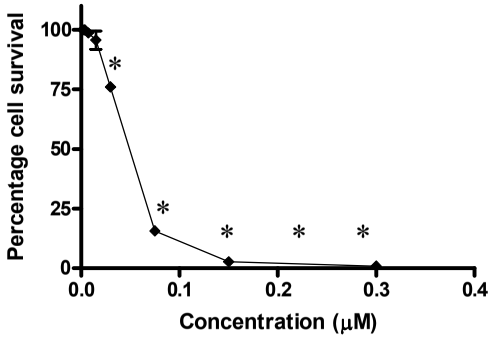

Figure 3.48 Effects of UH 126.1 on the growth of MCF-7[1]

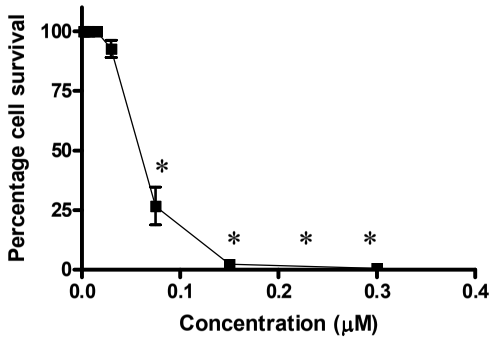

Figure 3.49 Effects of UH 127.1 on the growth of MCF-7[1]

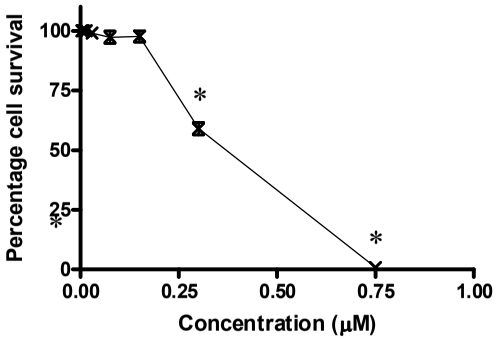

Figure 3.50 Effects of UH $[Au(dppe)_2]Cl$ on the growth of MCF-7[1]

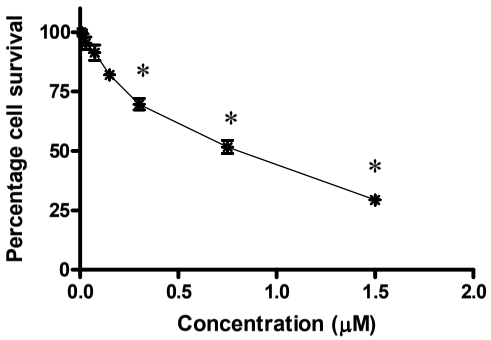

Figure 3.51 Effects of cisplatin on the growth of MCF-7[1]

* $p \leq 0.05$ when compared to the untreated control

1. Each endpoint represents the mean of three different experiments ± standard error of mean (SEM)

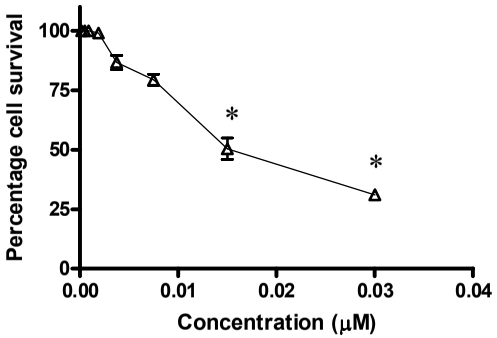

Figure 3.52 Effects of UH 75.1 on the growth of A2780[1]

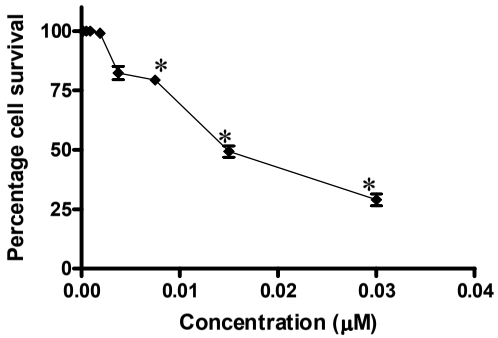

Figure 3.53 Effects of UH 107.1 on the growth of A2780[1]

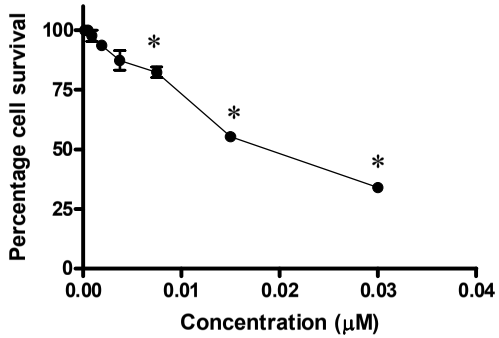

Figure 3.54 Effects of UH 126.1 on the growth of A2780[1]

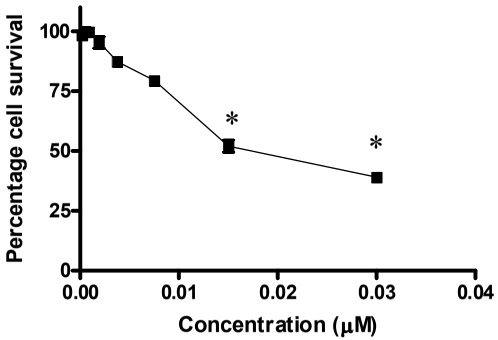

Figure 3.55 Effects of UH 127.1 on the growth of A2780[1]

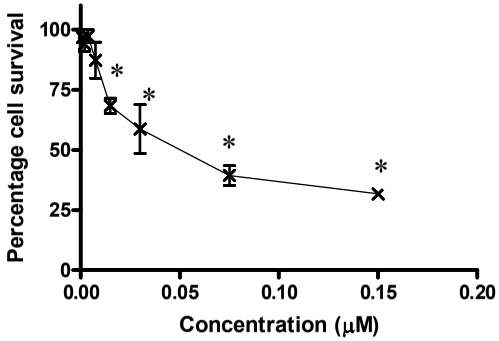

Figure 3.56 Effects of UH $[Au(dppe)_2]Cl$ on the growth of A2780[1]

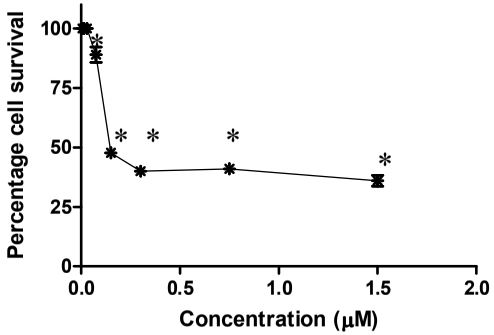

Figure 3.57 Effects of cisplatin on the growth of A2780[1]

* $p \leq 0.05$ when compared to the untreated control

1. Each endpoint represents the mean of three different experiments ± standard error of mean (SEM)

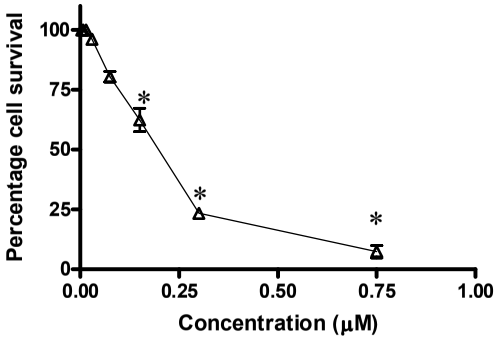

Figure 3.58 Effects of UH 75.1 on the growth of A2780cis[1]

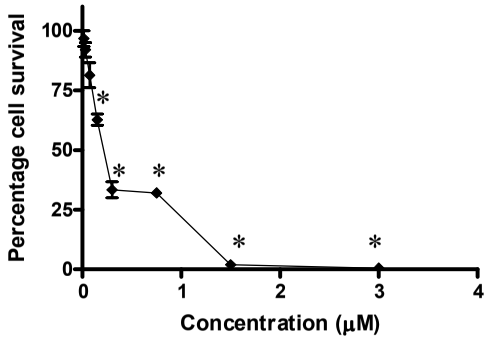

Figure 3.59 Effects of UH 107.1 on the growth of A2780cis[1]

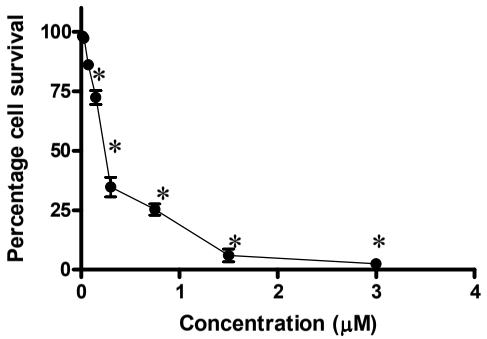

Figure 3.60 Effects of UH 126.1 on the growth of A2780cis[1]

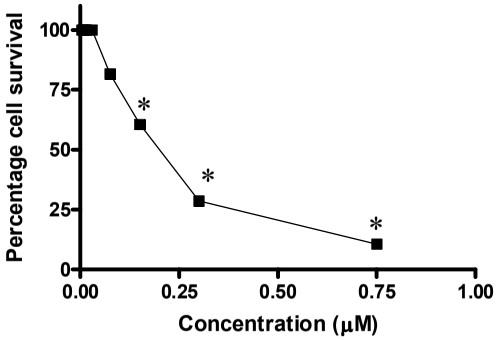

Figure 3.61 Effects of UH 127.1 on the growth of A2780cis[1]

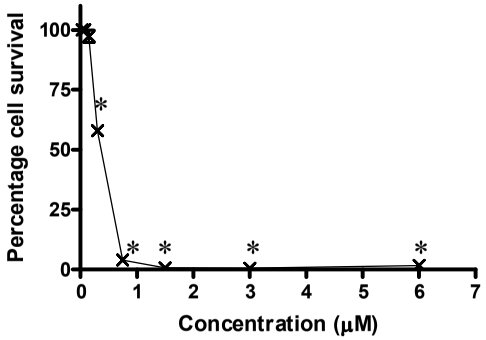

Figure 3.62 Effects of UH $[Au(dppe)_2]Cl$ on the growth of A2780cis[1]

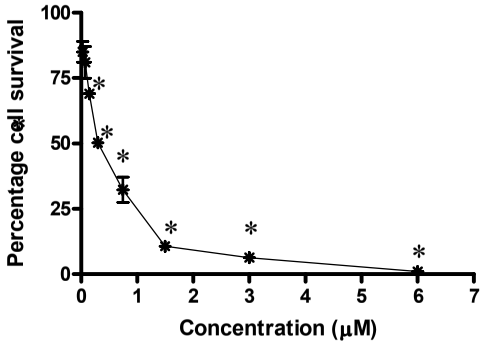

Figure 3.63 Effects of cisplatin on the growth of A2780cis[1]

* $p \leq 0.05$ when compared to the untreated control

1. Each endpoint represents the mean of three different experiments ± standard error of mean (SEM)

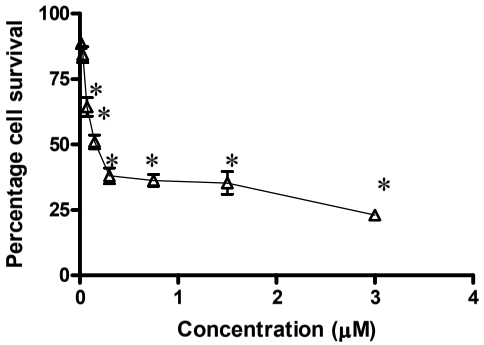

Figure 3.64 Effects of UH 75.1 on the growth of fibroblasts[1]

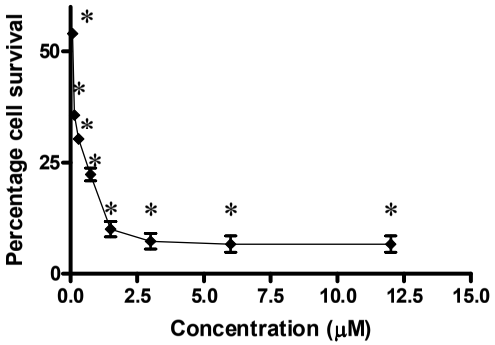

Figure 3.65 Effects of UH 107.1 on the growth of fibroblasts[1]

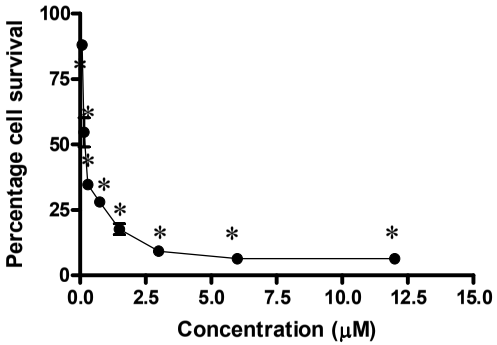

Figure 3.66 Effects of UH 126.1 on the growth of fibroblasts[1]

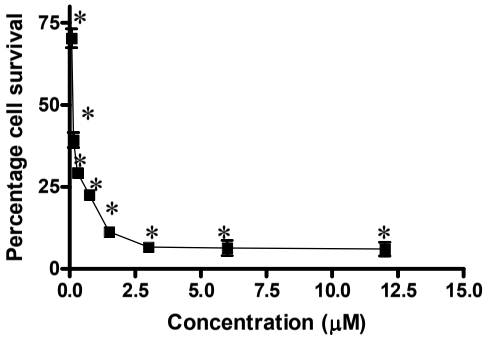

Figure 3.67 Effects of UH 127.1 on the growth of Fibroblasts[1]

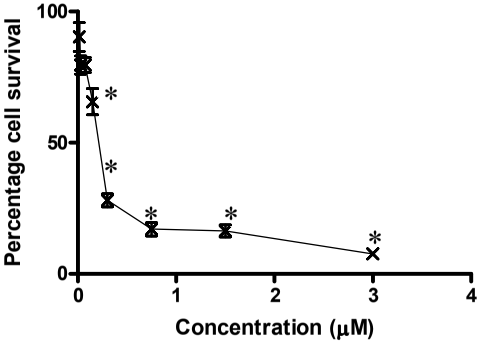

Figure 3.68 Effects of UH $[Au(dppe)_2]Cl$ on the growth of fibroblasts[1]

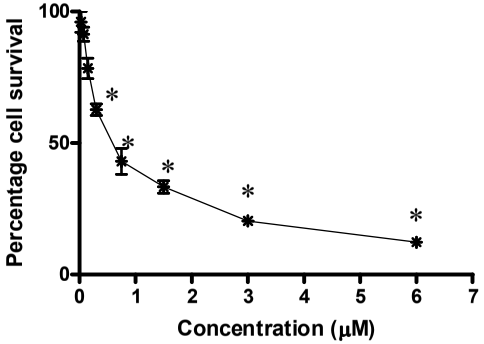

Figure 3.69 Effects of cisplatin on the growth of fibroblasts[1]

* $p \leq 0.05$ when compared to the untreated control

1. Each endpoint represents the mean of three different experiments ± standard error of mean (SEM)

Table 3.2. Mean drug concentration (μM) causing 50% cell death (IC_{50}) and the calculated tumour specificities of various cell lines and cell cultures after treatment with four novel compounds, $[Au(dppe)_2]Cl$ and cisplatin

Cells	HeLa	Jurkat	CoLo	MCF7	A2780	A2780cis	Chicken embryo Fibroblasts	Human Lymphocytes (resting)	Human Lymphocytes (PHA stimulated)	Tumour specificity
Compounds	**IC_{50} (μM) ± SEM of cells after treatment with each of the experimental compounds[1]**									
UH 75.1	0.081 ± 0.000	0.344 ± 0.115	0.016 ± 0.003	0.062 ± 0.002	0.016 ± 0.002	0.195 ± 0.016	0.170 ± 0.028	1.390 ± 0.178	1.097 ± 0.120	**3.7**
UH 107.1	0.063 ± 0.010	0.325 ± 0.060	0.007 ± 0.002	0.047 ± 0.002	0.015 ± 0.001	0.207 ± 0.006	0.085 ± 0.002	1.708 ± 0.218	1.204 ± 0.244	**4.5**
UH 126.1	0.050 ± 0.011	0.119 ± 0.010	0.005 ± 0.000	0.077 ± 0.008	0.015 ± 0.001	0.241 ± 0.013	0.169 ± 0.019	3.052 ± 0.885	1.559 ± 0.076	**9.4**
UH 127.1	0.065 ± 0.005	0.075 ± 0.030	0.007 ± 0.000	0.060 ± 0.004	0.016 ± 0.001	0.200 ± 0.003	0.121 ± 0.007	2.095 ± 0.010	1.454 ± 0.085	**8.7**
$[Au(dppe)_2]Cl$	0.603 ± 0.084	0.081 ± 0.003	0.156 ± 0.013	0.333 ± 0.011	0.051 ± 0.013	0.330 ± 0.004	0.200 ± 0.017	1.007 ± 0.300	0.192 ± 0.006	**0.9**
Cisplatin	0.413 ± 0.098	0.962 ± 0.061	0.312 ± 0.037	0.824 ± 0.010	0.123 ± 0.030	0.371 ± 0.007	0.503 ± 0.070	39.775 ± 4.888	11.650 ± 0.245	**17.3**

1. Average of three independent experiments

Table 3.3. Mean drug concentration (µM) causing 50% cell death (IC_{50}) and the calculated resistance factors (RFs) of the A2780 and A2780cis cell lines after treatment with four novel compounds, $[Au(dppe)_2]Cl$ and cisplatin

Cells	**A2780**	**A2780cis**	**Resistance factor (RF)**
Compounds	**IC_{50} (µM) ± SEM of cells after treatment with each of the experimental compounds[1]**		
UH 75.1	0.016 ± 0.002	0.195 ± 0.016	**12.19**
UH 107.1	0.015 ± 0.001	0.207 ± 0.006	**13.80**
UH 126.1	0.015 ± 0.001	0.241 ± 0.013	**16.07**
UH 127.1	0.016 ± 0.001	0.200 ± 0.003	**12.5**
$[Au(dppe)_2]Cl$	0.051 ± 0.013	0.330 ± 0.004	**6.47**
Cisplatin	0.123 ± 0.030	0.371 ± 0.007	**3.016**

1. Average of three independent experiments

Table 3.4. Spearman correlation coefficient depicting the relationship between the octanol/water partition coefficients and the cytotoxic potencies of all the tested compounds (UH 75.1, UH 86.2, UH 58.1, UH 145.1, UH 107.1, UH 126.1, UH 127.1, [Au(dppe)2]Cl and cisplatin) against HeLa cells, CoLo cells, Jurkat cells, resting lymphocytes and PHA stimulated lymphocytes.

Spearman correlation coefficient depicting the relationship between the octanol/water partition coefficients and the cytotoxic potencies of all the tested compounds against various cancer cell lines and normal cell cultures

	HeLa	**CoLo**	**Jurkat**	**Human Lymphocytes (resting)**	**Human Lymphocytes (PHA stimulated)**
Spearman r	-0.35	-0.44	-0.75	-0.233	-0.30
r2	0.12	0.20	0.56	0.05	0.09
P value	0.18	0.11	0.01	0.55	0.44
Significant correlation	No	No	Yes	No	No

3.7 DISCUSSION

In order to evaluate the anticancer potency and selectivity of UH 86.2, UH 75.1, UH 58.1, UH 145.1, UH 107.1, UH 126.1 and UH 127.1, cytotoxicity assays were performed.

The lipophilic cation, $[Au(dppe)_2]Cl$, was found to be a potent non-selective cytotoxicant, as has been previously described (Hoke *et al*. 1988). Although all cells displayed a general sensitivity to $[Au(dppe)_2]Cl$, it exhibited the lowest tumour specificity in comparison to the other compounds tested in this study.

The selectivity of cisplatin has been described elsewhere (Highley *et al.* 2000), and was also evident in the present study in which cisplatin exhibited the highest *in vitro* tumour specificity when compared to the other experimental compounds.

The anticancer activity of the novel compounds was compared to $[Au(dppe)_2]Cl$ and cisplatin. All the novel compounds displayed significant cytotoxicity against all cancer cells at concentrations <0.5μM. Furthermore, all the novel compounds exhibited better *in vitro* selectivity than $[Au(dppe)_2]Cl$. All seven novel compounds were tested initially on three cancer cell lines (HeLa cells, CoLo cells and Jurkat cells) and two normal cell cultures (resting and PHA stimulated lymphocytes). The four novel compounds that displayed the best cytotoxicity/selectivity profiles based on these results, were UH 75.1, UH 107.1, UH 126.1 and UH 127.1. Further testing, which included additional cell cultures (MCF-7 cells, A2780 cells, A2780cis cells and chicken embryo fibroblasts), were conducted with these four compounds. According to these results, the two azole-containing compounds, UH 126.1 and UH 127.1 exhibited the highest tumour specificities in comparison with UH 75.1 and UH 107.1. It was concluded that UH 126.1 and UH 127.1 are the two most promising novel compounds.

Pertaining to the cross-resistance that was studied in this experiment, it is noteworthy that the A2780cis (cisplatin-resistant ovarian cancer) cells were more resistant to the novel compounds and $[Au(dppe)_2]Cl$, than to cisplatin.

This increased resistance, might be an indication that overlapping mechanisms of action are at play, although differences in the transport mechanisms may also contribute to this observation. This may in part be attributed to the rate of efflux of the experimental compounds from the cells, or alternatively the size of the novel compounds could also contribute to their recognition as xenobiotics. Another possibility is that the novel compounds might react with cellular thiols (Berners-Price *et al*. 1988), which may influence the resistance of cells (Heffeter *et al.* 2008), although the exact mechanism of resistance against the experimental compounds is yet to be determined.

Pertaining to the relationship between the octanol/water PCs and the cytotoxic effects of anticancer compounds, it has been found that a correlation between lipophilicity and the selectivity exists for lipophilic cations of type $[Au(p\text{-}p)_2]+$ (Berners-Price *et al.* 1999). The compounds investigated in this study are, however, neutral, linear bridged di-gold species. The aim was therefore to determine whether such a correlation is echoed with the evaluation of these novel compounds. According to the results, no significant correlations were seen between the octanol/water PCs and cytotoxic potencies of the compounds against HeLa cells, CoLo cells, normal resting and PHA stimulated lymphocytes. In contrast to this, a significant negative correlation between the octanol/water PC and cytotoxicity against Jurkat cells were displayed. Pertaining to this cancer line, an increase in the lipophilicity of the compounds is associated with a decrease in IC_{50} values (i.e. increased cytotoxic potency). The reason for the exception of this cell line is not yet known.

The two most promising novel gold-containing compounds with azole bases (UH 126.1 and UH 127.1), were used in further investigations in this study, which aimed to provide insight into a possible mechanism by which cytotoxicity could be induced, as well as an *in vivo* toxicity study.

CHAPTER FOUR

ASSESSMENT OF DNA DAMAGE VIA APTOSIS OR NECROSIS

4.1 INTRODUCTION

In general, the aim of anticancer agents is to induce cancer cell death. The two distinct types of cell death *in vitro,* are apoptosis and necrosis (Searle *et al*. 1982). Apoptosis is described as a controlled form of cell death resulting from an activated intrinsic mechanism (Somosy 2000). Necrosis is a traumatic, but passive form of cell death resulting from extrinsic damage to the cell (Somosy 2000). Characteristics of apoptosis include cell shrinkage, dehydration, a fragmented nucleus, irregular bulging of the plasma membrane (cytoplasmic blebbing), chromatin condensation, and apoptotic bodies, which are then phagocytised by macrophages (Kerr *et al*. 1987; Kiechle *et al*. 2002). The characteristics of necrosis, however, are failing ion pumps, cell swelling and lysis of the cell with the release of inflammatory mediators (Searle *et al*. 1982).

There are two distinct pathways for apoptotic signal transduction: (i) extrinsic/receptor-linked apoptosis or (ii) intrinsic/mitochondria-mediated apoptosis (Kiechle *et al*. 1998; Mullauer *et al*. 2001; Reed 2000; Zimmerman *et al*. 2002).

The extrinsic/receptor-linked apoptotic pathway (left side of **Figure 4.1, page 54**), is induced by members of the death-receptor family, including tumour necrosis factor (TNF) receptor I and member 6 (Fas-gene) of the TNF family. Upon binding of the Fas-gene ligand to the Fas-receptor, receptor clusters are formed, which lead to the formation of a death-inducing signalling complex (Bredesen, 2000; Hengartner, 2000). Multiple procaspase-8 molecules are recruited via the adaptor molecule FADD (Fas-associated death domain protein), with subsequent activation of caspase-8, followed by caspase-3 activation (caspases are proteases that mediate apoptosis). Caspase-3 activation results in the final apoptotic events, dismantling and removal of the cell by macrophages (Ker *et al.* 1987; Hengartner, 2000).

The intrinsic/mitochondria-mediated pathway (right side of **Figure 4.1, page 54**) is initiated upon accumulation of a cytotoxic compound within the mitochondrial membranes. Via dephosphorylation, proteolysis or other mechanisms, a pro-apoptotic member of the Bcl-2 family is activated. This is followed by the release of molecules from the mitochondria, mainly including cytochrome c, which associates with apoptotic protease activating factor 1 (Apaf-1) and procaspase-9 to form the apoptosome. This in turn, leads to the activation of the executioner caspases (caspases 3,6,7). Caspase-3 activation and activity is antagonized by the IAP (inhibitor of apoptosis) proteins, which are in turn antagonized by the Smac (second mitochondria-derived activator of caspase) protein, which is released from mitochondria. Activation of the executioner caspases is followed by the final apoptotic events: proteins involved in cytoskeletal functions are degraded followed by cell shrinkage and the collapse of the nucleus and the cell (Hengartner, 2000; Hill *et al*. 2003; Huppertz *et al*. 1999).

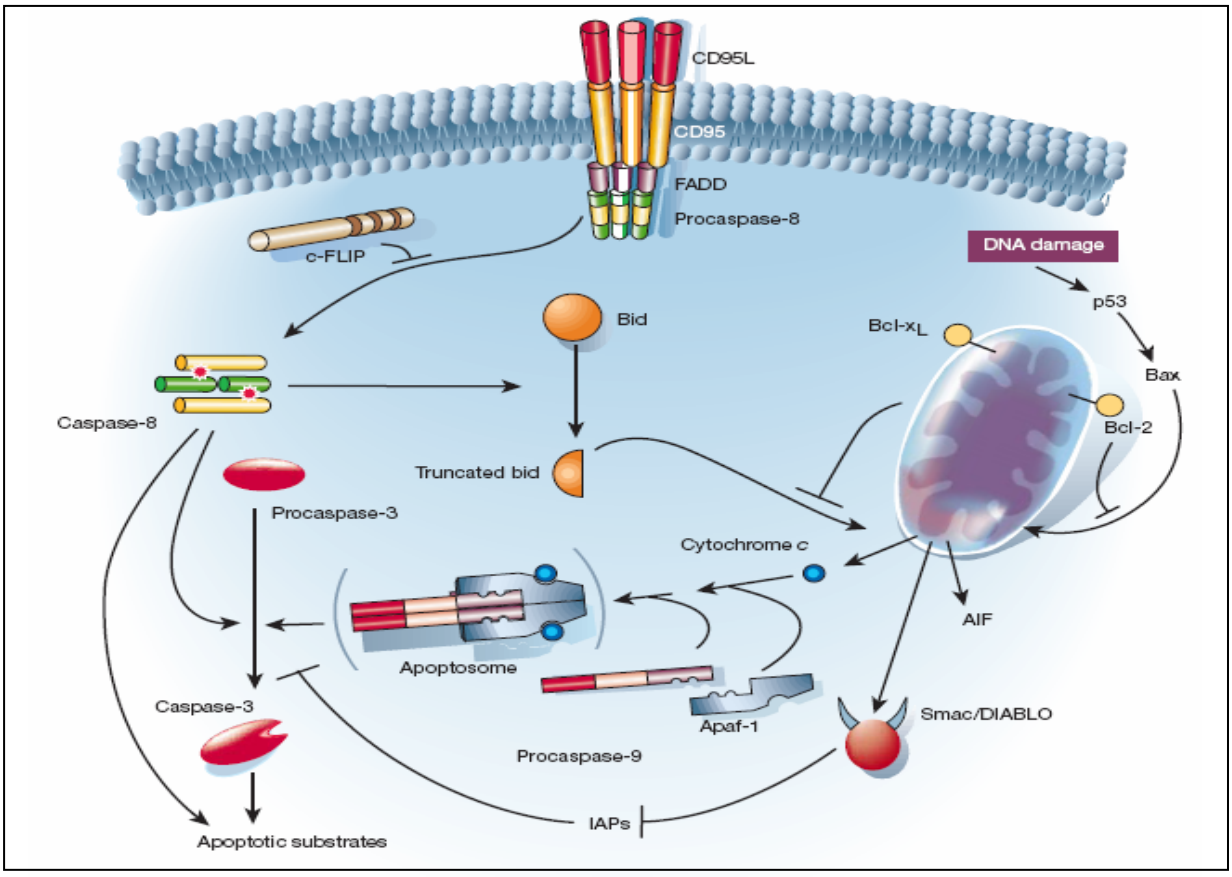

Figure 4.1. Two major apoptotic pathways in mammalian cells (Hengartner, 2000).

A flow cytometric method is widely used to determine whether the experimental compounds induce their cytotoxic effects in Jurkat cells via the apoptotic or necrotic pathway (Michie *et al*. 2003). Two stains, Annexin-V and propidium iodide (PI), are able to bind to specified markers of apoptosis (phosphatidylserine) or necrosis (DNA) respectively. The binding of these stains is quantified via flow cytometry, i.e. binding of Annexin-V to phosphatidylserine indicates that the apoptotic pathway was initiated, whereas binding of PI to DNA indicates necrosis. At the onset of initiated apoptosis, phosphatidylserine shifts from the inside of the cell membrane and presents on the outside of the cell membrane, which enables fluorescence conjugated Annexin-V (Annexin-V FITC) to bind. During necrosis, rapid, irreversible cell lysis occurs that enables PI-DNA binding (Michie *et al*. 2003).

4.2 AIM

To determine whether the novel azole-based gold-containing compounds, UH 126.1 and 127.1, initiate the apoptotic or necrotic cell death pathway in Jurkat cells.

4.3 MATERIALS

Annexin-V FITC

A volume of 5µl of Annexin-V FITC (fluorescein isothiocyanate), a photostable conjugate of Annexin-V, obtained from BD Bioscience, JHB, SA. The stain was refrigerated at 4ºC until use.

Binding buffer

Prepared by dissolving 238mg HEPES, 876mg NaCl, 26.5mg $CaCl_2$, 37.3mg KCl and 9.5mg $MgCl_2$ in 100ml of deionised water. The pH was adjusted to 7.2 with NaOH. The solution was refrigerated at 4ºC until use.

Cell counting fluid

A volume of 1ml of a 0.1% crystal violet solution and 2ml glacial acetic acid was

dissolved in 97ml of distilled water. The solution was mixed well and refrigerated at 4ºC until use.

Experimental compounds

A 10mM stock solution was prepared by dissolving the appropriate mass of each compound (UH 126.1, UH 127.1, $[Au(dppe)_2]Cl$ and cisplatin) in dimethyl sulphydroxide (DMSO) (obtained from Merck, Darmstadt, Germany). The volume of 50µl of each compound was aliquoted in eppendorf vials and stored at -70°C. Dilutions were prepared in the appropriate supplemented medium.

Jurkat cells

Human T –lymphocyte leukaemia (NRBM no TIB-152) were maintained in RPMI 1640 medium with 10% bovine FCS.

Phosphate buffered saline (PBS)

A mass of 0.923g of FTA hemagglutinin buffer powder (The Scientific Group, JHB, SA) was dissolved in 100ml of distilled water. The pH was adjusted to 7.2. The solution was refrigerated at 4ºC until use.

Propidium Iodide (PI)

PI powder was obtained from BD Bioscience, JHB, SA. A 50µg/m PBS solution was prepared and refrigerated at 4ºC until use.

Roswell Park Memorial Institute Medium (RPMI) 1640

RPMI 1640 powder (Sigma-Aldrich, JHB, SA) was dissolved in sterile water with the aid of a sterile stirrer. The pH of the solution was adjusted to 4 with 1M HCl to ensure complete solubilisation. Thereafter, 2mg of $NaHCO_3$ was added to each litre of the medium. The pH was readjusted to 7.1 through the addition of either 1M HCl or 1M NaOH. The medium was filter-sterilized through a 0.22µm filter and divided into 500ml aliquots. A volume of 55ml was removed from the 500ml aliquot and the remaining solution was supplemented with 5ml of a 1% penicillin/streptomycin solution and 50ml sterile HI FCS. The medium was stored at 4ºC until use.

4.4 METHODS

4.4.1 Passaging the cells

1. Jurkat cells were cultured and maintained in RPMI medium with 10% bovine FCS at 37ºC in an incubator supplemented with 5% CO_2.
2. The culture medium was discarded from a 75cm^2 flask
3. The cell suspension was transferred to a 15ml centrifuge tube and centrifuged at 1000 rpm for 5 minutes.
4. The supernatant was discarded after which 1ml medium supplemented with foetal calf serum (FCS) were added to the cell pellet and aspirated to form a suspension.

4.4.2 Counting the cells

1. A volume of 50µl of the cell suspension was added to 450µl white cell counting fluid (**see section 4.4.1, page 57)**.
2. This suspension was then added to the Haemocytometer and cells were counted using a Reichert-Jung Microstar 110 microscope at a magnification of 40 times.
3. The cells were re-suspended to obtain the relevant cell concentration for each assay.

4.4.3 Experimental procedure

1. Cells (1x10^6 cells per ml) (**see section 4.4.2, page 57**) were incubated with the experimental compounds for 24 and 48 hours at 37ºC with 5% CO_2. Drug concentrations (i) equal to the IC_{50} value, (ii) double the IC_{50} value and (iii) five times the IC_{50} value was used (**refer to Chapter 3, Tables 3.1 and 3.2, pages 43 and 48**.) No compound was added to the control cells.
2. After the incubation period, the cells were centrifuged for 5 min at 200g and washed twice by adding and then removing PBS.
3. Cells were re-suspended in 1ml binding buffer.
4. A 100µl volume of the cell suspension was transferred to a flow cytometer tube for each compound, for each concentration, i.e. three tubes were prepared for each compound.

5. 5µl of the Annexin V-FITC and 10µl of the PI solutions were added to each tube.
6. Cell suspensions were mixed gently and incubated at room temperature (20-25^{0}C) for 15 min in the dark.
7. 400µl of binding buffer was added to each tube.
8. Cells were analysed using the FC 500 Series Beckman Coulter flow cytometer.

4.5 EXPRESSION OF RESULTS

In this study, it was determined whether Annexin-V and/or PI stain was bound to a cell, via a flow cytometric method. Annexin-V and PI was only able to bind to non-viable cells in this experiment. Annexin-V positive staining indicated induction of the apoptotic pathway, whereas induction of the necrotic pathway was indicated via PI positive staining. The percentage of cells that was bound to Annexin-V and/or PI stain was quantified. A histogram was generated via intrinsic Beckman Coulter flow cytometric software, which indicated PI positive staining on the x-axis and Annexin-V positive staining on the y-axis. According to the intensity measured for each stain, the histogram was divided into specified areas/gates, indicating initial (early) apoptosis, advanced (late) apoptosis and necrosis respectively. Results are expressed as percentage of cells ± SEM. Statistical evaluation was done by a Mann-Whitney non-parametric test (**refer to Appendix A, 3.1, a-b, pages 133-134**) with GRAPHPAD Statistical Software© program (**refer to Appendix A, 3.1, c, page 134**). The difference was considered statistically significant at $p \leq 0.05$.

4.6 RESULTS

A flow cytometric method was used in order to determine whether UH 126.1, UH 127.1, $[Au(dppe)_2]Cl$ and cisplatin initiate the apoptotic or necrotic cell death pathway when exerting their cytotoxic effects in Jurkat cells. Jurkat cells were incubated in the presence of UH 126.1, UH 127.1, $[Au(dppe)_2]Cl$ or cisplatin at three different concentrations: (i) equal to the IC_{50}, (ii) double the IC_{50}, and (iii) five times the IC_{50}. for each compound. The concentrations were previously determined (**refer to Chapter 3, Table 3.2, page 48**). Untreated Jurkat cells were also included to serve as a control. The cells were analysed after incubation periods of 24 hours and 48 hours. Two stains, Annexin-V FITC

and PI, were added to the Jurkat cells before flow cytometric analysis. It has been proven that Annexin-V FITC binds to phospatidylserine (which is present on apoptotic cells), whereas PI binds to DNA, which is indicative of irreversible cell lysis (i.e. necrosis) (Michie *et al*. 2003). The cells, which were positive for the Annexin-V FITC and PI stains, were quantified via flow cytometry. A flow cytometric histogram was generated, indicating PI staining on the x-axis and Annexin-V positive staining on the y-axis (**Figure 4.2, page 60**). According to the intensity measured for each stain, the histogram was divided into specified areas/gates, indicating initial (early) apoptosis, advanced (late) apoptosis and necrosis respectively (**Figure 4.2, page 60**). An apoptotic pathway is indicated by a high intensity of Annexin-V stain (as indicated by the arrow in **Figure 4.3, page 60)**, whereas a necrotic pathway would be indicated by a high intensity of PI stain (as indicated by the arrow in **Figure 4.4, page 60)**.

The results of this study are graphically presented in **Appendix C, page 143** (**Figures 1 – 26)**. When assessing these graphic results, it is evident that all the tested compounds (UH 126.1, UH 127.1, $[Au(dppe)_2]Cl$ and cisplatin) induced the apoptotic cell death pathway in a similar way as indicated by the arrow in **Figure 4.3, page 60.**

Quantified data is summarized in **Table 4.1, page 61.** According to these results, UH 126.1, UH 127.1 and cisplatin, induced initial apoptosis in Jurkat cells after 24 hours at all three concentrations. This is indicated by the significant increase in cells detected in the initial apoptosis region of the histogram, when compared to the untreated control cells in this region. Pertaining to the lipophilic cation, $[Au(dppe)_2]Cl$, advanced apoptotic cells and necrotic cells were already detected after 24 hours. It is noteworthy that a significant increase in percentage of non-viable cells was detected at the highest concentration (IC_{50} x 5) of $[Au(dppe)_2]Cl$ in comparison to the other compounds.

A remarkable increase in percentage of non-viable cells is seen from 24 hours to 48 hours, which was induced by all the tested compounds (**Table 4.1, page 61)**. This increase is echoed for the untreated control cells. It is evident that cell lysis (necrosis) was induced after 48 hours by all the tested compounds. A significant increase in

necrotic cells was detected at all three concentrations of all the tested compounds when compared to the untreated control. UH 126.1 and UH 127.1 induced a drastic increase in non-viable cells (at the highest concentrations (IC_{50} x 5)), when compared to that of the other tested compounds.

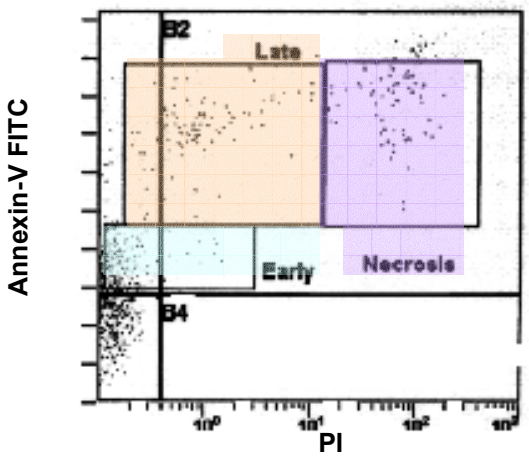

Figure 4.2. Histogram of untreated Jurkat cells

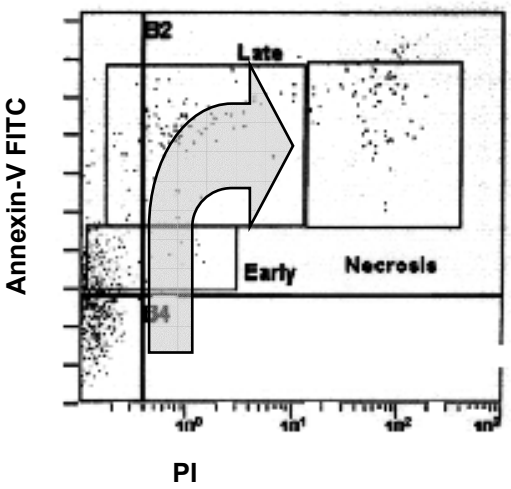

Figure 4.3. Histogram of untreated Jurkat cells indicating the apoptotic pathway

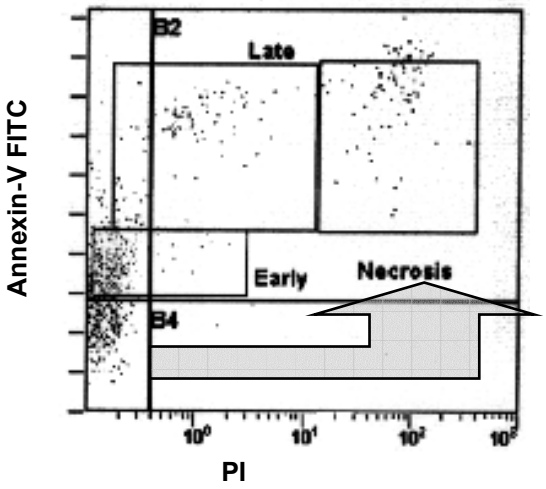

Figure 4.4. Histogram of untreated Jurkat cells indicating the necrotic pathway

Table 4.1. Cell death pathway analysis of Jurkat cell lines after exposure to three different concentrations (μM) of each experimental compound at two different exposure times

Assessment of cell death induction in Jurkat cells		Incubation time: 24 hours				Incubation time: 48 hours			
Compound	**Concentration (μM)**	**Initial Apoptosis**	**Advanced Apoptosis**	**Necrosis**	**Non-viable cells**	**Initiated Apoptosis**	**Advanced Apoptosis**	**Necrosis**	**Non-viable cells**
		Mean percentage (%) cells ± SEM [1]			**%**	**Mean percentage (%) cells ± SEM [1]**			**%**
Control	N/A	3.31 ± 0.61	1.97 ± 0.22	1.03 ± 0.57	6.31	32.9 ± 0.18	7.10 ± 0.30	8.86 ± 0.05	48.86
UH 126.1	0.119 (IC_{50})	5.98 ± 0.24*	2.12 ± 0.13	1.23 ± 0.27	9.33	27.73 ± 0.09	6.96 ± 0.15	16. 83 ± 0.28*	51.52
	0.238 (IC_{50}×2)	6.4 ± 0.64*	2.25 ± 0.11	1.23 ± 0.17	9.88	25.46 ± 0.13	8.75 ± 0.29	18.72 ± 0.36*	52.93
	0.595 (IC_{50}×5)	3.89 ± 0.19	3.53 ± 0.27*	5.39 ± 0.49*	12.81	10.75 ± 0.11*	19.34 ± 0.08*	52.55 ± 0.04*	82.64
UH 127.1	0.075 (IC_{50})	5.05 ± 0.61*	2.44 ± 0.01	1.47 ± 0.17	8.96	29.59 ± 0.02	9.21 ± 0.14	18.87 ± 0.18*	53.67
	0.150 (IC_{50}×2)	7.17 ± 0.35*	2.29 ± 0.02	1.33 ± 0.27	10.79	28.79 ± 0.17	10.29 ± 0.15	22.58 ± 0.18*	61.66
	0.375 (IC_{50}×5)	6.50 ± 0.39*	3.66 ± 0.10*	6.23 ± 0.18*	16.39	16.65 ± 0.06*	16.42 ± 0.17*	43.39 ± 0.09*	76.46
$[Au(dppe)_2]Cl$	0.081 (IC_{50})	3.39 ± 0.58	6.25 ± 0.99*	5.75 ± 1.32*	15.39	27.36 ± 0.04	8.05 ± 0.21	19.51 ± 0.18*	54.92
	0.162 (IC_{50}×2)	2.75 ± 0.47	6.17 ± 0.60*	6.15 ± 0.96*	15.07	25.20 ± 0.11	9.83 ± 0.05	26.46 ± 0.17*	61.49
	0.405 (IC_{50}×5)	2.81 ± 0.22	18.13 ± 0.18*	17.66 ± 0.09*	38.6	15.87 ± 0.02	5.92 ± 0.19	38.16 ± 0.02*	59.95
Cisplatin	0.413 (IC_{50})	5.26 ± 0.32*	2.03 ± 0.14	1.3 ± 0.05	8.59	30.08 ± 0.15	7.79 ± 0.15	16.41 ± 0.28*	54.28
	0.826 (IC_{50}×2)	4.99 ± 0.59*	1.92 ± 0.12	1.22 ± 0.13	8.31	32.99 ± 0.09	10.52 ± 0.24	15.17 ± 0.33*	58.68
	2.065 (IC_{50}×5)	3.4 ± 0.23	1.98 ± 0.08	1.35 ± 0.25	6.73	33.01 ± 0.06	9.78 ± 0.25	15.96 ± 0.30*	58.75

* $p \leq 0.05$ when compared to the untreated control

1. Average of three experiments

4.7 DISCUSSION

The induction of apoptosis via anticancer compounds is a desirable result in cancer chemotherapy (Yalowitz *et al*. 2002). The induction of the necrotic pathway is, however, associated with side effects such as the release of inflammatory mediators (Searle *et al*. 1982). Apoptosis is associated with intrinsic or extrinsic apoptotic activators that induce the intracellular apoptotic cascade, which progresses until resulting in cell death (Hengartner, 2000). In necrosis, however, cell death is attributed to cell swelling and external damage that causes rapid lysis (Searle *et al*. 1982; Somosy 2000).

In the present study, the cell death pathway induced by the experimental compounds was investigated via a flow cytometric method. Jurkat cells were exposed to the tested compounds (UH 126.1, UH 127.1 $[Au(dppe)_2]Cl$ and cisplatin), at three different concentrations for 24 hours, and 48 hours, respectively. According to the results, there was a remarkable increase in non-viable (dead) cells by increasing exposure to the tested compounds from 24 hours to 48 hours. Duration of exposure evidently requires consideration when investigating possible treatment regimes for this class of compound (**Table 4.1, page 61)**.

Results indicated that all the tested compounds, at all three different concentrations after 24 hours and 48 hours of exposure, induced the apoptotic cell death pathway in Jurkat cells (**Figures 1-26, Appendix C, page 143**). Necrotic cells are, however present after 48 hours of exposure (**Table 4.1, page 61)**. The occurrence of necrotic cells at this stage is explained by the binding of PI to DNA of these cells. It is likely that exposure of up to 48 hours would cause exposure of the DNA as a result of lysed membranes. Cell damage at this stage is irrepairable.

The lipophilic cation, $[Au(dppe)_2]Cl$, induced apoptosis, which rapidly progressed to advanced apoptosis and necrosis after 24 hours. These results indicate rapid accumulation of the compound within the cells, which enables the rapid activation of intrinsic apoptotic mediators (Hill *et al*. 2003; Huppertz *et al*. 1999). It has been found that, due to the lipophilic, cationic nature of $[Au(dppe)_2]Cl$, the compound accumulates within the

mitochondria (Davis *et al*. 1985), and is followed by the release of cytochrome c, subsequent activation of the executioner caspases (caspases 3,6,7) and the final apoptotic events (Hill *et al*. 2003; Huppertz *et al*. 1999). It has been proposed that mitochondria are the primary target of the gold(I) phosphine anticancer activity (Hoke *et al.* 1989; Rush *et al.* 1987), and it has been documented that $[Au(dppe)_2]Cl$ induces intrinsic/mitochondria-mediated apoptosis (Mahepal *et al*. 2008; Smith *et al*. 1989). In contrast to this, it is known that cisplatin induces extrinsic/receptor-linked apoptosis, which does not involve the mitochondria (Yu *et al*. 2008), but are reliant on the formation of the death-inducing signalling complex, with subsequent activation of caspase-8 (Bredesen, 2000; Hengartner, 2000).

The results of this study indicate that the novel compounds, UH 126.1 and UH 127.1, induce the apoptotic cell death pathway when exerting their cytotoxic effects in Jurkat cells. It is not yet elucidated in this experiment whether UH 126.1– and UH 127.1–induced apoptosis is due activation of the extrinsic/receptor-linked apoptotic pathway or the intrinsic/mitochondrial apoptotic pathway.

CHAPTER FIVE

MITOCHONDRIAL MEMBRANE POTENTIAL

5.1 INTRODUCTION

Two distinct cell death pathways have been described according to previous findings: the apoptotic and necrotic pathways (Searle *et al*. 1982). Furthermore, there can be differentiated between two distinct apoptotic pathways, the extrinsic/receptor-linked pathway or the intrinsic/mitochondria-mediated pathway. It has been established in this study that the novel gold-containing compounds with azole bases (UH 126.1 and UH 127.1,), induce the apoptotic pathway when exerting cytotoxic effects in Jurkat cells (**see Chapter 4, section 4.6, page 58**). It was not, however, elucidated whether apoptosis is initiated via the extrinsic/receptor-linked apoptotic pathway or the intrinsic/mitochondria-mediated apoptotic pathway.

As described previously (**refer to Chapter 4, section 4.1, page 53**), the mitochondrial apoptotic pathway is triggered by cytochrome c upon release from mitochondria. In contrast to this, members of the death-receptor super family trigger the extrinsic pathway, with subsequent activation of caspase-8 (Bredesen, 2000; Hengartner, 2000), leading to cell death.

Mitochondria play a key role in the intrinsic/mitochondria-mediated apoptotic pathway (Bredesen, 2000; Hengartner, 2000). The mitochondrial membrane potential (MMP), is defined as the voltage difference across the mitochondrial inner membrane, with the outside being positive and the inside being negative, that generates the proton-motive force, driving the synthesis of ATP by the process of oxidative phosphorylation. The status of the MMP is an important parameter of mitochondrial function (Salido *et al.* 2007). It has been shown that there is an association between the release of cytochrome c from mitochondria and the loss of the MMP (Gruss-Fischer and Fabian 2002). A collapse of MMP indicates mitochondrial toxicity (Ferraresi *et al.* 2004). Depolarisation of the MMP, due to chemical compounds (such as the novel compounds UH 126.1 and UH 127.1), will thus be indicative of mitochondrial involvement in the cell death pathway.

Many types of indicator molecular probes and methods have been used for estimating the electrical potential across the inner mitochondrial membrane. Lipophilic cations accumulate in the mitochondrial membranes (which possess a negative intermembrane charge), because of their delocalised positive charge and solubility in both the inner mitochondrial membrane and matrix space (Grotyohann *et al*. 1999; Smith *et al*. 1989). The lipophilic cation dye, JC-1 (5,5',6,6'-tetrachloro-1,1',3,3' tetraethylbenzimidazolyl-carbocyanine iodide), is able to detect changes in mitochondrial membrane potential at single cell level (Cossarizza *et al*. 1993). JC-1 shows a green fluorescence when existing as a monomer in the cytosol and an orange fluorescence when it aggregates and accumulates in the mitochondria. When JC-1 accumulates in intact mitochondria, the mitochondria are stained orange. In apoptotic cells, however, the MMP collapses, and the dye is not able to enter the mitochondria. A primarily green fluorescence is thus seen in apoptotic cells with depolarized MMPs (Smiley *et al*. 1991).

A standard flow cytometric method was used to test the effect of the experimental compounds on Jurkat cells and normal PHA stimulated lymphocytes (Bortner and Cidlowski 1999; Chen 1988). Valinomycin was included as a positive control, for it is known to have a depolarising effect on the mitochondrial membrane potential (Cosarizza *et al*. 1993).

5.2 AIM

To determine whether the novel gold compounds UH 126.1 and UH 127.1 induce the collapse (depolarisation) of the mitochondrial membrane potential (MMP).

5.3 MATERIALS

Cell counting fluid

A volume of 1ml of a 0.1% crystal violet solution and 2ml glacial acetic acid was dissolved in 97ml of distilled water. The solution was mixed well and refrigerated at 4ºC until use.

Experimental compounds

A 10mM stock solution was prepared by dissolving the appropriate mass of each compound (UH 126.1, UH 127.1, $[Au(dppe)_2]Cl$ and cisplatin) in dimethyl sulphydroxide (DMSO) (obtained from Merck, Darmstadt, Germany). The volume of 50µl of each compound was aliquoted in eppendorf vials and stored at -70°C. Dilutions were prepared in the appropriate supplemented medium.

Human lymphocytes

Cells were derived from preservative free heparinized peripheral human blood. Procedures for isolation of lymphocytes are discussed in **Appendix B.2, page 141.**

JC-1

A solution of 25ug JC-1 / ml PBS was prepared and refrigerated at 4ºC until use (JC-1 obtained from Sigma-Aldrich, Steinheim, Germany).

Jurkat cells

Human T –lymphocyte leukaemia (NRBM no TIB-152) were maintained in RPMI 1640 medium with 10% bovine FCS.

Phosphate buffered saline (PBS)

A mass of 0.923g of FTA hemagglutinin buffer powder (The Scientific Group, JHB, SA) was dissolved in 100ml of distilled water. The pH was adjusted to 7.2. The solution was refrigerated at 4ºC until use.

Propidium Iodide (PI)

PI powder was obtained from BD Bioscience, JHB, SA. A 50µg/m PBS solution was prepared and refrigerated at 4ºC until use.

Roswell Park Memorial Institute Medium (RPMI) 1640

RPMI 1640 powder (Sigma-Aldrich, JHB, SA) was dissolved in sterile water with the aid of a sterile stirrer. The pH of the solution was adjusted to 4 with 1M HCl to ensure

complete solubilisation. Thereafter, 2mg of $NaHCO_3$ was added to each litre of the medium. The pH was readjusted to 7.1 through the addition of either 1M HCl or 1M NaOH. The medium was filter-sterilized through a 0.22µm filter and divided into 500ml aliquots. A volume of 55ml was removed from the 500ml aliquot and the remaining solution was supplemented with 5ml of a 1% penicillin/streptomycin solution and 50ml sterile HI FCS. The medium was stored at 4ºC until use.

5.4 METHODS

5.4.1 Passaging the cells

1. Jurkat cells were cultured and maintained in RPMI medium with 10% bovine FCS at 37ºC in an incubator supplemented with 5% CO_2.
2. The culture medium was discarded from a 75cm^2 flask.
3. The cell suspension was transferred to a 15ml centrifuge tube and centrifuged at 1000 rpm for 5 minutes.
4. The supernatant was discarded after which 1ml medium supplemented with foetal calf serum (FCS) were added to the cell pellet and aspirated to form a suspension.

5.4.2 Counting the cells

1. A volume of 50µl of the cell suspension was added to 450µl white cell counting fluid (**refer to section 5.4.1, page 67**).
2. This suspension was then added to the Haemocytometer and cells were counted using a Reichert-Jung Microstar 110 microscope at a magnification of 40 times.
3. The cells were re-suspended to obtain the relevant cell concentration (**refer to section 5.4.3, page 67)** for each assay.

5.4.3 Experimental procedure

1. Flow cytometer tubes were prepared with 1800µl cells at concentrations of:
   - PHA stimulated lymphocytes: 2×10^6 cells per ml
   - Jurkat: 2×10^5 cells per ml

2. The cells were incubated for 1hour at 37ºC with 5% CO_2 before adding 200µl of the required concentrations of each compound to the cell suspension. Drug concentrations equal to the IC_{50} value, double the IC_{50} value and five times the IC_{50} value was be used (**refer to Chapter 3, Tables 3.1 and 3.2, pages 43 and 48**). No compound was added to the control cells.
3. The cells were incubated at 37ºC with 5% CO_2 and analysed after 24 and 48 hours.
4. After the incubation period, 10µl valinomycin (10 µM) was added to the cell suspension and incubated for 10 minutes.
5. The cell suspensions were centrifuged for 5 minutes at 2000rpm (800g) and the supernatant was discarded.
6. Cells were resuspended with 100µl of 25ug/ml JC-1 and 900µl RPMI 1640 medium with 10% bovine FCS.
7. The cell suspension were incubated for 20 minutes at 37ºC with 5% CO_2 and centrifuged for 5 minutes at 2000rpm (800g).
8. After discarding the supernatant, the cells were washed twice with the addition of 2ml PBS.
9. The cells were then resuspended in 1ml PBS containing 10% heat inactivated FCS.
10. Cells were analysed within 1 hour using the FC 500 Series Beckman Coulter flow cytometer.

5.5 EXPRESSION OF RESULTS

Flow cytometric software (intrinsic to the FC 500 Series Beckman Coulter flow cytometer) quantified the JC-1 intensity and colour of the stained Jurkat cells and lymphocytes. Results are graphically presented as a ratio ± SEM, where FL1 represents apoptotic green stained cells with collapsed MMPs and FL2 represents orange stained cells with intact mitochondria. For determining MMP in Jurkat cells, the ratio is expressed as FL1/FL2. In the case of PHA stimulated lymphocytes, the ratio is expressed as FL2/FL1. Statistical evaluation was done by a Mann-Whitney non-parametric test (**refer to Appendix A, 4.1, a-b, page 135**) with GRAPHPAD Statistical Software©

program (**refer to Appendix A, 4.1, c, page 135**). The difference was considered statistically significant at $p \leq 0.05$.

5.6 RESULTS

The experimental compounds (UH 126.1, UH 127.1, $[Au(dppe)_2]Cl$, cisplatin and valinomycin) were added to the Jurkat cells and PHA stimulated lymphocytes at three different concentrations for each experimental compound (i) equal to the IC_{50}, (ii) double the IC_{50}, and (iii) five times the IC_{50} for a period of 24 hours. Valinomycin was used as a positive control at a fixed concentration of 10 µM. The lipophilic stain, JC-1, was added to the cells after the 24-hour incubation period. JC-1 was seen as a green fluorescence when existing as a monomer in the cytosol and an orange fluorescence when it aggregated and accumulated in intact mitochondria. Orange stained cells represent cells with intact mitochondria. When the MMP of the cells collapsed, the dye was not able to enter the mitochondria, and a primarily green fluorescence was seen. For determination of the MMP in Jurkat cells, results are expressed as a ratio: FL1/FL2, where FL1 represents green stained cells and FL2 represents orange stained cells with intact mitochondria. Depolarisation of the MMP in Jurkat cells is thus indicated by an increase in the measured ratio compared to the control cells. In Jurkat cell analysis (**Figures 5.1-5.3, pages 72-74**), the ratio is expressed as FL1/FL2 (y-axis). The relative concentrations of each compound are displayed on the x-axis of the graphic presentations (**Figures 5.1-5.3, pages 72-74**). In contrast to this, the depolarisation of the MMP in PHA stimulated lymphocytes (**Figures 5.4-5.6, pages 75-77**), is indicated by a decrease in the measured ratio when compared to the untreated control cells. In this case the ratio is expressed as FL2/FL1 (y-axis). The relative concentrations of each compound are displayed on the x-axis of the graphic presentations (**Figures 5.4-5.6, pages 75-77)**.

The results of this study indicated that valinomycin (at a fixed concentration of 10 µM), caused the depolarisation of the MMP in Jurkat cells. A significant increase in the measured ratio was observed when compared to the untreated control cells (**Figures 5.1-5.3, pages 72-74**). These results were echoed when valinomycin was added to PHA stimulated lymphocytes (**Figures 5.4-5.6, pages 75-77**).

When assessing the effect of $[Au(dppe)_2]Cl$ on the MMP of Jurkat cells, collapse (depolarisation) of the MMP increased in a dose-dependant manner. As the concentration of $[Au(dppe)_2]Cl$ increased , the measured ratio increased as well (**Figures 5.1-5.3, pages 72-74**). These results were mirrored when $[Au(dppe)_2]Cl$ was added to PHA stimulated normal lymphocytes (**Figures 5.4-5.6, pages 75-77**). In this case, however, depolarisation of the MMP was indicated with a decrease in the measured ratio, i.e. with increased concentrations of $[Au(dppe)_2]Cl$, a decrease in the measured ratio (FL2/FL1) was obtained (**Figures 5.4-5.6, pages 75-77**). It is evident that higher concentrations of $[Au(dppe)_2]Cl$ induced more significant depolarisation of the MMP in both Jurkat cancer cells and PHA stimulated lymphocytes.

With the addition of cisplatin to Jurkat cells and PHA stimulated lymphocytes, the measured ratios did not differ statistically from that of the untreated control cells in both cell cultures. These results were obtained at all three concentrations [(i) equal to the IC_{50}, (ii) double the IC_{50}, and (iii) five times the IC_{50}] (**Figures 5.1-5.6, pages 72-77)**. According to the results, cisplatin did not induce the depolarisation of the MMPs of either Jurkat cells (**Figures 5.1-5.3, pages 72-74**), or PHA stimulated lymphocytes (**Figures 5.4-5.6, pages 75-77**).

The exposure of Jurkat cells to UH 126.1 did not result in a significant loss of MMP when added at a concentration equal to the IC_{50} (**Figure 5.1, page 72)**, or double that of the IC_{50} (**Figure 5.2, page 73)**. There was, however, a significant increase in the measured ratio (FL1/FL2) with the addition of UH 126.1 at a concentration five times that of the IC_{50} to Jurkat cells (**Figure 5.3, page 74)**. This indicates depolarisation of the MMP in Jurkat cells induced by UH 126.1 at a very high concentration (five times that of the IC_{50}). When this compound was added to PHA lymphocytes (at concentrations double, and five times that of the IC_{50}), a significant decrease in the measured ratio (FL2/FL1) was obtained (**Figures 5.5-5.6, pages 76-77)**. No significant differences were seen between the ratio of the untreated control cells (PHA stimulated lymphocytes), and

that which was obtained for UH 126.1 at a concentration equal to the IC_{50} (**Figure 5.4, page 75)**. According to the results, UH 126.1 induced depolarisation of the MMP in PHA stimulated lymphocytes at concentrations double, and five times that of the IC_{50}.

When assessing the effect of UH 127.1 (at concentrations equal to- double- and five times that of the IC_{50}) on the MMP of Jurkat cells, it was determined that the measured ratios (FL1/FL2) did not differ statistically from that of the untreated control cells (**Figures 5.1-5.3, pages 72-74**). It is thus evident that this compound did not induce the collapse of the MMP in Jurkat cells. When this compound was added to PHA lymphocytes (at concentrations equal to- double- and five times that of the IC_{50}), no significant differences were obtained between the ratio's of the untreated control cells and the UH 127.1 treated cells. A trend, however, is depicted in these graphic presentations (**Figures 5.4-5.6, pages 75-77)**: a decrease in the measured ratio (FL2/FL1) is directly proportionate with an increase of the UH 127.1 concentration.

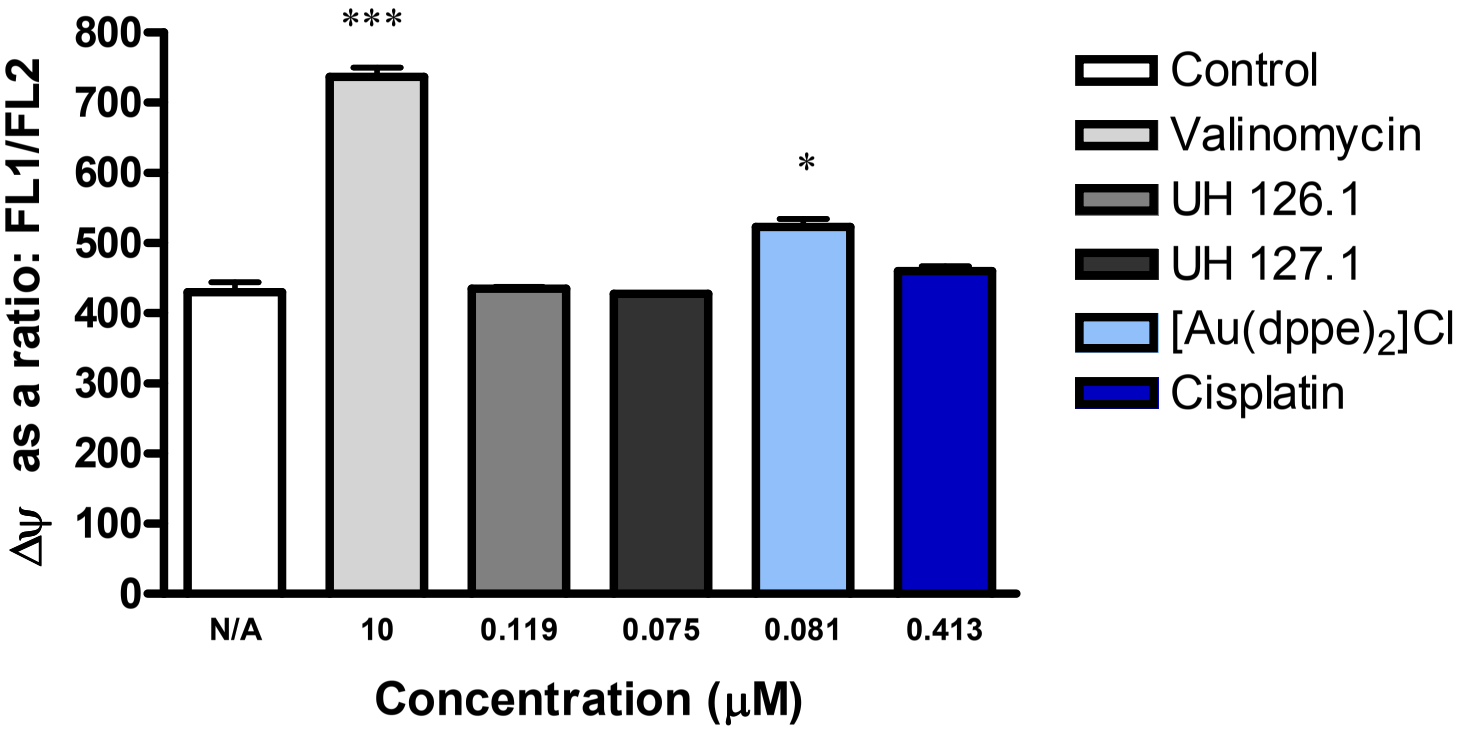

Figure 5.1. Flow cytometric analysis of the mitochondrial membrane potential (MMP) of Jurkat cells stained with JC-1 after exposure to valinomycin, UH 126.1, UH 127.1, $[Au(dppe)_2]Cl$ and cisplatin for 24 hours. The concentration of each experimental compound is equal to the IC_{50} determined for Jurkat cells. FL 1 indicates green fluorescence and FL2 indicates orange fluorescence. Error bars reflect the standard error of the mean (SEM). *$p \leq 0.05$ when compared to the untreated control; ***$p \leq 0.001$ when compared to the untreated control.

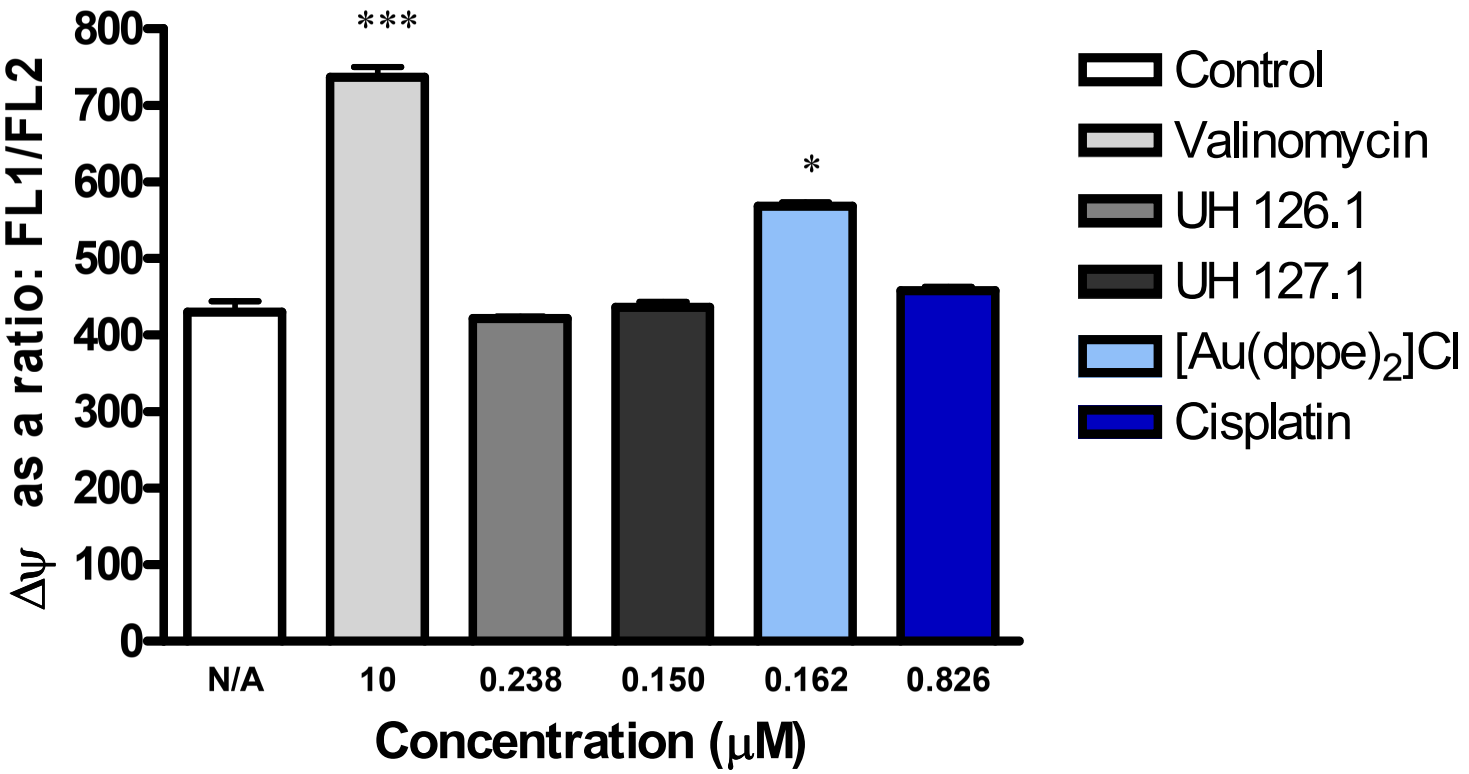

Figure 5.2. Flow cytometric analysis of the mitochondrial membrane potential (MMP) of Jurkat cells stained with JC-1 after exposure to valinomycin, UH 126.1, UH 127.1, $[Au(dppe)_2]Cl$ and cisplatin for 24 hours. The concentration of each experimental compound is 2 x IC_{50} determined for Jurkat cells. FL 1 indicates green fluorescence and FL2 indicates orange fluorescence. Error bars reflect the standard error of the mean (SEM). *$p \leq 0.05$ when compared to the untreated control; ***$p \leq 0.001$ when compared to the untreated control.

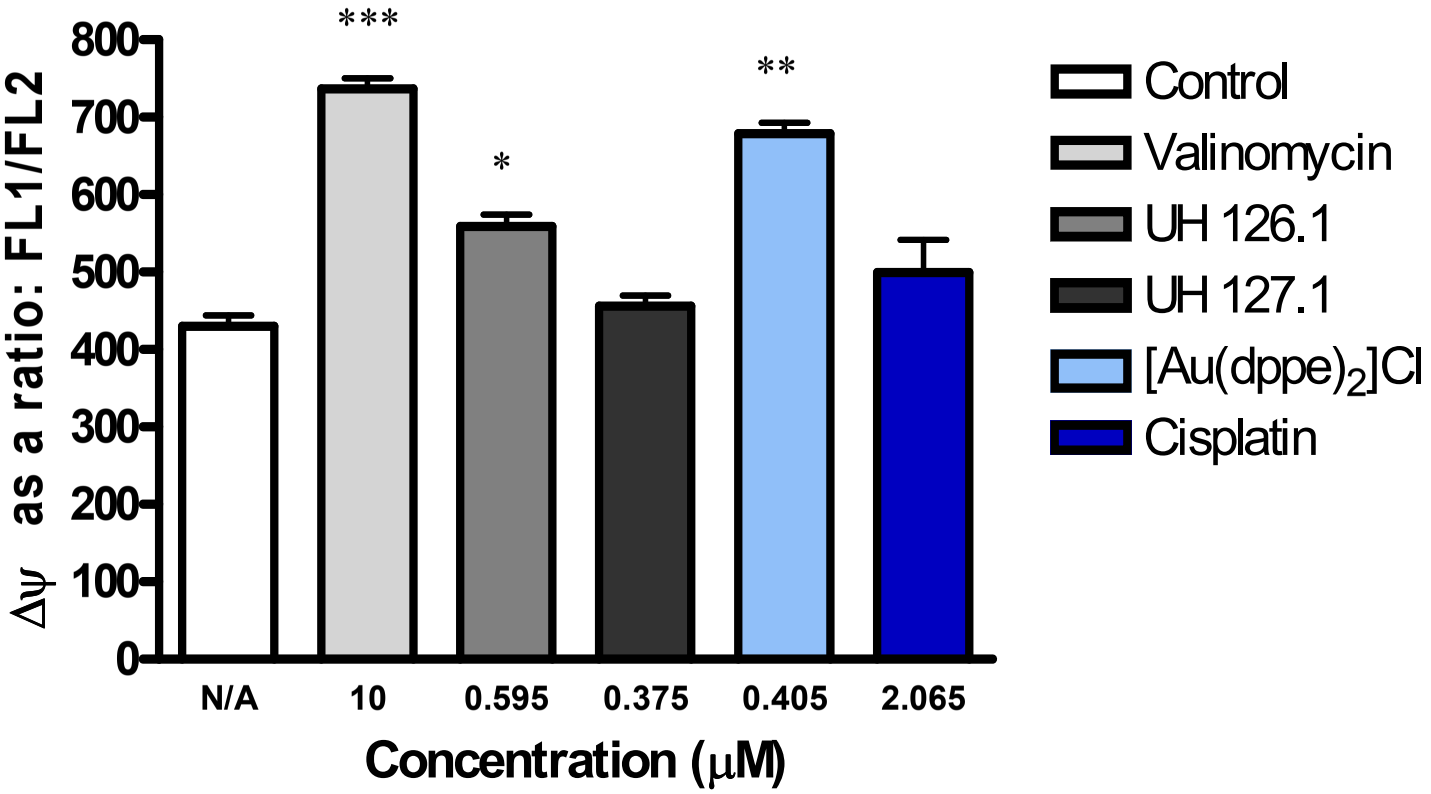

Figure 5.3. Flow cytometric analysis of the mitochondrial membrane potential (MMP) of Jurkat cells stained with JC-1 after exposure to valinomycin, UH 126.1, UH 127.1, $[Au(dppe)_2]Cl$ and cisplatin for 24 hours. The concentration of each experimental compound is 5 x IC_{50} determined for Jurkat cells. FL 1 indicates green fluorescence and FL2 indicates orange fluorescence. Error bars reflect the standard error of the mean (SEM). *$p \leq 0.05$ when compared to the untreated control; **$p \leq 0.01$ when compared to the untreated control; ***$p \leq 0.001$ when compared to the untreated control.

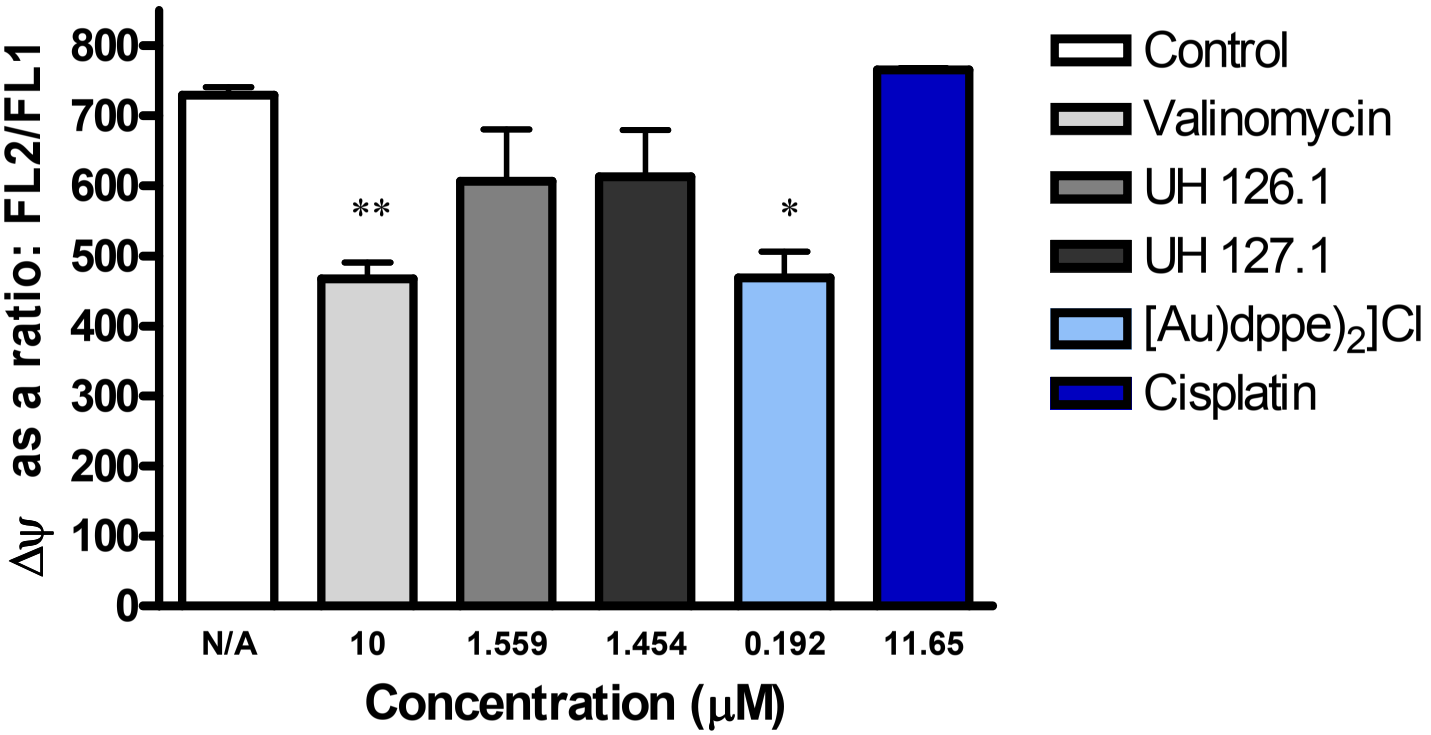

Figure 5.4. Flow cytometric analysis of the mitochondrial membrane potential (MMP) of PHA stimulated lymphocytes stained with JC-1 after exposure to valinomycin, UH 126.1, UH 127.1, [Au(dppe)$_2$]Cl and cisplatin for 24 hours. The concentration of each experimental compound is equal to the IC_{50} determined for PHA stimulated lymphocytes. FL 1 indicates green fluorescence and FL2 indicates orange fluorescence. Error bars reflect the standard error of the mean (SEM). *$p \leq 0.05$ when compared to the untreated control; **$p \leq 0.001$ when compared to the untreated control.

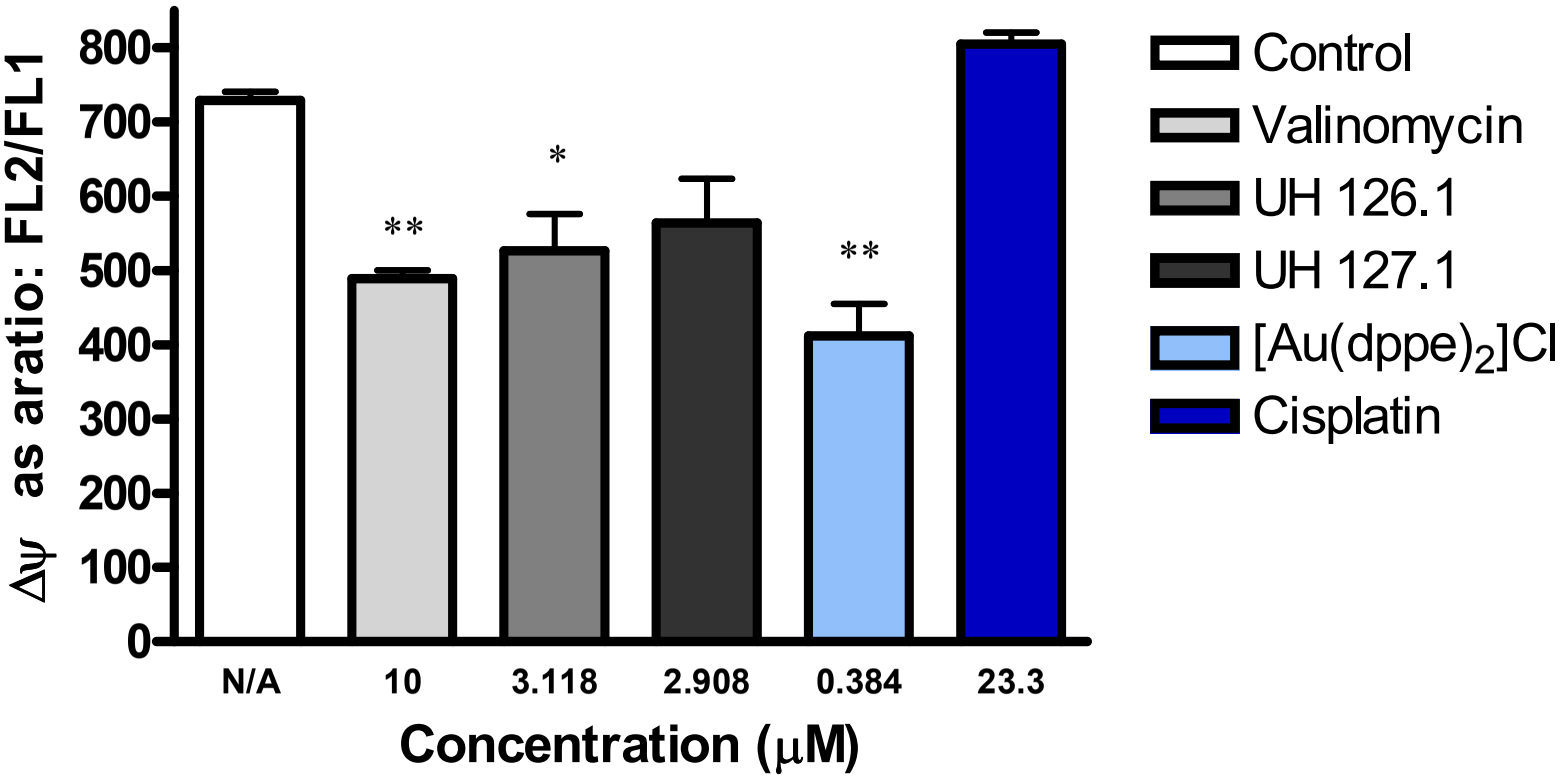

Figure 5.5. Flow cytometric analysis of the mitochondrial membrane potential (MMP) of PHA stimulated lymphocytes stained with JC-1 after exposure to valinomycin, UH 126.1, UH 127.1, $[Au(dppe)_2]Cl$ and cisplatin for 24 hours. The concentration of each experimental compound is 2 x IC_{50} determined for PHA stimulated lymphocytes. FL 1 indicates green fluorescence and FL2 indicates orange fluorescence. Error bars reflect the standard error of the mean (SEM). *$p \leq 0.05$ when compared to the untreated control; **$p \leq 0.01$ when compared to the untreated control.

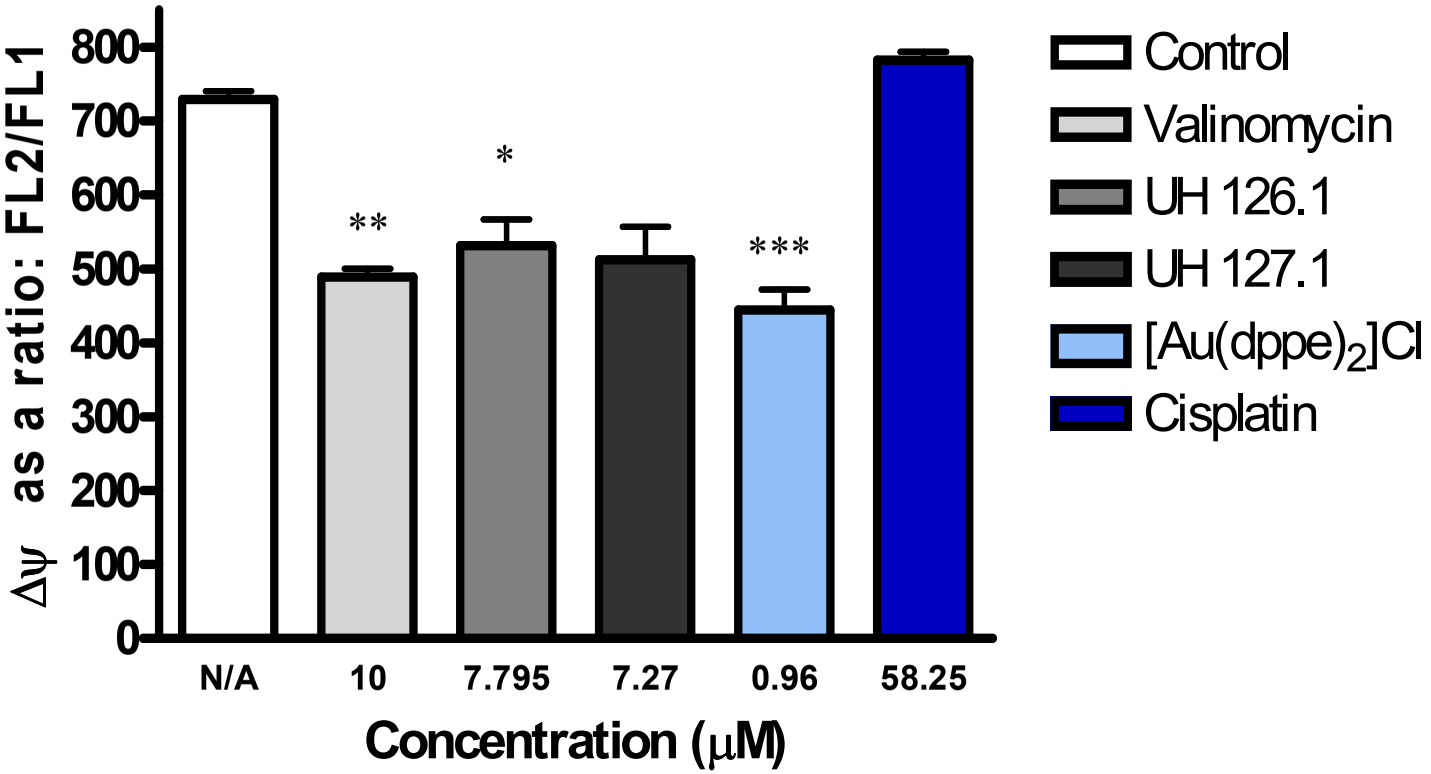

Figure 5.6. Flow cytometric analysis of the mitochondrial membrane potential (MMP) of PHA stimulated lymphocytes stained with JC-1 after exposure to valinomycin, UH 126.1, UH 127.1, $[Au(dppe)_2]Cl$ and cisplatin for 24 hours. The concentration of each experimental compound is 5 x IC_{50} determined for PHA stimulated lymphocytes. FL 1 indicates green fluorescence and FL2 indicates orange fluorescence. Error bars reflect the standard error of the mean (SEM). *$p \leq 0.05$ when compared to the untreated control; **$p \leq 0.01$ when compared to the untreated control; ***$p \leq 0.001$ when compared to the untreated control.

5.7 DISCUSSION

The collapse of the MMP was determined by using Jurkat cancer cells and normal PHA stimulated lymphocytes. The tested compounds (the lipophilic cation $[Au(dppe)_2]Cl$, the novel gold(I)-azole combination compounds UH126.1 and UH 127.1, cisplatin and the positive control valinomycin), was added to the cells for a period of 24 hours. The effect of each compound on the MMPs of these two cell cultures was determined via flow cytometry.

It is proposed that the mitochondria are the primary target for the gold(I)phosphine compounds (Berners-Price *et al*. 2002). These findings are supported by the results obtained in this experiment. The induction of MMP collapse indicated the involvement of mitochondria when inducing cytotoxicity via the apoptotic pathway. In this study, the gold(I)phosphine, $[Au(dppe)_2]Cl$, induced MMP collapse at all the tested concentrations in both Jurkat cells and PHA stimulated lymphocytes. The depolarisation of the MMP increased in a dose-dependant manner with the addition of $[Au(dppe)_2]Cl$ to the cells. The lack of selectivity of this compound is evident in that the MMP was depolarised significantly in the cancer cells as well as normal cells.

As expected, cisplatin did not induce the collapse of the MMP of Jurkat cells or PHA stimulated lymphocytes. This is explained by the proposed mechanism of action of cisplatin that has been described previously (Thurston *et al*. 2007; Yu *et al*. 2008). Cisplatin induces cytotoxicity through the formation of DNA intrastrand cross-links and does not involve the mitochondria (Thurston *et al*. 2007; Yu *et al*. 2008).

The novel compound, UH 126.1, induced the depolarisation of the MMP in Jurkat cells at a very high concentration (five times that of the IC_{50}). This compound also caused the collapse of the MMP when added to PHA stimulated lymphocytes at concentrations double- and five times that of the IC_{50}.

No effects on the MMP were induced with the addition of UH 127.1 to Jurkat cells. When this compound was added to PHA lymphocytes, it was observed that an increase in

MMP depolarisation was accompanied by increased concentrations of added UH 127.1. However, this was not statistically significant.

Although the MMP remained almost unaltered by UH 126.1 and UH 127.1 at low concentrations, some involvement of mitochondria was indicated at higher concentrations in both Jurkat cells (at a very high concentration of UH 126.1) and PHA stimulated lymphocytes (at high concentrations of UH 126.1 and UH 127.1), as evidenced by MMP depolarisation. From this evidence presented, at the lower concentrations, it is not likely that mitochondria are the primary target of UH 126.1 and UH 127.1, however, the involvement of mitochondria at higher concentrations cannot be discounted.

CHAPTER SIX

DETERMINATION OF EFFECTS ON CELL CYCLE DIVISION

6.1 INTRODUCTION

All cancer cells are able to proliferate unchecked, which enables them to surpass biochemical checkpoints that normally assess cellular viability and control growth (Perchellet *et al*. 2005). In order to inhibit the hyper proliferation state of cancer cells, most anticancer drugs target the cell cycle (Lee and Schmitt, 2003) at certain checkpoints. At these checkpoints, it is confirmed whether the cell can proceed or whether it should abort further division due to the detection of cell damage.

The cell cycle can be divided into two phases namely interphase and mitosis (Fairbanks and Andersen 1999). During interphase cell growth takes place in the first gap (G1) phase, DNA duplication happens during the synthesis (S) phase and cells continue to grow during the second gap (G2) phase. Mitosis consists of orderly cell division into two daughter cells over various stages (**Figure 6.1, page 81**). There are checkpoints between the G1 and S phase, during the S phase, at the end of the G2 phase and at the end of mitosis (Perchellet *et al*. 2005).

Some of the checkpoints require the interaction of enzymes, cyclins and cyclin-dependent kinases (cdks), which make these enzymes and cdks valuable drug targets (Perchellet *et al*. 2005). During the G1 phase, messenger RNAs and proteins necessary for DNA replication are synthesized. The cyclin D/cdk 4+6 complex phosphorylates the retinoblastoma (Rb) protein, after which the transcription factor, E2F, is released. Subsequently, the genes for the components essential for DNA synthesis (i.e. cyclins E and A, DNA polymerase, thymidine kinase, dihydrofolate reductase etc.) are activated. The activated cyclin E/cdk 2 complex is critical for transition from G1 to S phase. During S phase, phosphorylation of cyclin E/cdk 2 and cyclin A/cdk 1+2 activates proteins/enzymes involved in DNA synthesis. Cells then progress to G2 phase, during which cells contain double the number of chromosomes and must duplicate all other

components during mitosis. Cyclin A/cdk 1+2 and cyclin B/cdk 2 are active during G2 phase and regulate entry into mitosis. The presence of cyclin B/cdk 2 complex in the nucleus is required for commencement of mitosis (Rang *et al*. 2007). It is thus evident that cdk- and enzyme inhibitors can regulate the cell cycle negatively, leading to activation of the apoptotic cascade (**Figure 6.1, page 81**) (Rang *et al*. 2007).

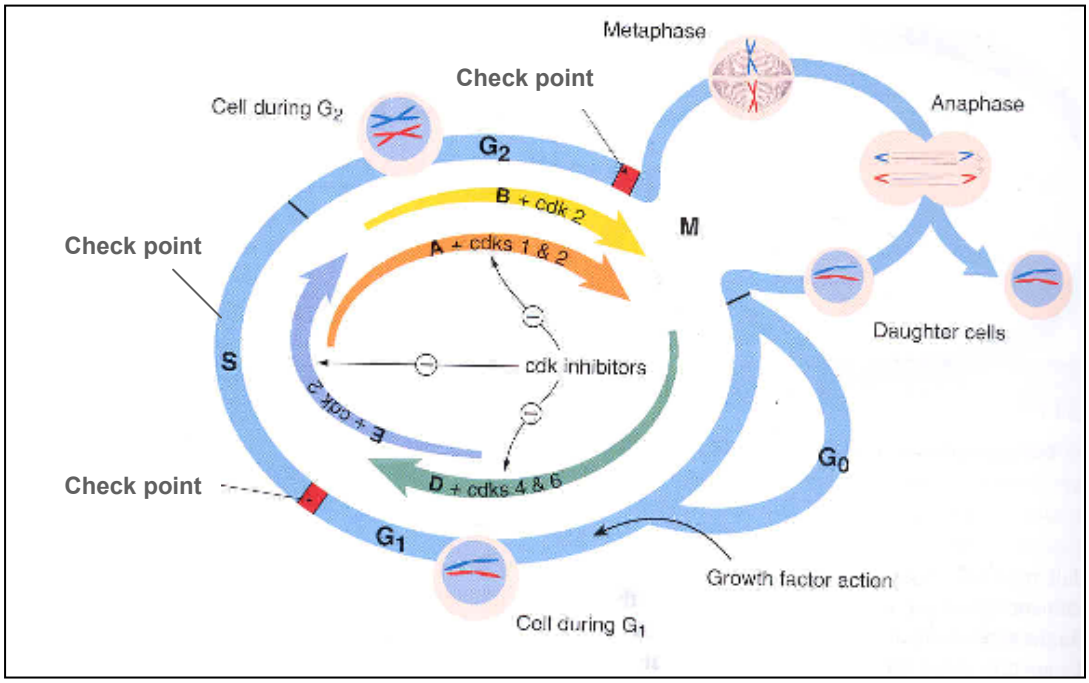

Figure 6.1. Schematic diagram of the cell cycle, showing the role cyclin/cyclin-dependant kinase complexes. Adapted from Rang *et al*. 2007; Lewin 1995.

Drugs can interfere with the cell cycle directly, such as (i) drugs that interfere with DNA synthesis (e.g. cisplatin) (Thurston *et al.* 2007), (ii) drugs that introduce DNA damage (e.g. some au(I)phosphines) (Berners-Price *et al.* 1986) and (iii) drugs that inhibit the function of the mitotic spindle (e.g. taxanes) (Schmidt and Bastians 2007). Alternatively, compounds can target the cell cycle indirectly via interference with cdks (e.g. azole derivatives) (Chen *et al*. 2008; Forgue-Laffite 1992; Sengupta *et al*. 2007) and enzymes (e.g. topoisomerase inhibitors) (Ichiro *et al.* 2007) that are necessary for cell replication.
A standard flow cytometric method was used for the cell cycle analysis of Jurkat cells, as described by Scott *et al*. (2004). Propidium Iodide (PI) is a nucleic acid stain, which

quantitatively indicates the DNA content present in each phase of the cell cycle. Cells that are in the G1 phase have a defined amount of DNA (i.e. diploid chromosomal DNA content). During S phase, cells contain DNA levels between the above-mentioned defined amount and double the defined amount. Within the G2/M phases, cells have double the amount of DNA (i.e. tetraploid chromosomal DNA content). There is thus a standard number of DNA present in each phase of the cell cycle. Hence, by quantifying the amount of DNA present in a cell, it can be determined in which phase the cell cycle has been arrested.

6.2 AIM

To determine the effect of the novel compounds, UH 126.1 and UH 127.1 on the cell cycle progression of Jurkat cells.

6.3 MATERIALS

Cell counting fluid

A volume of 1ml of a 0.1% crystal violet solution and 2ml glacial acetic acid was dissolved in 97ml of distilled water. The solution was mixed well and refrigerated until use.

Experimental compounds

A 10mM stock solution was prepared by dissolving the appropriate mass of each compound (UH 126.1, UH 127.1, $[Au(dppe)_2]Cl$ and cisplatin) in dimethyl sulphydroxide (DMSO) (obtained from Merck, Darmstadt, Germany). The volume of 50µl of each compound was aliquoted in eppendorf vials and stored at -70°C. Dilutions were prepared in the appropriate supplemented medium.

Jurkat cells

Human T –lymphocyte leukaemia (NRBM no TIB-152) were maintained in RPMI 1640 medium with 10% bovine FCS.

Phosphate buffered saline (PBS)

A mass of 0.923g of FTA hemagglutinin buffer powder (The Scientific Group, JHB, SA) was dissolved in 100ml of distilled water. The pH was adjusted to 7.2.

Propidium Iodide

A [50µg/ml] solution was made up in either PBS or sodium citrate (BD Bioscience, JHB, SA)

Roswell Park Memorial Institute Medium (RPMI) 1640

RPMI 1640 powder (Sigma-Aldrich, JHB, SA) was dissolved in sterile water with the aid of a sterile stirrer. The pH of the solution was adjusted to 4 with 1M HCl to ensure complete solubilisation. Thereafter 2mg of $NaHCO_3$ was added to each litre of the medium. The pH was readjusted to 7.1 through the addition of either 1M HCl or 1M NaOH. The medium was filter-sterilized through a 0.22µm filter and divided into 500ml aliquots. A volume of 55ml was removed from the 500ml aliquot and the remaining solution was supplemented with 5ml of a 1% penicillin/streptomycin solution and 50ml sterile HI FCS. The medium was stored at 4ºC until use.

RNAse

A concentration of 2mg/ml was made by dissolving RNAse (Sigma-Aldrich, Steinheim, Germany) in 1.12%w/v sodium citrate.

6.4 METHODS

6.4.1 Passaging the cells

1. Jurkat cells were cultured and maintained in RPMI medium with 10% bovine FCS at 37ºC in an incubator supplemented with 5% CO_2.
2. The culture medium was discarded from a 75cm^2 flask.
3. The cell suspension was transferred to a 15ml centrifuge tube and centrifuged at 1000 rpm for 5 minutes.

4. The supernatant was discarded after which 1ml medium supplemented with foetal calf serum (FCS) were added to the cell pellet and aspirated to form a suspension.

6.4.2 Counting the cells

1. A volume of 50µl of the cell suspension was added to 450µl white cell counting fluid (**refer to section 6.4.1, page 83)**.
2. This suspension was then added to the Haemocytometer and cells were counted using a Reichert-Jung Microstar 110 microscope at a magnification of 40 times.
3. The cells were re-suspended to obtain the relevant cell concentration for this experiment (3×10^5 cells per ml).

6.4.3 Experimental procedure

1. Jurkat cells, at the concentration of 3×10^5 cells per ml (**refer to section 6.4.2, page 84**), were incubated in culture flasks with the required concentrations (equal to the IC_{50}, double the IC_{50}, five times the IC_{50}) (**refer to Chapter 3, Table 3.1, page 43**) of each experimental compound at 37ºC in an incubator supplemented with 5% CO_2.
2. The cell suspensions were incubated in the presence of the experimental compounds for 24 and 48 hours at three different concentrations.
3. After the required incubation period, the cells were centrifuged at 200g for 5 min.
4. The cells were then resuspended in a volume of 500µl PBS and chilled on ice for 10 minutes.
5. Standard flow cytometer tubes containing 500µl of ice cold 100% ethanol were prepared.
6. The cold cell suspension was aspirated rapidly into the cold ethanol.
7. The suspension remained on ice for 15 minutes.
8. The cell suspension was centrifuged for 3 minutes at 300g after which as much supernatant as possible was removed without disturbing the cell pellet.
9. 125µl RNAse was added to the cells in each tube.
10. The cell suspensions were incubated in a water bath for 15 minutes at 37ºC.

11. After incubation, 125µl of propidium iodide (PI) stain solution (BD Bioscience, JHB, SA) was added to the cells and mixed.
12. The cell suspensions were kept in the dark at room temperature for at least 30 minutes before analysis on the flow cytometer (FC 500 Series Beckman Coulter).

6.5 EXPRESSION OF RESULTS

DNA concentration profiles were produced through PI staining of nucleic acid within ethanol-induced membrane-permeabilised cells. The PI staining was quantified and cells were classified into three different phases of the cell cycle: G1 phase, S phase or G2/M phase. The results were acquired in the form of a histogram (created by internal FC 500 Series Beckman Coulter flow cytometric software), and were then quantified, which classified the total number of cells into one of three phases, i.e. G1 phase, S phase or G2/M phase. Results are expressed as the mean percentage of cells in each phase ± SEM. Statistical evaluation was done by a Mann-Whitney non-parametric test (**refer to Appendix A, 5.1, a-b, page 136**) with GRAPHPAD Statistical Software© program (**refer to Appendix A, 5.1, c, page 136**). The difference was considered statistically significant at $p \leq 0.05$.

6.6 RESULTS

The percentage of Jurkat cells classified to each phase of the cell cycle is presented in **Table 6.1, page 88**. The Jurkat cells were exposed to the experimental compounds at three different concentrations: (i) equal to the IC_{50}, (ii) double the IC_{50}, and (iii) five times the IC_{50} over two different exposure times (24 hours and 48 hours). Cells were quantified and classified into three different phases of the cell cycle: G1 phase, S phase or G2/M phase.

Results showed that the greatest percentage of the Jurkat cells that were treated with $[Au(dppe)_2]Cl$, accumulated in the G1 phase with a concurrent decrease of cells in the S phase and G2/M phase (**Table 6.1, page 88**). After 24 hours incubation, significant accumulation of cells in the G1 phase was induced by $[Au(dppe)_2]Cl$ at all three

concentrations. Cell accumulation in the G1 phase was 72.27% for the concentration equal to the $IC_{50,}$ 74.43% for the concentration double the IC_{50} and 67.02% for the concentration five times the IC_{50} in comparison with the untreated control (62.02%). Similarly, even after 48 hours, significant accumulation in the G1 phase was induced by all three concentrations of $[Au(dppe)_2]Cl$. Hence, at concentrations (i) equal to the IC_{50}, (ii) double the IC_{50} ,and (iii) five times the IC_{50} cell accumulations of 62.75%, 63.97%, and 62.44% were observed when compared to the untreated control of 55.93% respectively.

Data exhibited a trend that Jurkat cells, exposed to UH 126.1 (for 24 and 48 hours at concentrations equal to the previously determined IC_{50}, double the IC_{50}, and five times the IC_{50}) accumulated in the G1 phase when compared to the untreated control (**Table 6.1, page 88**). After 24 hours, 66.76%, 64.51% and 69.75% ($p \leq 0.05$) of cells that were treated with the three respective concentrations of UH 126.1, accumulated in the G1 phase vs. 62.02% for untreated control cells. A significant decrease in percentage of cells in the S phase was detected where concentrations double the IC_{50}, and five times the IC_{50} were added to the cells. Results were similar after 48 hours where UH 126.1 induced accumulation of cells in G1 phase at all three concentrations [57.78%, 64.22% ($p \leq 0.05$), 60.34% ($p \leq 0.05$)] compared to the untreated control (53.93%).

Results indicated that no significant accumulation in any of the phases were induced in the Jurkat cells after addition of UH 127.1 for a period of 24 hours at concentrations equal to the previously determined IC_{50}, and five times the IC_{50}. There was, however, an increase in cells in the G1 phase when UH 127.1 was added at a concentration double that of the IC_{50}, with a subsequent decrease in the percentage of cells in the S phase (27.23% vs. 33.41% of untreated control cells) (**Table 6.1, page 88**). The accumulation of UH 127.1 treated cells in the G1 phase was more apparent after 48 hours [58.01%, 59.39% and 64.62% ($p \leq 0.05$) for the respective concentrations vs. 55.93% of untreated control cells] (**Table 6.1, page 88**).

According to the results, cisplatin caused a significant accumulation of cells in the S phase of the cell cycle at all three concentrations after exposure to Jurkat cells after both 24 hours (38.95%, 36.15% and 41.22% respectively) and 48 hours (40.46%, 39.23% and 42.65% respectively) when compared with the untreated control (33.41% after 24 hours and 34.02% after 48 hours). This was accompanied by a co-comittant decrease percentage of cells that accumulated in the G1 and G2 phases (**Table 6.1, page 88**).

When compared to the untreated control, cell progression to the G2/M phase decreased significantly after 48 hours of exposure to the experimental compounds ($[Au(dppe)_2]Cl$, UH 126.1, UH 127.1 and cisplatin). The percentage of untreated control cells in the G2/M phase after 24 hours (4.56%), doubled after 48 hours (10.05%), whereas the percentages of drug treated cells in the G2/M phase remained virtually unchanged from 24 hours to 48 hours (**Table 6.1, page 88**). This is indicative that all four experimental compounds ($[Au(dppe)_2]Cl$, UH 126.1, UH 127.1, and cisplatin) inhibited/arrested further cell replication.

Table 6.1 Cell cycle analysis of Jurkat cell lines after exposure to three different concentrations (μM) of each experimental compound at two different exposure times.

Assessment of cell cycle progression in Jurkat cells		Incubation time: 24 hours			Incubation time: 48 hours		
Experimental Compound	**Concentration (μM)**	**G1 phase**	**S phase**	**G2/M phase**	**G1 phase**	**S phase**	**G2/M phase**
		Mean percentage (%) cells ± SEM [1]					
Control	N/A	62.02 ± 0.05	33.41 ± 0.03	4.56 ± 0.45	55.93 ± 0.10	34.02 ± 0.01	10.05 ± 0.01
UH 126.1	0.119 (IC_{50})	66.76 ± 0.09	27.45 ± 0.21	5.76 ± 0.90	57.78 ± 0.09	37.62 ± 0.20	4.60 ± 1.01*
	0.238 (IC_{50}×2)	64.51 ± 0.04	29.52 ± 0.03*	5.99 ± 0.56	64.22 ± 0.08*	31.25 ± 0.10	4.20 ± 0.45*
	0.595 (IC_{50}×5)	69.75 ± 0.08*	25.20 ± 0.08*	5.06 ± 0.72	60.34 ± 0.01*	33.53 ± 0.04	6.13 ± 0.08*
UH 127.1	0.075 (IC_{50})	60.31 ± 0.03	32.47 ± 0.08	7.22 ± 0.41	58.01 ± 0.03	35.56 ± 0.05	5.76 ± 0.20*
	0.150 (IC_{50}×2)	66.62 ± 0.11	27.23 ± 0.15*	6.16 ± 0.51	59.39 ± 0.06	33.80 ± 0.07	6.80 ± 0.22*
	0.375 (IC_{50}×5)	61.18 ± 0.03	32.49 ± 0.09	6.33 ± 0.20	64.62 ± 0.03*	29.27 ± 0.10	5.44 ± 0.16
$[Au(dppe)_2]Cl$	0.081 (IC_{50})	72.27 ± 0.05*	24.64 ± 0.09*	3.09 ± 0.54	62.75 ± 0.07*	32.89 ± 0.14	4.36 ± 0.44*
	0.162 (IC_{50}×2)	74.43 ± 0.04*	22.56 ± 0.12*	2.99 ± 0.03	63.97 ± 0.08*	30.57 ± 0.14*	5.46 ± 0.45*
	0.405 (IC_{50}×5)	67.02 ± 0.19	23.05 ± 0.38*	9.91 ± 0.90	62.44 ± 0.03*	34.62 ± 0.07	2.42 ± 0.36*
Cisplatin	0.413 (IC_{50})	57.33 ± 0.06	38.95 ± 0.08*	3.72 ± 0.86	53.94 ± 0.01*	40.46 ± 0.07*	5.60 ± 0.47*
	0.826 (IC_{50}×2)	60.80 ± 0.09	36.15 ± 0.09*	3.05 ± 0.73	54.13 ± 0.08	39.23 ± 0.02*	6.64 ± 0.51*
	2.065 (IC_{50}×5)	51.61 ± 0.16	41.22 ± 0.16*	7.17 ± 0.70	51.06 ± 0.06*	42.65 ± 0.05*	6.29 ± 0.35*

* $p \leq 0.05$ when compared to the untreated control

1. Average of three experiments

6.7 DISCUSSION

The effect of UH 126.1 and UH 127.1 on the cell cycle progression of Jurkat cells was determined in this experiment. According to Lee and Schmitt (2003), the cell cycle is a valuable target in cancer chemotherapy, due to the end result being apoptotic cell death.

The results clearly indicated that the lipophilic control compound, $[Au(dppe)_2]Cl$, caused cell accumulation in the G1 phase with a concurrent decrease in the percentage of cells classified to the S phase and G2/M phase being observed. These results correlate with previous findings, which stated that gold(I)phosphines induce cell growth inhibition by means of elongation of the G1 phase in cells (Zhang and Lippard 2003). This could be explained by previous findings, which stated that, although not the primary mechanism of action, some gold(I) phosphines induce DNA-protein cross-links and DNA strand breaks (Berners-Price *et al*. 1986).

In this study, cisplatin induced an increase of cells accumulating in the S phase. (Bergamo *et al*. 1999; Wilkins *et al.* 1997). This finding is consistent with previous studies and might be ascribed to the S phase being slowed down (Sorenson and Eastman 1988), or due to complete S phase arrest (Ishibashi and Lippard 1998). Since DNA synthesis occurs during the S phase, the accumulation of cells in this phase upon exposure to cisplatin, is consistent with the well known mode of action of the drug, which involves the formation of platinum bonded purine intrastrand cross-links (Wang and Lippard 2005).

The data demonstrated a trend that the novel azole-containing compounds cause cell accumulation in the G1 phase with a resultant decrease in the percentage of cells continuing to the S phase and G2/M phase. Various studies have indicated that azole derivatives induce cell cycle arrest in the G1 phase due to different mechanisms. Some of these mechanisms include inhibition of the cdks, inhibiting cell cycle regulator enzymes (such as polymerases, dehydrofolate reductase etc.) (Chen *et al*. 2008; Forgue-Laffite 1992; Sengupta *et al*. 2007) and DNA adduct formation (Trapani *et al*. 2003).

All the experimental compounds induced cytotoxicity after an incubation period of 24 hours, leading to cell cycle arrest at that point (Lewin 1995). In contrast to this, the untreated control cells were able to progress to a further cell cycle, which resulted in an increase in cells proceeding to the G2/M phase. This was confirmed experimentally with only some (≈5%) of the drug treated proceeding to the G2/M phase after 48 hours, whereas 10.05% was observed for the untreated control cells.

It is deduced from this study that the novel azole-containing compounds, UH 126.1 and UH 127.1, induce cell accumulation in the G1 phase, possibly due to interference with cyclin dependant kinases or cell cycle regulator enzymes as in the case of other azole-derivatives (Chen *et al*. 2008; Forgue-Laffite 1992; Sengupta *et al*. 2007).

CHAPTER SEVEN

ASSESSMENT OF *IN VIVO* ACUTE TOXICITY

7.1 INTRODUCTION

Although previously tested gold compounds were cytotoxic to cancer cells, they were still too toxic *in vivo* for clinical use (Berners-Price *et al*. 1999; Hoke *et al*. 1989). Due to severe hepatotoxicity, cardiotoxicity, and vascular toxicity in Beagle dogs during a pre-clinical study of $[Au(dppe)_2]Cl$, further development was abandoned (Hoke *et al*. 1989). Pertaining to azoles, side effects such as severe gastrointestinal side effects, hepatotoxicity, myelosuppression, neutropenia, and nausea have limited the clinical use of azole derivatives, however, the further investigation of azoles combined with other classes of chemotherapeutic agents has been identified as an area worth investigation (Rodriguez and Acosta 1995; Magedov *et al*. 2007). The use of metals in medicine has precedence, since even to this day platinum containing compounds are the most widely used chemotherapeutic agents. However, even for this class of compounds severe side effects (such as emesis, nephro- oto- and neurotoxicity, asthenia and gastrointestinal toxicity) limit their clinical use, which necessitates the continued investigations into the development of new classes of metal containing anti-tumour agents (Boulikas 2004).

The newly synthesized compounds containing gold and azoles were tested *in vivo* in a mouse model according to the method used by Berners-Price *et al*. (1999). It is known that elevated plasma levels of AST (aspartate amino transferase), ALT (alanine amino transferase) and GGT (gamma-glutamyl transpeptidase) are indicative of liver damage (Schiff *et al*. 2006). Parameters indicative of nephrotoxicity include elevated plasma urea and creatinine levels (Gross *et al*. 2005; Sinha *et al*. 2008). Plasma concentrations of these liver and kidney markers together with organ and body weights, whole blood analysis and observation of the mice were used as indicators of induced toxicity in the experimental animals. In this study, the *in vivo* acute toxicity of the novel compounds, UH 126.1 and UH 127.1, was determined.

7.2 AIM

To determine the *in vivo* toxicity of the novel compounds UH126.1 and UH 127.1 in mice.

7.3 MATERIALS

Animals

Female syngeneic Balb/C mice of 6-8 weeks from the same breeding batch were used (Berners-Price *et al*. 1986). Animals were housed in groups of six in individually ventilated (IVC) mouse cages in rooms with controlled environmental conditions (temperature: 22±2ºC, humidity: 40%-60%). Environmental enrichments were allowed. The animals were fed irradiated Purina 5LG4 and water *ad libitum*.

7.4 METHODS

7.4.1 Dosage, route of administration and sample size

In this acute toxicity study, experimental compounds (UH 126.1 and UH 127.1) were injected intraperitoneally (i.p.) Intermediate starting dosages of 6µmol/kg and 3µmol/kg daily from day one to five were administered i.p. to the experimental animal groups. These dosages were selected as suitable starting doses based on the maximum tolerated dose of $[Au(dppe)_2]Cl$, documented as 3µmol/kg in the literature (Berners-Price *et al*. 1986), and on the *in vitro* cytotoxic findings in this study. Although the starting doses for the experimental compounds are higher than the maximum tolerated dose of $[Au(dppe)_2]Cl$, the tumour specificities of both the experimental compounds UH 126.1 and UH 127.1 are however ± nine fold higher than that of $[Au(dppe)_2]Cl$ (**refer to Chapter 3, Table 3.2, page 48)**. It was determined that, should any adverse events occur, lower dosages would be administered during the following phase. The weight of each mouse was determined to adapt the dosages according to their body weight. Due to the water insoluble nature of the experimental compounds, the chosen solvent for this study was a DMSO (0,5%) - olive oil solution. Olive oil, as a drug-carrying vehicle, has been used in previous studies (Anger *et al*. 2006; De la Portilla *et al*. 2004). A final dose volume of 0,5ml per mouse was administered i.p. The DMSO-olive oil solution was also

administered to the control groups during each phase. The dosages were prepared immediately prior to each i.p. injection with a 26 gauge insulin needle.

A total of 45 female syngeneic Balb/C mice were used in this study (Berners-Price *et al*. 1986). The study was divided into three phases (phase one, two and three). Each phase was designed to consist of three groups of mice, where a maximum of six mice were assigned to each group. Hence, a maximum of 18 mice were allowed for each phase. Phase one (**Table 7.1, page 94**) investigated the novel compound UH 126.1 at two intermediate starting dosages (3µmol/kg and 6µmol/kg) for five consecutive days in comparison with an untreated control group. Phase two (**Table 7.2, page 94**) investigated the novel compound UH 127.1 at two intermediate starting dosages (3µmol/kg and 6µmol/kg) for five consecutive days in comparison with a control group. The study proceeded to phase three where the dosage was lowered for both compounds due to observed adverse effects during phases one and two. Phase three (**Table 7.3, page 94**) investigated the novel compounds UH 126.1 and UH 127.1 at a lower dosage (1,5µmol/kg) for five consecutive days in comparison with a control group.

The animals were weighed daily and monitored for pain and distress (behavioural changes). Toxicity was determined by evaluation of reduced food and water intake resulting in weight loss (more than 20% original weight), observation of abnormal movement (particularly as it pertains to the ability of the animal to obtain food and water) and ease of breathing. Any animal showing signs of pain and distress would have been euthanized immediately with CO_2 overdose. If two or more animals in a group were to show these signs, the whole group would have been euthanized and no further testing of the specific dosage would take place.

After the last day of the investigation (day six), mice were euthanized with isofluorane, where after maximum blood was drawn via cardiac puncture by a staff member at University of Pretoria Biomedical Research Centre (UPBRC). The Department of

Clinical Pathology at the Faculty of Veterinary Science, University of Pretoria was responsible for haematological analysis and enzyme level determination.

Table 7.1. Description of phase one

	Dosage
Control group	Olive oil-DMSO solution, 0,5ml daily from day 1 to 5 administered i.p. to 6 mice (0,5% DMSO)
UH 126.1	0,5 ml of 3µmol/kg daily from day 1 to 5 administered i.p. to 6 mice (0,5% DMSO)
UH 126.1	0,5 ml of 6µmol/kg daily from day 1 to 5 administered i.p. to 6 mice (0,5% DMSO)

Table 7.2. Description of phase two

	Dosage
Control group	Olive oil-DMSO solution, 0,5ml daily from day 1 to 5 administered to 6 mice (0,5% DMSO)
UH 127.1	0,5 ml of 3µmol/kg daily from day 1 to 5 administered i.p. to 6 mice (0,5% DMSO)
UH 127.1	0,5 ml of 6µmol/kg daily from day 1 to 5 administered i.p. to 6 mice (0,5% DMSO)

Table 7.3. Description of phase three

	Dosage
Control group	Olive oil-DMSO solution, 0,5ml daily from day 1 to 5 administered to 6 mice (0,5% DMSO)
UH 126.1	0,5 ml of 1,5µmol/kg daily from day 1 to 5 administered i.p. to 6 mice (0,5% DMSO)
UH 127.1	0,5 ml of 1,5µmol/kg daily from day 1 to 5 administered i.p. to 6 mice (0,5% DMSO)

7.4.2 Parameters of toxicity

Toxicity was determined by evaluation of reduced food and water intake resulting in weight loss (more than 20% original weight), observation of abnormal movement (particularly as it pertains to the ability of the animal to obtain food and water) ease of breathing, and observed piloerection. In addition to observed adverse effects, standard liver markers (AST, ALT and GGT) and kidney markers (urea and creatinine) were analysed by the Department of Clinical Pathology at the Faculty of Veterinary Science, University of Pretoria. A whole blood profile was done on all the blood samples.

7.5 EXPRESSION OF RESULTS

7.5.1 Body weight changes

The mean body weight changes ± SEM, in grams, are graphically presented in **Figures 7.1-7.3, pages 101-103**. Each group served as its own control. The mean body weight of each group of mice on each day (day 2-6) was compared to the mean body weight of the same group as measured on first day of the study. For example the mean body weight on day 4 of the mice in the group that received UH 126.1 (3µmol/kg) was compared to the mean body weight of this same group as measured on day one. Statistical evaluation was done by a Wilcoxon signed-rank non-parametric test (**refer to Appendix A, 6.1, a-b, page 137**) with GRAPHPAD Statistical Software© program (**refer to Appendix A, 6.1, c, page 137**). The difference was considered statistically significant at $p \leq 0.05$.

The mean percentage body weight changes are presented graphically in **Figure 7.4, page 104**, with the first day of study being represented as 100% body weight. The mean body weight percentages for each group of mice on each of days 2-6 were calculated with the formula:

body weight % =

[mean body weight (group x) (day x) / mean body weight (group x) (day 1)] x 100

7.5.2 Liver and kidney markers, haematology, organ weights

Results pertaining to the plasma liver enzymes and plasma kidney markers are expressed as the mean ± SEM. The organ weights and haematology results are indicated as the mean ± SD.

The organ weight / body weight ratio was determined with the formula:

Ratio = (mean organ weight / mean body weight) x 1000

Results are expressed as mean ratio ± SEM.

The mean values ± SEM/SD for each measured parameter, including liver and kidney markers, organ weight ratios and haematology, were obtained for the untreated control group in each phase. Statistical evaluation was done with a Kruskal-Wallis non-parametric test (**refer to Appendix A, 6.2, a-b, pages 137-138**) with GRAPHPAD Statistical Software© program (**refer to Appendix A, 6.2, c, page 138**) in order to determine whether a statistically significant variation existed between the measured values of the untreated control groups of a specific parameter at different phases of the study. The analysis revealed that there was no significant variation between the untreated control values measured at each phase for each of the respective parameters (AST, ALT, GGT, urea, creatinine, organ weight ratio, haematological parameters) (data not shown).

Hence, the average of the means for each of the untreated control groups measured in each phase was used to determine whether there is a statistical difference between the measured parameters in the drug treated groups vs. control groups. To conduct this analysis the Mann-Whitney non-parametric test (**refer to Appendix A, 6.3, a-b, page 138**) and GRAPHPAD Statistical Software© program (**refer to Appendix A, 6.3, c, page 139**), was used.

7.6 RESULTS

Groups of mice were treated in each phase as previously described in **Tables 7.1, 7.2 and 7.3, page 94.**

7.6.1 Observed adverse effects

The animals were observed on a daily basis in order to detect any abnormal behaviour that might indicate toxicity of the compounds. Adverse effects observed during the study included diarrhoea, severe piloerection and hyperactivity following dosage administration in the groups receiving UH 126.1 (at dosages of 3 and 6µmol/kg) in phase 1 and UH 127.1 (at dosages of 3 and 6µmol/kg) in phase 2. Piloerection, however, was not observed in the control group or the groups receiving 1.5µmol/kg of UH 126.1 or UH 127.1 (phase 3). Significant weight loss was apparent in phases 1 and 2 for the groups receiving UH 126.1 and UH 127.1 at dosages of 3 and 6µmol/kg (**Figures 7.1 -7.2, pages 101-102**). After initial weight loss in the groups receiving the lower dose (1.5µmol/kg) of UH 126.1 and UH 127.1, an increase in body weight was observed in phase 3 (**Figure 7.3, page 103**). It is possible that the weight loss was due to untreated diarrhoea, which severely affected the groups receiving 3 and 6µmol/kg of both compounds. Very slight diarrhoea, which was observed in the mice that received 1.5µmol/kg of both compounds, resolved almost completely, after which consecutive weight gain from day 3 onwards was observed in these groups.

While **Figures 7.1-7.3, pages 101-103,** display mass changes in grams, this data is expressed as percent (%) changes in weight in **Figure 7.4, page 104**. The data was normalised in order to start at a weight percentage of 100% on day one for all of the control- and test groups. It is evident that all of the control groups gained body weight from day one to six. However, for the groups that received UH 126.1 and UH 127.1 at 3µmol/kg and 6µmol/kg, respectively, a significant total weight loss was observed. On day six, percentage weight loss for the 3µmol/kg and 6µmol/kg doses of UH 126.1 was 5% and 7%, respectively, while for UH 127.1 at the same concentrations, weight reductions of 10% and 15% were detected. After significant initial weight loss (20%) on day two in the group that received 1.5µmol/kg of UH 126.1 an increase in body weight

was detected. The total percentage of weight loss as measured on day six was 3% for the group that received UH 126.1 at 1.5µmol/kg, and 6% for the group that received UH 127.1 at the same concentration. Weight gain would possibly have continued in the mice in both these groups were it not for the termination of the study.

7.6.2 Liver serum markers

The plasma levels of the liver markers, ALT, AST and GGT, were determined in this study for all the treatment groups (untreated control, UH 126.1 and UH 127.1, at concentrations of 1.5, 3 and 6µmol/kg as described in **Tables 7.1-7.3, page 94**). It is known that elevated AST and ALT levels are indicative of hepatocellular death and fatty degeneration, whereas elevated GGT levels are associated with hepatobiliary (cholestatic) blockage (Amacher 1998). The definition of liver injury is "an increase greater than two times the upper limit of normal range (ULN) in ALT or conjugated bilirubin or a combined increase in AST, Alk P, and total bilirubin provided that one of them is greater than two times the ULN" (Benichou 1990). The ULN of AST and ALT for female Balb/C mice (6-8weeks old), is indicated as 140 U/L and 18 U/L, respectively (Derelanko *et al.* 2002).

This study revealed that the detected plasma levels of AST and ALT in all of the treatment groups were less than twice the ULN as shown in **Figures 7.5-7.6, pages 105-106**. Furthermore, neither of the experimental compounds, UH 126.1 or UH 127.1, caused significant increases in plasma AST (**Figure 7.5, page 105**) or ALT (**Figure 7.6, page 106**) levels when compared to the untreated control group. AST levels were slightly increased with administration of UH 126.1 (1,5 µmol/kg) and UH 127.1 (1,5µmol/kg and 6µmol/kg) (**Figure 7.5, page 105**) when compared to the untreated control group. This was, however, not significant.

The ULN for GGT in Balb/C mice is not available (Derelanko *et al.* 2002). Results indicated a significant increase in GGT in the group that received UH 127.1 (6µmol/kg) when compared to the untreated control as shown in **Figure 7.7, page 107**.

7.6.3 Kidney serum markers

In this study, plasma creatinine and urea levels were determined in order to investigate possible nephrotoxicity. These are commonly used tests for determination of reduced renal function (Bishop 2005). Elevated urea and creatinine levels might indicate renal dysfunction (Bishop 2005). Normal published values in female Balb/C mice (6-8 weeks old) have been indicated as 5-9 mmol/L for urea, and 44-79.2 µmol/L for creatinine (Derelanko *et al.* 2002). Although all of the plasma urea and creatinine values in this study fall within these ranges, it must be taken into account that the study conditions (duration of study, environment, diet etc.) might have influenced these outcomes. It is, therefore, more reliable to compare each of the experimental groups with the untreated control group as was done in this study. Results from the present study revealed no significant increase in plasma creatinine levels (**Figure 7.8, page 108**), however, significant elevation of plasma urea concentrations (**Figure 7.9, page 109**) was detected in the mice that received UH 126.1 at the concentration of 1.5µmol/kg and UH 127.1 at the concentration of and 3µmol/kg, when compared to the untreated control.

7.6.4 Organ weights

It was determined in this study whether there was an increase in the organ weights of the mice by calculating the organ/body-weight ratio. Results are summarised in **Table 7.4, page 110**. At the end of the study there was a slight, but significant increase in the kidney weights of all the mice that received the experimental compounds (UH 126.1 and UH 127.1) at all of the concentrations tested. Liver weight increases were detected at lower doses of 1.5 and 3µmol/kg of the experimental compounds. The heart weights of the mice that were given UH 127.1 at doses of 3 and 6µmol/kg, also increased significantly.

7.6.5 Haematology

The results of the full blood counts are displayed in **Table 7.5, page 111**. Haematology results revealed that, in comparison with the untreated control group, there were slight but significant increases in the red cell count (RCC), haemoglobin (Hb) and haematocrit (HT) in groups that received UH 126.1 at doses of 3 and 6 µmol/kg. Data also indicated a slight decrease in mean corpuscular volume (MCV) in the groups that received UH 127.1 at concentrations of 1.5 and 3µmol/kg. Similarly, the mean corpuscular

haemoglobin (MCH), mean corpuscular haemoglobin concentration (MCHC) and red cell distributive width (RDW) in the groups that received 3 and 6µmol/kg of UH 127.1 also decreased when compared to the untreated control.

No significant changes were measured in the white cell counts (WCC) when values obtained for the test groups were compared to that of the untreated control group. This excludes the presence of infections and indicates that the bone marrow was not suppressed (Pagana et al.1998).

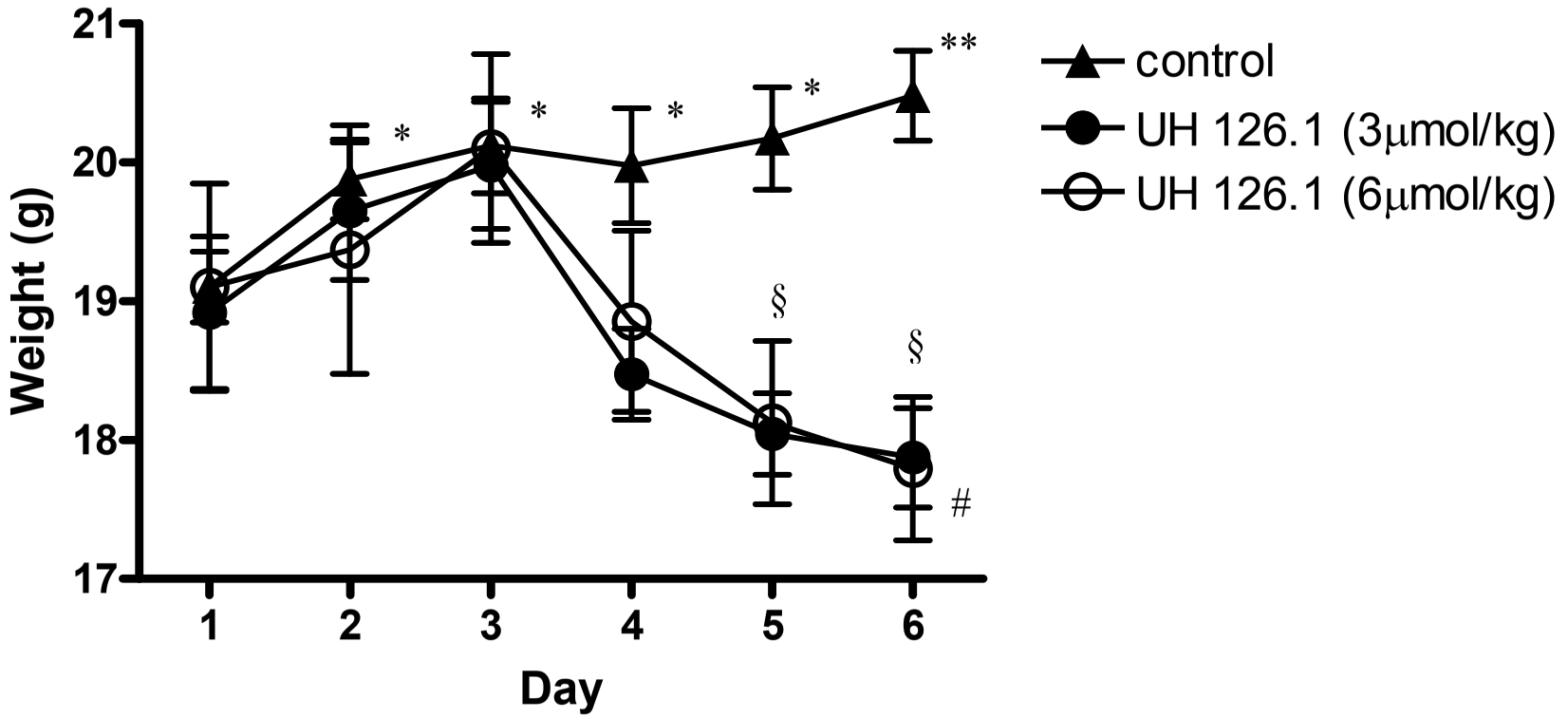

Figure 7.1. The mean daily body weights (g) of mice that received the DMSO-olive-oil solvent alone or UH 126.1 at two different concentrations for five consecutive days (phase 1). Error bars represent the standard error of the mean (SEM); * $p \leq 0.05$ when mean weight of the untreated control group on the relevant day is compared to the mean weight on day 1 of the same group; ** $p \leq 0.01$ when mean weight of the untreated control group on the relevant day is compared to the mean weight on day 1 of the same group; § $p \leq 0.05$ when the mean weight of the group receiving UH 126.1 (3 μmol/kg) on the relevant day is compared to the mean weight on day 1 of the same group; # $p \leq 0.05$ when the mean weight of the group receiving UH 126.1 (6 μmol/kg) on the relevant day is compared to the mean weight on day 1 of the same group.

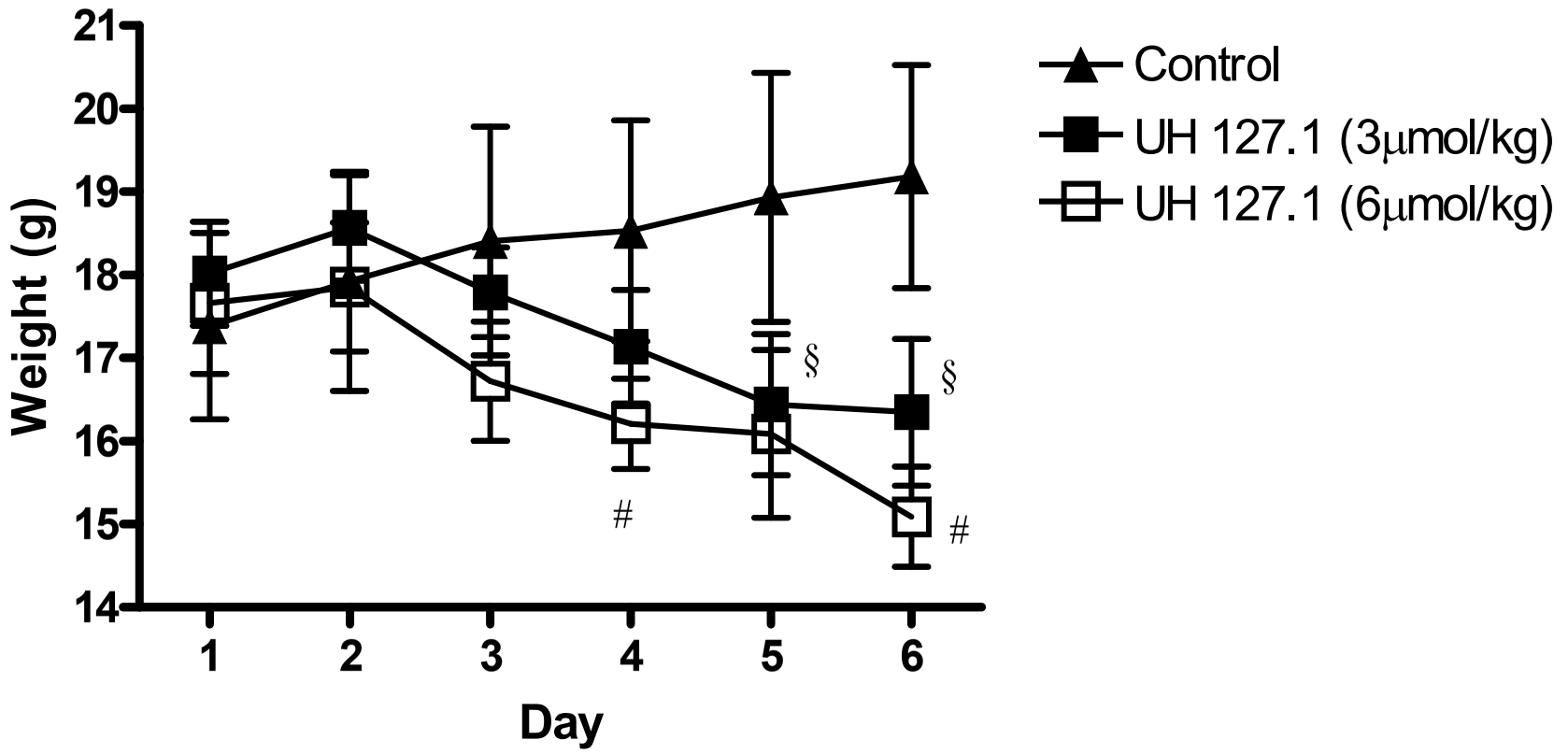

Figure 7.2. The mean daily body weights (g) of mice that received DMSO-olive-oil solvent alone or UH 127.1 at two different concentrations for five consecutive days (phase 2). Error bars represent the standard error of the mean (SEM); § $p \leq 0.05$ when the mean weight of the group receiving UH 127.1 (3 µmol/kg) on the relevant day is compared to the mean weight on day 1 of the same group; # $p \leq 0.05$ when the mean weight of the group receiving UH 127.1 (6 µmol/kg) on the relevant day is compared to the mean weight on day 1 of the same group.

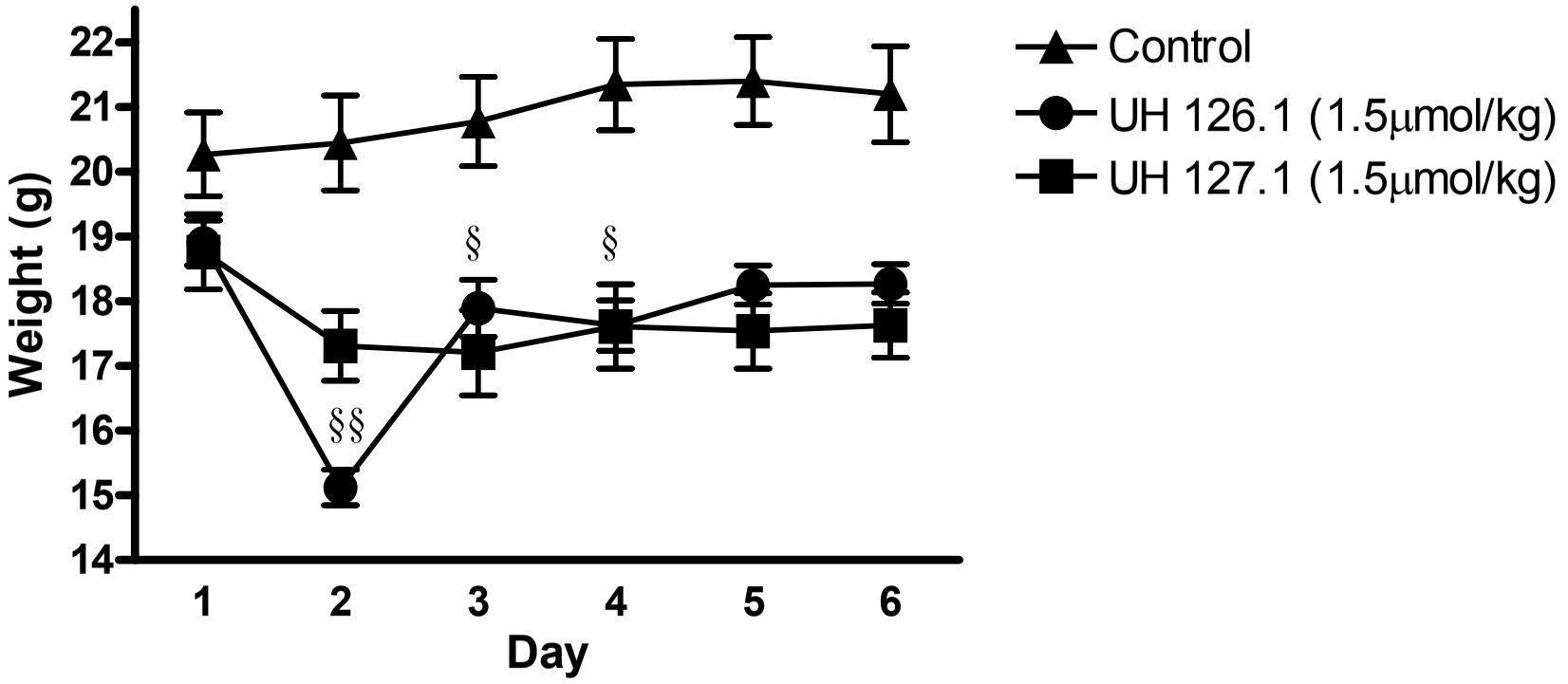

Figure 7.3. The mean daily body weights (g) of mice that received DMSO-olive-oil solvent alone, UH 126.1 or UH 127.1 at 1.5 µmol/kg for five consecutive days (phase 3). Error bars represent the standard error of the mean (SEM). § $p \leq 0.05$ when the mean weight of the group receiving UH 126.1 (1.5 µmol/kg) on the relevant day is compared to the mean weight on day 1 of the same group; §§ $p \leq 0.01$ when the mean weight of the group receiving UH 126.1 (1.5 µmol/kg) on the relevant day is compared to the mean weight on day 1 of the same group.

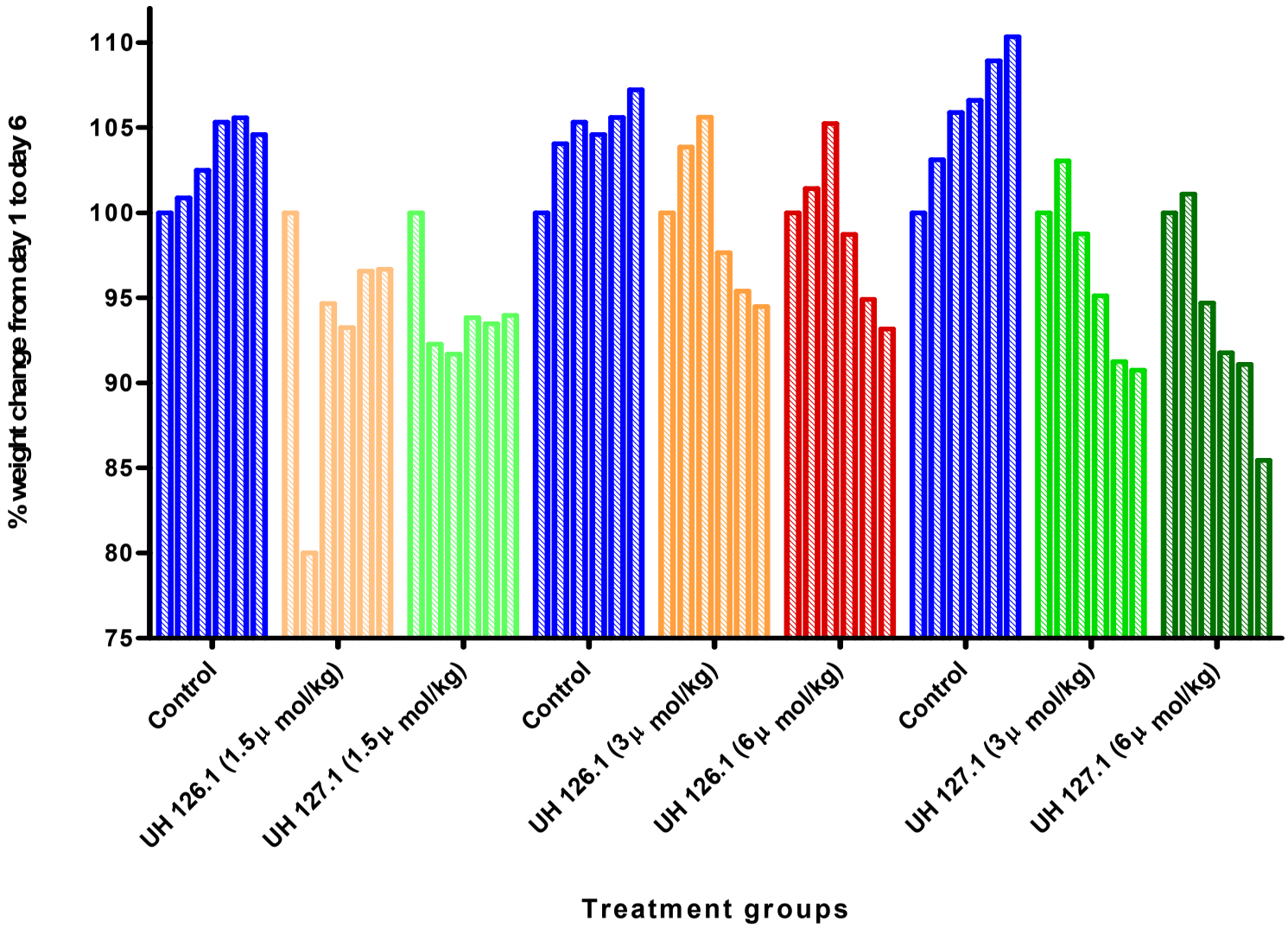

Figure 7.4. Summary of percentage body weight changes for all the control- and test groups from day one to six, including phase 1-3. Each bar represents one day. The initial weight percentage for all the groups on day one is represented as 100%.

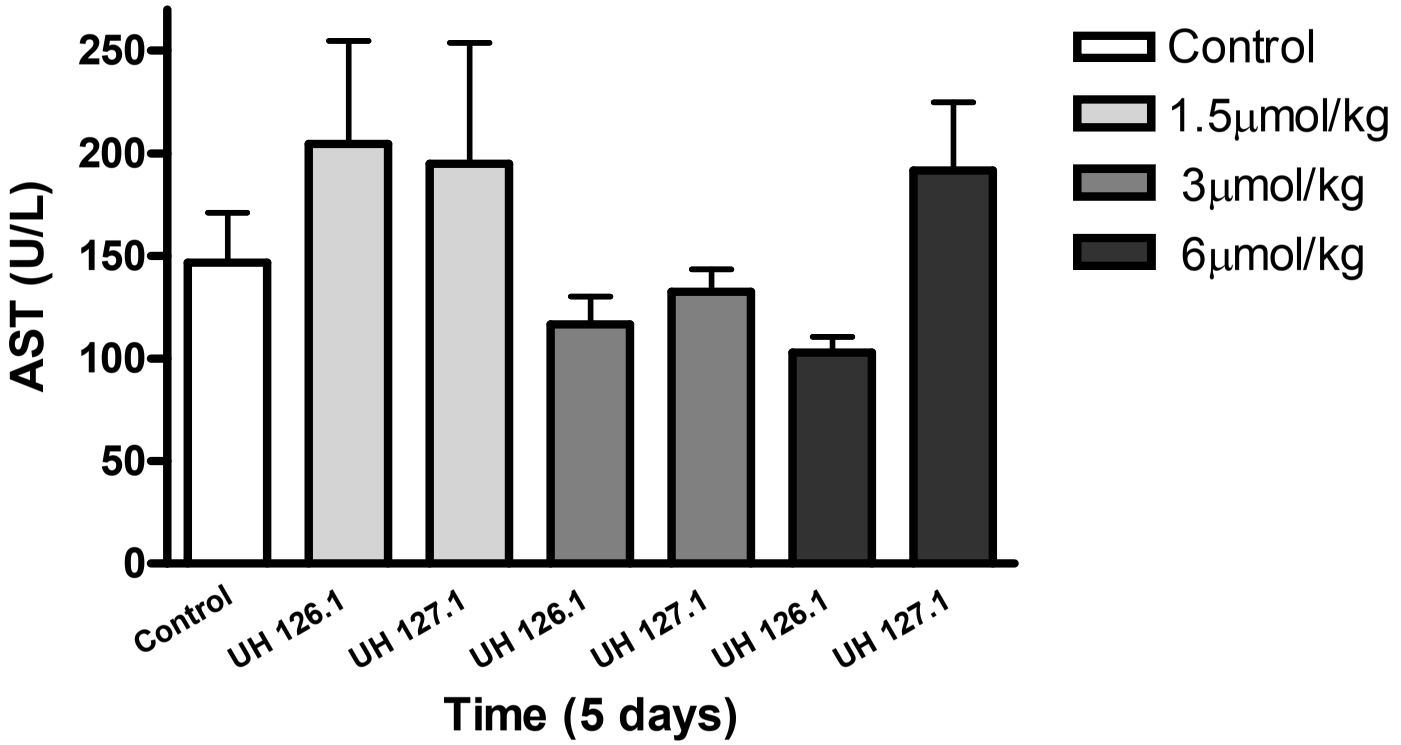

Figure 7.5. Mean plasma concentrations of AST in mouse plasma after administration of three different concentrations of UH 126.1 and UH 127.1 once daily for a period of five consecutive days. Error bars reflect the standard error of the mean (SEM).

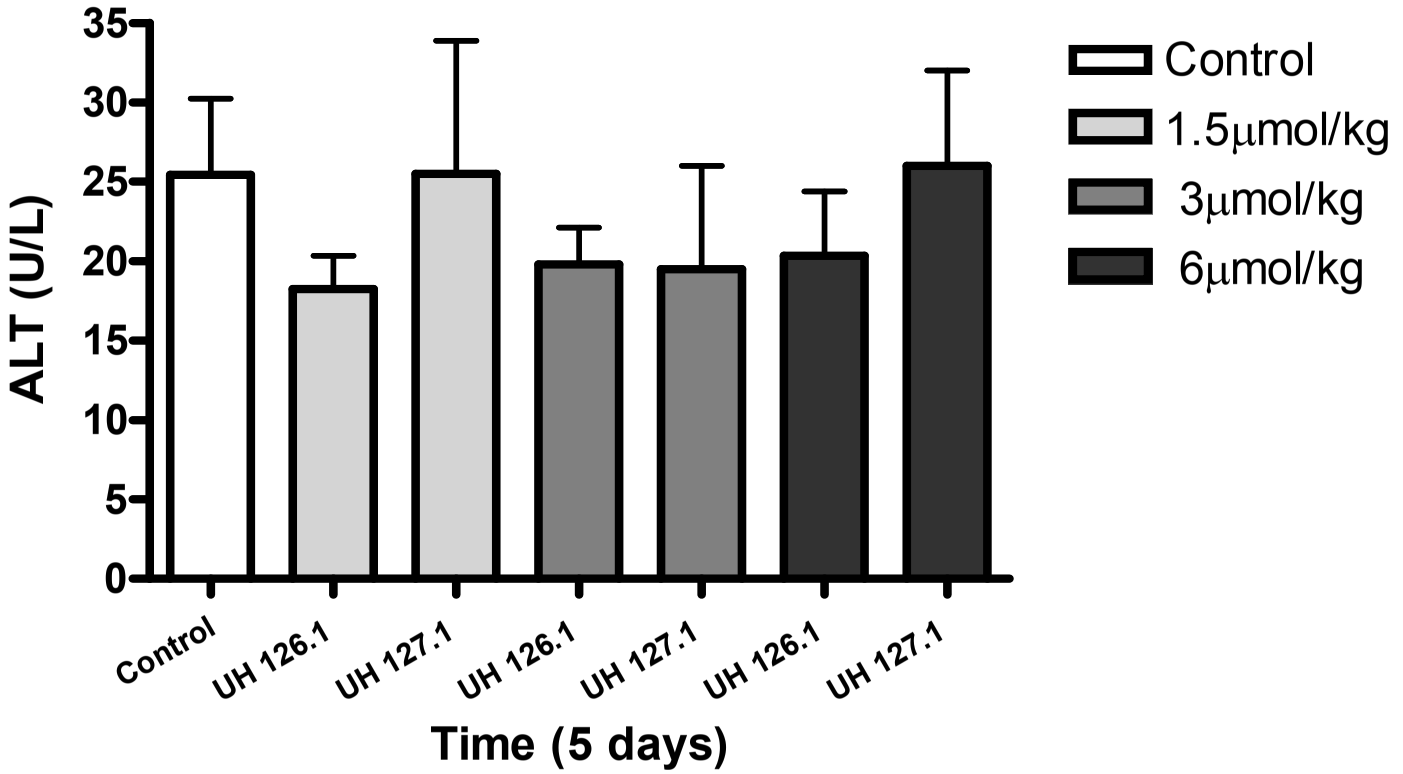

Figure 7.6. Mean plasma concentrations of ALT in mouse plasma after administration of three different concentrations of UH 126.1 and UH 127.1 once daily for a period of five consecutive days. Error bars reflect the standard error of the mean (SEM).

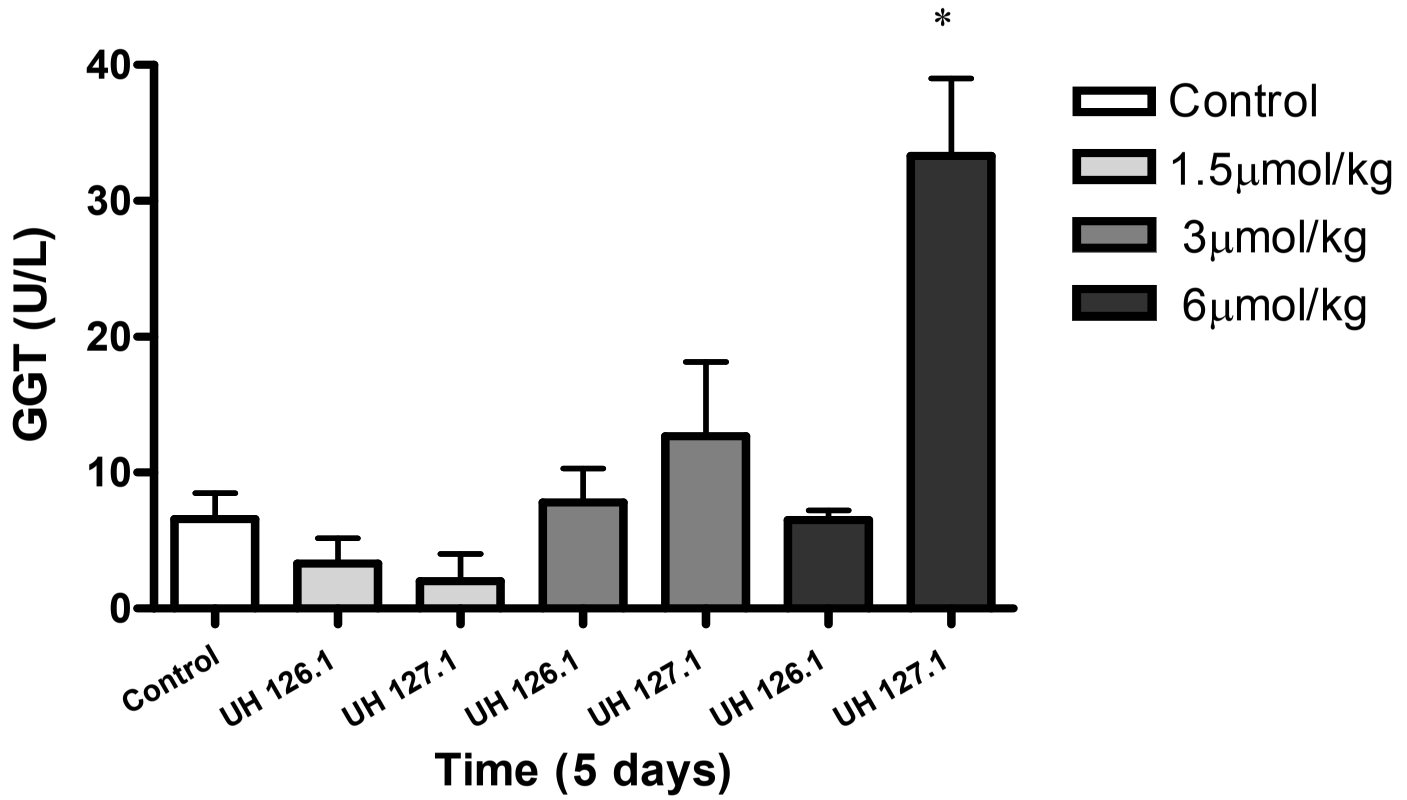

Figure 7.7. Mean plasma concentrations of GGT in mouse plasma after administration of three different concentrations of UH 126.1 and UH 127.1 once daily for a period of five consecutive days. Error bars reflect the standard error of the mean (SEM). * $p \leq 0.05$ when compared to the untreated control.

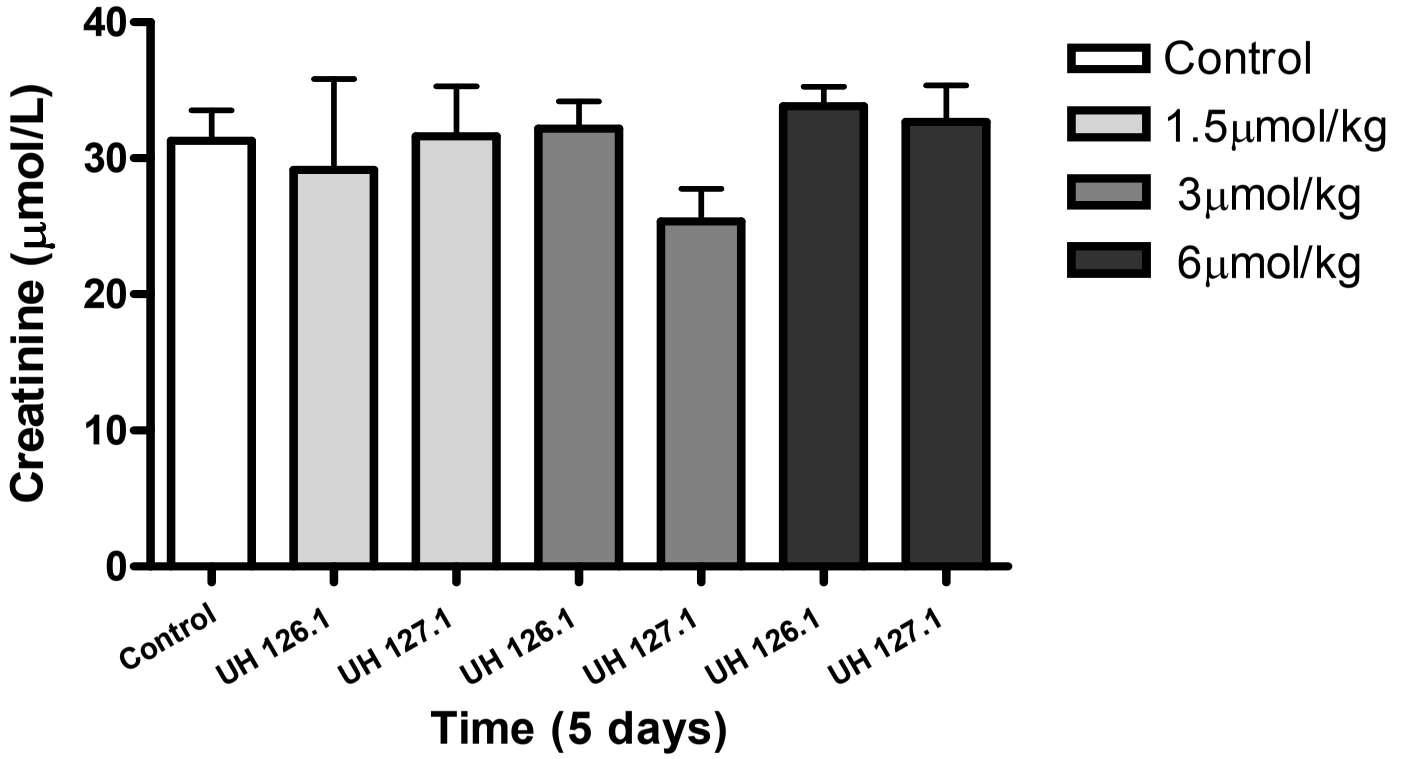

Figure 7.8. Mean plasma concentrations of creatinine in mouse plasma after application of three different doses of UH 126.1 and UH 127.1 over a period of five consecutive days. Error bars reflect the standard error of the mean (SEM).

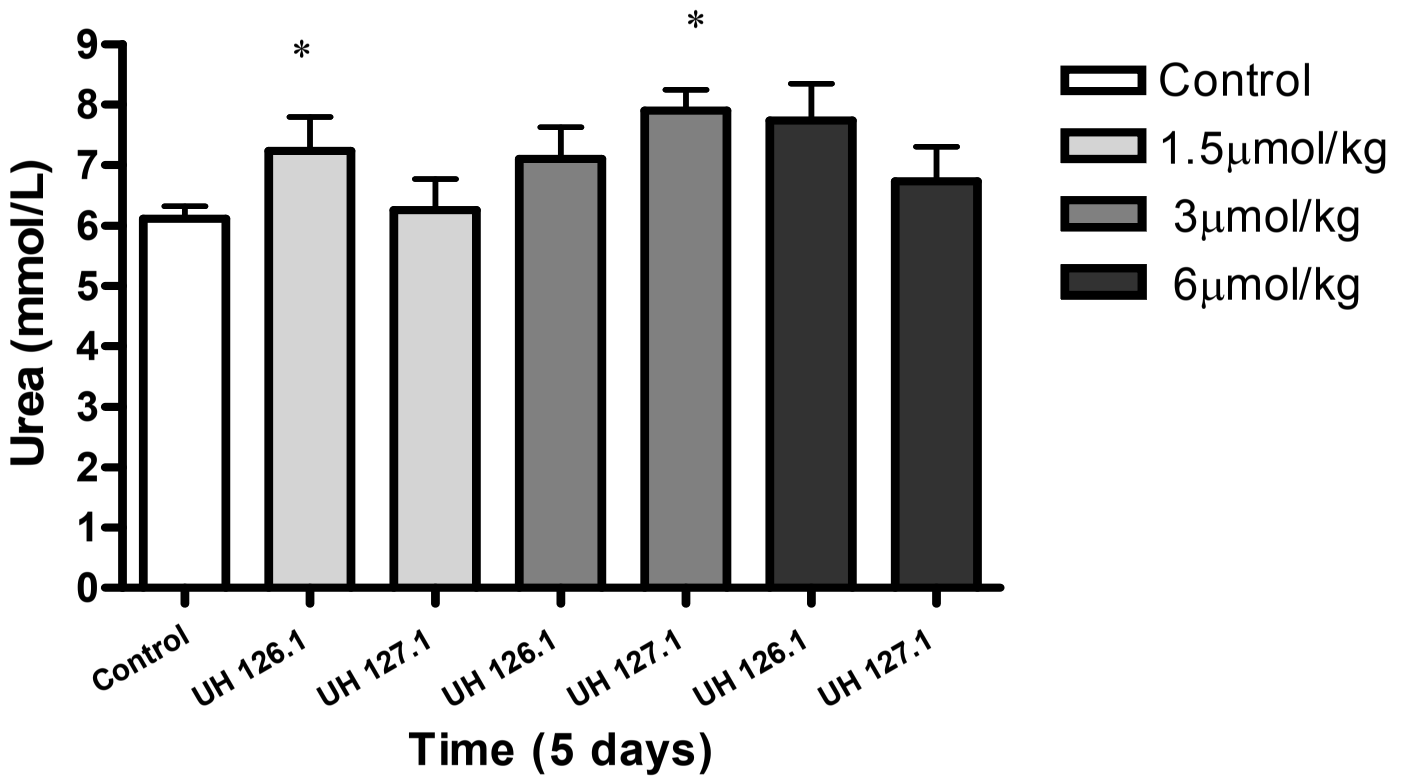

Figure 7.9. Mean plasma concentrations of urea in mouse plasma after administration of three different concentrations of UH 126.1 and UH 127.1 once daily for a period of five consecutive days. Error bars reflect the standard error of the mean (SEM). * $p \leq 0.05$ when compared to the untreated control.

Table 7.4. The effects of UH 127.1 and UH 127.1 on the organ weight / body-weight ratio. Data is expressed as mean ± standard error of the mean (SEM).

		Left kidney	Right kidney	Liver	Heart
Compound	**Concentration**	**Ratio [organ weight / body weight (1000)] ± SEM**			
Control (n=15)	**N/A**	5.326 ± 0.010	5.863 ± 0.012	45.293 ± 0.123	5.033 ± 0.016
UH 126.1 (n=6)	**1,5µmol/kg**	6.066 ± 0.007*	6.503 ± 0.011*	51.347 ± 0.054 *	4.972 ± 0.007
UH 126.1 (n=6)	**3µmol/kg**	6.100 ± 0.013*	6.323 ± 0.011*	49.301 ± 0.122*	5.036 ± 0.007
UH 126.1 (n=6)	**6µmol/kg**	5.900 ± 0.01*	6.069 ± 0.015*	44.675 ± 0.101	5.170 ± 0.013
UH 127.1 (n=6)	**1,5µmol/kg**	6.214 ± 0.013*	6.442 ± 0.011*	49.915 ± 0.122*	5.131 ± 0.007
UH 127.1 (n=3)	**3µmol/kg**	6.882 ± 0.000*	7.061 ± 0.002*	47.397 ± 0.046	5.685 ± 0.009*
UH 127.1 (n=3)	**6µmol/kg**	6.689 ± 0.009*	7.224 ± 0.008*	44.816 ± 0.053	7.358 ± 0.005*

* $p \leq 0.05$ when compared to the untreated control.

Table 7.5. The mean full blood counts of mice that received three different doses of UH 126.1 and UH 127.1 for five consecutive days. Data is expressed as mean ± standard error of the mean (SEM)

	Control (n=15)	UH 126.1 1.5 µmol/kg (n=6)	UH 126.1 3 µmol/kg (n=6)	UH 126.1 6 µmol/kg (n=6)	UH 127.1 1.5 µmol/kg (n=6)	UH 127.1 3 µmol/kg (n=3)	UH 127.1 6 µmol/kg (n=3)
Hb (g/l)	153.8 ± 16.40	144.5 ± 6.70	165.83 ± 13.00*	170.67 ± 15.12*	136.67 ± 15.04*	145.67 ± 2.89	142.33 ± 3.78
RCC (× 10^{12}/l)	9.10 ± 0.61	8.92 ± 0.41	9.75 ± 0.40*	9.69 ± 0.16*	8.54 ± 0.97	9.37 ± 0.05	9.25 ± 0.25
HT (l/l)	0.43 ± 0.03	0.42 ± 0.02	0.46 ± 0.02*	0.45 ± 0.01*	0.40 ± 0.05	0.44 ± 0.01	0.42 ± 0.01
MCV (fl)	47.05 ± 1.29	47.03 ± 0.48	46.75 ± 0.67	46.50 ± 0.55	46.25 ± 0.45*	46.40 ± 0.44	45.60 ±1.15*
MCH (g/dl)	16.92 ± 1.59	16.17 ± 0.37	17.07 ± 1.55	17.62 ± 1.62	16.00 ± 0.19	15.53 ± 0.23*	15.37 ± 0.38*
MCHC (g/dl)	35.97 ± 3.24	34.40 ± 0.49	36.42 ± 3.24	37.92 ± 3.53	34.62 ± 0.33	33.43 ± 0.23*	33.80 ± 0.10*
WCC (× 10^{9}/l)	5.53 ± 3.50	7.35 ± 6.51	7.26 ± 5.01	4.33 ± 2.03	3.46 ± 0.76	4.23 ± 2.14	7.80 ± 2.35
RDW (%)	18.23 ± 0.97	18.08 ± 1.08	17.48 ± 0.58	17.63 ± 1.19	17.58 ± 0.56	19.43 ± 0.97*	20.17 ± 1.12*

*$p \leq 0.05$ when compared to the untreated control.

7.7 DISCUSSION

The acute toxicity of the novel azole derivatives, UH 126.1 and UH 127.1, was determined in female Balb/C mice by assessing the following markers after five days of drug exposure: (i) evaluation of observed adverse effects and weight loss, (ii) liver markers (AST, ALT, GGT), (iii) kidney markers (urea and creatinine) and (iv) organ weight evaluation. The compounds were injected i.p. once daily for five consecutive days at concentrations of 1,5µmol/kg, 3µmol/kg and 6µmol/kg, respectively.

In the present study, toxicity was indicated by severe piloerection and diarrhoea in the mice that received 3 and 6µmol/kg of UH 126.1 and UH 127.1. At these two concentrations, both compounds induced significant weight loss (5% and 7% for UH 126.1; 10% and 15% for UH 127.1) (**refer to Figure 7.4, page 104**). In the mice receiving the lower dosage of UH 126.1 and UH 127.1 (1.5µmol/kg), minimal adverse events were observed, i.e. no piloerection and minimal diarrhoea. In these two groups, the mice recovered from initial weight loss on the second day of the study and weight gain continued from day three until termination of the study. Previous studies have indicated weight loss as a valuable parameter of drug-induced toxicity (Clarke *et al.* 2000; Gorbacheva *et al.* 2005). It is thus evident that UH 126.1 and UH 127.1 at 3 and 6µmol/kg induced severe piloerection, gastrointestinal side effects (diarrhoea) and significant body weight loss in this study. It is known that gastrointestinal toxicity is one of the dose-limiting side effects for some azole derivatives (Magedov *et al*. 2007; Rodriguez and Acosta 1995).

Pertaining to liver marker evaluation as indicators of hepatotoxicity, AST and ALT are the most frequent investigated enzymes for this purpose (Meeks *et al* 1991). According to Benichou (1990), the definition of liver injury is an increase greater than two times the upper limit of normal range (ULN) in ALT or conjugated bilirubin or a combined increase in AST, Alk P, and total bilirubin provided that one of them is greater than two times the ULN (Benichou 1990). This study revealed that neither the AST or ALT enzyme levels were greater than twice the upper limit of normal as indicated for Balb/C 6-8week old female mice (**refer to section 7.6.2 and Figures 7.5-7.6, pages 105-106**).

Furthermore, the results did not indicate any significant elevation of AST or ALT levels for the mice in the test groups when compared to the untreated control group. These observations are consistent with the absence of hepatotoxicity.

In considering the dose-dependent increase in GGT plasma levels when UH 127.1 was administered as shown in **Figure 7.7, page 107**, an argument, however, for hepatotoxicity can be made. Although this was the only instance where liver enzyme levels were significantly raised, an increase in the liver weight/body ratio was detected in the groups that received 1.5 and 3µmol/kg of UH 126.1, and 1.5µmol/kg of UH 127.1. The organ weight increases are noteworthy when keeping in mind that the experimental compounds were administered for only five days. It is possible that the mice compensated for initial drug-induced hepatotoxicity, which is why no significant elevation of the AST and ALT levels was detected (Amacher 1998). The data indicated that UH 127.1, at a concentration of 6µmol/kg, induced cholestatic effects (decreased bile secretion or obstruction of bile flow into the digestive tract), which is indicative of hepatotoxicity. The increased liver weight / body weight ratios that were induced by UH 126.1 and UH 127.1 might also be indicative of hepatotoxicity, which might present clinically in a prolonged study.

Creatinine and urea plasma levels were determined in this study, since elevated urea and creatinine levels are often indicators of renal dysfunction (Bishop 2005). As a by-product of muscle metabolism, creatinine is produced at a constant rate and eliminated by renal clearance. In the case of nephrotoxicity, the glomerular filtration rate (GFR) is decreased, which will limit the excretion of creatinine, while causing an increase in plasma creatinine levels (Bishop 2005). In this study, the measured creatinine serum levels (indicative of GFR) remained unchanged in all the treatment groups (**refer to Figure 7.8, page 108)**. The absence of plasma creatinine elevation in the study, however, can be due to an over estimation of GFR, which is accompanied by muscle wasting, as was observed for the animals used in this study (Bishop 2005). From these observations, therefore, nephrotoxicity cannot be excluded.

A significant increase in plasma urea levels was detected in the groups that received UH 126.1 (1.5µmol/kg) and UH 127.1 (3µmol/kg) when compared to the untreated control group, as shown in **Figure 7.9, page 109**.

Furthermore, haematology results illustrated a slight increase in Hb, RCC and HT in the groups that received UH 126.1 (3 and 6 µmol/kg). In the groups that received UH 127.1 at concentrations of 1.5 and 3µmol/kg, slight decreases in MCV were observed, while at concentrations of 3 and 6µmol/kg of UH 127.1, decreases in MCH, MCHC and RDW were also detected (**see Table 7.5, page 111)**. These findings are sometimes associated with kidney damage (Pagana *et al*. 1998), although it is not elucidated whether this is the case in the present study.

A significant increase in the heart weight / body weight ratio was also detected in the mice that received 3 and 6µmol/kg of UH 127.1 (**refer to Table 7.4, page 110**). These results might be indicative of UH 127.1-induced cardiotoxicity. It has been established that cardiotoxicity might perpetuate further kidney damage in animals (as was seen in the animals used in this experiment), due to decreased cardiac output, which might lead to increased extracellular fluid volume with a subsequent further decrease in GFR and thus exacerbated kidney damage (Rang *et al.* 2007).

Results revealed minimal adverse effects in the groups that received 1,5µmol/kg of both compounds. However, increased kidney weight / body weight ratios and liver weight / body weight ratios, when compared to the untreated control, is indicative that some toxicity is induced by both UH 126.1 and 127.1. From this study, it is suggested that the maximum tolerated dose (MTD) for UH 126.1 and UH 127.1 in Balb/C mice is 1,5µmol/kg. This should be confirmed in a chronic study.

CHAPTER EIGHT

SUMMARY & CONCLUSION

8.1 SUMMARY

The purpose of this study was to investigate the cytotoxic potency, selectivity and toxicity of seven novel gold compounds that either contains purine bases or azole bases. The compounds containing nucleoside analogues (purines) are UH 86.2, UH 75.1, UH 58.1, and UH 145.1. The compounds containing azoles are UH 107.1 (imidazole derivative), UH 126.1 (pyrazole derivative), and UH 127.1 (triazole derivative). The activity of these novel compounds were compared to the well documented anticancer compounds, $[Au(dppe)_2]Cl$ and cisplatin. The first aim of this study was to identify whether a correlation between the lipophilicity and cytotoxicity of the novel compounds exists. Further aims of the study included the identification of the two most promising novel compounds based on the cytotoxicity assay results, and to investigate a possible mechanism by which these two compounds induce cytotoxicity. Finally, the *in vivo* toxicity of the two most promising novel compounds was explored.

Pertaining to the relationship between the lipophilicity and the cytotoxic effects of anticancer compounds, previous studies determined that, for gold-containing cationic bisphosphine complexes, a decrease in lipophilicity correlated with enhanced selectivity, while with increased lipophilicity, potency was increased (Berners-Price *et al*. 1999). Although the novel compounds have neutral, linear two-coordinated structures, an objective of this study was to investigate whether a correlation exists between the lipophilicity and cytotoxic activities of the novel compounds. It has previously been observed that, for linear two-coordinate bisphosphine di-gold complexes, that rearrangement to the cationic bisphosphine species occurs in biological media. The possibility thus exists, that for the novel compounds explored in this study, that the four-coordinate cationic bisphosphine analogue is the pharmacologically active species, giving further credence to exploring lipophilicity vs. cytotoxicity relationships in this study. The results from octanol/water PC determinations, revealed that the purine-containing compounds (UH 86.2, UH 75.1, UH 58.1, and UH 145.1), as well as the azole-containing

compound, UH 127.1, exhibited hydrophilic properties, while the azole-containing compounds, UH 107.1 and UH 126.1 were found to be lipophilic. In contrast to results by Berners-Price *et al*. (1999), that reported a direct proportionality between lipophilicity and cytotoxicity, for the current study, involving HeLa cells, CoLo cells, normal resting and PHA stimulated lymphocytes, no correlation was observed. For the Jurkat cell line, however, an increase in lipophilicity for the series of compounds studied was accompanied by an increase in cytotoxicity. The reason for the exception is not yet fully understood.

Cytotoxicity was evaluated using the MTT assay. All seven novel compounds were tested initially on three cancer cell lines (HeLa cells, CoLo cells, Jurkat cells) and two normal cell cultures (resting and PHA stimulated lymphocytes). Analysis revealed that the compounds, UH 75.1, UH 107.1, UH 126.1 and UH 127.1, displayed the best cytotoxicity / selectivity profiles. The cytotoxic effects of these compounds were tested on additional cell cultures, including MCF-7 cells, A2780 cells, A2780cis cells and chicken embryo fibroblasts. The results revealed that for the compounds tested, that the cells that typically exhibit resistance to cisplatin (A2780cis cells) are similarly cross-resistant to the novel drugs investigated in this study. This may be attributed to overlapping mechanisms of action, although differences in the transport mechanisms may also contribute to this observation. Another possibility is that the novel compounds might react with cellular thiols (Berners-Price *et al*. 1988), which may influence the resistance of cells (Heffeter *et al.* 2008), although the exact mechanism of resistance against the experimental compounds is not yet understood. Data from these extended studies, revealed that, the two azole-containing compounds (UH 126.1 and UH 127.1), exhibited the highest tumour specificities. These two compounds were selected for further experiments, which investigated (i) possible mechanisms by which they might exert their cytotoxic effects and (ii) their acute *in vivo* toxicity.

The first step towards unravelling the possible mechanism of action of the novel compounds, UH 126.1 and UH 127.1, was to investigate the induced cell death pathway. Two distinct cell death pathways have been described according to previous findings: the

apoptotic and necrotic pathways (Searle *et al*. 1982). The apoptotic pathway can be induced by either the extrinsic/receptor-linked pathway or the intrinsic/mitochondria-mediated pathway. It has been established in this study that both UH 126.1 and UH 127.1 induce the apoptotic pathway when exerting their cytotoxic effects in Jurkat cells. It was not, however, elucidated whether apoptosis was initiated via the extrinsic/receptor-linked apoptotic pathway or the intrinsic/mitochondria-mediated apoptotic pathway. Mitochondria play a key role in the intrinsic/mitochondria-mediated apoptotic pathway (Bredesen, 2000; Hengartner, 2000). In order to determine whether mitochondria are involved in the cytotoxic action of the novel compounds, UH 126.1 and UH 127.1, the status of the mitochondrial membrane potential (MMP) was determined in Jurkat cells that were exposed to these compounds.

The status of the MMP is an important parameter of mitochondrial function (Salido *et al.* 2007). It is known that there is an association between the release of cytochrome c from mitochondria and the loss of the MMP (Gruss-Fischer and Fabian 2002). A collapse of MMP indicates mitochondrial toxicity (Ferraresi *et al.* 2004). Depolarisation of the MMP, due to chemical compounds (such as the novel compounds UH 126.1 and UH 127.1), will thus be indicative of mitochondrial involvement in the cell death pathway. Results of the present study indicated that the novel compound, UH 126.1, induced the depolarisation of the MMP in Jurkat cells at a very high concentration (five times that of the IC_{50}). This compound also caused the collapse of the MMP when added to PHA stimulated lymphocytes at concentrations double- and five times that of the IC_{50}. UH 127.1, however, did not induce MMP depolarisation when added to Jurkat cells. When this compound was added to PHA lymphocytes, it was observed that an increase in MMP depolarisation was accompanied by increased concentrations of added UH 127.1. However, this was not statistically significant.

Although the MMP remained almost unaltered by UH 126.1 and UH 127.1 at low concentrations, some involvement of mitochondria was indicated at higher concentrations in both Jurkat cells (at a very high concentration of UH 126.1) and PHA stimulated lymphocytes (at high concentrations of UH 126.1 and UH 127.1), as evidenced by MMP

depolarisation. From this evidence presented, at the lower concentrations, it is not likely that mitochondria are the primary target of UH 126.1 and UH 127.1, however, the involvement of mitochondria at higher concentrations cannot be discounted.

The next step was to investigate the effect the novel azole-containing compounds on the cell cycle of Jurkat cells. All cancer cells are able to proliferate unchecked, which enables them to surpass biochemical checkpoints that normally assess cellular viability and control growth (Perchellet *et al*. 2005). In order to inhibit the hyper proliferation state of cancer cells, most anticancer drugs target the cell cycle at certain checkpoints (Lee and Schmitt, 2003). At these checkpoints, it is confirmed whether the cell can proceed to the next phase or whether it should abort further division due to the detection of cell damage. Some of the checkpoints require the interaction of enzymes, cyclins and cyclin-dependent kinases (cdks), which make these enzymes and cdks valuable drug targets (Perchellet *et al*. 2005).

From this study, it was deduced that the novel azole-containing compounds, UH 126.1 and UH 127.1, induce cell accumulation in the G1 phase, possibly due to interference with cyclin dependant kinases or cell cycle regulator enzymes as in the case of other azole-derivatives (Chen *et al*. 2008; Forgue-Laffite 1992; Sengupta *et al*. 2007).

Following the *in vitro* tests that were performed during this study, an acute *in vivo* toxicity study was performed to investigate the toxic effects of UH 126.1 and UH 127.1, this involved dosing female Balb/C mice for five consecutive days at different concentrations (1,5µmol/kg, 3µmol/kg and 6µmol/kg).

Symptoms of toxicity were observed including, significant weight loss, severe piloerection and slight diarrhoea in the test groups that received 3 and 6µmol/kg of both UH 126.1 and UH 127.1. Evidence also revealed signs of nephrotoxicity and hepatotoxicity. Due to minimal adverse effects observed in the groups that received these compounds at the concentration of 1,5µmol/kg, this is the suggested MTD. Further dose-

range studies with UH 126.1 and UH 127.1 are, however, needed in order to evaluate clinical efficacy.

8.2 CONCLUSION

The hypothesis of this study was that the novel compounds will have a high tumour specificity and will be less toxic than $[Au(dppe)_2]Cl$ in mice, owing to the extended coordination of gold to the additionally anti-tumour active nitrogen-containing heterocycles included in this study. According to the results, the novel compounds, UH 126.1 and UH 127.1, did indeed have much higher *in vitro* tumour specificities than that of $[Au(dppe)_2]Cl$. The *in vitro* tumour specificities for UH 126.1 and UH 127.1 were determined to be 9.4 and 8.7 respectively, in contrast with a much lower value of 0.9 that was determined for $[Au(dppe)_2]Cl$. In evaluating the relative toxicities of UH 126.1 and UH 127.1 against $[Au(dppe)_2]Cl$, the MTD of both experimental compounds were found to be 1.5µmol/kg, which compared to the 3µmol/kg observed for the gold-phosphine control compound. It is likely that efficacy studies with UH 126.1, UH 127.1 and $[Au(dppe)_2]Cl$, may be a more reliable indicator of toxicity. These studies are further warranted, given the higher selectivity exhibited by both UH 126.1 and UH 127.1 when compared the control, $[Au(dppe)_2]Cl$.

REFERENCES

Acton BM, Jurisicova A, Jurisica I, Casper RF. *Alterations in mitochondrial membrane potential during preimplantation stages of mouse and human embryo development*. Molecular Human Reproduction 2004; 10(1); 23-32

Allan JC. *Learning about statistics*. Macmillan South Africa publishers 1982: 219-244

Amacher DE. *Serum Transaminase Elevations as Indicators of Hepatic Injury Following the Administration of Drugs*. Regulatory Toxicology and Pharmacology 1998; 27: 119-130

Anger DL, Crankshaw DJ, Foster WG. *Spontaneous appearance of uterine tumours in vehicle and 3-methylcholanthrene-treated Wistar rats.* Reproductive Toxicology 2006; 22: 760–764

Barnard CFJ, Fricker SP, Vaughan OJ. *Medical applications of inorganic chemicals. Insights into speciality inorganic chemicals.* Cambridge: Royal Society of Chemistry 1995: 35–60

Benichou, C. Criteria of drug-induced liver disorders. *Report of an international consensus meeting*. J. Hepatol. 1990; 11: 272–276

Bergamo A, Gagliardi V, Scarcia A, Furlani E, Alessio E, Mestroni G, Sava G. *In vitro Cell Cycle Arrest, In vivo Action on Solid Metastasizing Tumors, and Host Toxicity of the Antimetastatic Drug NAMI-A and Cisplatin.* JPET 1999; 289: 559-564

Bernardi P, Scorrano L, Colonna R, Petronelli V, Di Lisa F. *Mitochondria and Cell Death.* European Journal of Biochemistry 1999; 264: 687-701

Berners-Price SJ, Bowen RJ, Galettis P, Healy PC, McKeage MJ. *Structural and Solution Chemistry of Gold(I) and Silver(I) Complexes of Bidentate Pyridyl Phosphines: Selective Anti-tumour Agents*. Coordination Chemistry Reviews 1999; 185–186: 823–836

Berners-Price SJ, Mirabelli CK, Johnson RK, Mattern MR, McCabe FL, Faucette LF Sung C, Mong S, Sadler PJ, Crooke ST. *In vivo Antitumor Activity and In vitro Cytotoxic Properties of Bis[1,2-bis(diphenylphosphino)ethane}gold(I) Chloride*. Cancer Research 1986; 46: 5486-5493

Berners-Price SJ, Sadler PJ. *Phosphines and metal phosphines complexes: relatioship of chemistry to anticancer and other biological activity*. Structure bonding 1988; 70:27 - 102

Bishop YM. *The Veterinary Formulary, sixth edition*. Pharmaceutical press 2005: 119

Bortner CD, Cidlowski JA. *Caspase independent/dependent regulation of K(+), cell shrinkage, and mitochondrial membrane potential during lymphocyte apoptosis*. J Biol Chem 1999; 274(31): 21953-62

Boulikas T. *Low toxicity and anticancer activity of a novel liposomal cisplatin (Lipolatin) in mouse xenografts.* Oncology reports. 2004; 12(1): 3-12

Bradshaw TD, Shi DF, Schultz RJ, Paull KD, Kelland L, Wilson A, Garner C, Fiebig H, Wrigley S, Stevens MFG. *Influence of 2-(4- aminophenyl)benzothiazoles on growth of human ovarian carcinoma cells in vitro and in vivo*. Br J Cancer 1998; 78: 421–429

Bradshaw TD, Wrigley S, Shi DF, Schultz RJ, Paull KD, Stevens MFG. *2-(4-Aminophenyl)benzothiazoles: novel agents with selective profiles of in vitro anti-tumour activity*. Br J Cancer 1998; 77: 745–752

Bredesen DE. *Apoptosis: overview and signal transduction pathways*. Journal of Neurotrauma 2000; 17 (10): 801–810

Burger KNJ, Staffhorst RWHM, De Vijlder HC, Velinova MJ, Bomans PH, Frederik PM, De Kruijff B. *Nanocapsules: lipid-coated aggregates of cisplatin with high cytotoxicity.* Nature Medicine 2002; 8: 81 - 84

Caldwell G, Neuse EW, Van Rensburg CEJ. *Cytotoxic activity of two polyaspartamide-based monoamineplatinum(II)conjugates against the HeLa cancer cell line*. Appl. Organometallic Chemistry 1999; 13: 189-194

Chen LB. *Mitochondrial membrane potential in living cells*. Annu Rev. Cell Biol 1988; 4: 155-188

Chen C, Hsu M, Huang L, Yamori T, Chung J, Lee F, Teng C, Kuo S. *Anticancer mechanisms of YC-1 in human lung cancer cell line, NCI-H226.* Biochemical Pharmacology 2008; 75: 360-368

Clarke SJ, Farrugia DC, Aherne GW, Pritchard DM, Benstead J, Jackman AL. *Balb/c Mice as a Preclinical Model for Raltitrexed-induced Gastrointestinal Toxicity*. Clinical Cancer Research 2000; 6:285-296

Cossarizza A, Baccarani-Contri GK, Fransceschi C. *A new method for the cytofluorimetric analysis of mitochomdrial membrane potential using the J-Aggregate forming lipophilic cation 5, 5',6, 6'-tetrachloro -1,1'3,3'- tetraethyl benzimidazol carbocyanine iodide (JC-1).* Biochemical and biophysical research communications 1993; 197 (1): 40-45

Dancey, J, Sausville E. A. *Issues and progress with protein kinase inhibitors for cancer treatment*. Nat. Rev. Drug Discovery 2003; 2: 296-313

Davis S, Weiss MJ, Wong JR, Lampidis TJ, Chen LB. *Mitochondrial and plasma membrane potentials cause unusual accumulation and retention of rhodamine 123 by human breast adenocarcinoma-derived MCF-7 cells.* Journal of Biological Chemistry 1985; 260 (25): 13844–13850

DeCaprio AP. *Toxicologic Biomarkers.* CRC Press 2005: 29

De la Portilla F, Ynfante I, Bejarano D, Conde J, Ferna´ndez A, Ma Ortega J, Carranza G. *Prevention of Peritoneal Adhesions by Intraperitoneal Administration of Vitamin E: An Experimental Study in Rats.* Dis Colon Rectum 2004

Denny WA, Atwell GJ, Baguely BC, Cain BF. *Potential antitumor agents. 29. Quantitative structure-activity relationships for the antileukemic bisquaternary ammonium heterocycles.* J. Med. Chem. 1979; 22(2): 134-50

Derelanko MJ, Hollinger MA. *Handbook of Toxicology, second edition*. CRC Press 2002: 762

De Souza CPC, Osmani SA. *Mitosis, Not Just Open or Closed*. Eukaryotic Cell 2007; 1521–1527

Elgemeie GH. *Thioguanine, Mercaptopurine: Their Analogs and Nucleosides as Antimetabolites.* Current Pharmaceutical Design 2003; 9: 2627-2642

Fairbanks DJ, Andersen WR. *Genetics the continuity of life*. Brooks/Cole publishing Company a division of International Thomson Publishing Inc 1999; 323

Fantin VR, Berardi MJ, Scorrana L, Korsmeyer SJ, Leder P. *A novel mitochondriotoxic small molecule that selectively inhibits tumour cell growth*. Cancer Cell 2002; 2: 29-42

Ferraresi R, Troiano L, Rossi D, Gualdi E, Lugli E, Mussini C, Cossarizza A. *Mitochondrial membrane potential and nucleosidic inhibitors of HIV reverse transcriptase: a cytometric approach*. Mitochondrion 2004; 4: 271-278

Forgue-Lafitte M, Coudray A, Fagot D, Mester J. *Effects of Ketoconazole on the Proliferation and Cell Cycle of Human Cancer Cell Lines*. Cancer Research 1992; 52: 6827-6831

Freimoser FM, Jakob CA, Aebi M, Tuor U. *The MTT [3-(4,5-Dimethylthiazol-2-yl)-2,5-Diphenyltetrazolium Bromide] Assay Is a Fast and Reliable Method for Colorimetric Determination of Fungal Cell Densities*. Applied And Enviromental Microbiology 1999: 65; 3727–3729

Freshney RI. *Culture of animal cells: a manual of basic technique.* 4th Ed. Wiley-Liss Publishers, New York 2000

Frey T.G. & Manella C.A. *The internal organization of mitochondria*. TIBS 2000: 25; 319-324

Fries JF, Bloch D, Spitz P, Mitchell DM. *Cancer in rheumatoid arthritis: a prospective long-term study of mortality*. Am J Med 1985; 78(Suppl. 1A): 56–59

Galmarini CM, Mackey JR, Dumontet C. *Nucleoside analogue sand nucleobases in cancer treatment*. Lancet Oncol 2002; 3: *415–424*

Gorbacheva VY, Kondratov RV, Zhang R, Cherukuri S, Gudkov AV, Takahashi JS, Antoch MP. *Circadian sensitivity to the chemotherapeutic agent cyclophosphamide depends on the functional status of the CLOCK/BMAL1 transactivation complex.* PNAS 2005; 102(9): 3407-3412

Gross JL, de Azevedo MJ, Silveiro SP, Canani LH, Caramori ML, Zelmanovitz T. *Diabetic nephropathy: diagnosis, prevention, and treatment*. Diabetes Care 2005; 28 (1): 164-176

Grotyohann LW, Scaduto RC Jr. *Measurement of mitochondrial membrane potential using fluorescent rhodamine derivatives*. Biophys. J 1999; 76: 469-77

Gruss-Fischer T, Fabian I. *Protection by ascorbic acid from denaturation and release of cytochrome c, alteration of mitochondrial membrane potential and activation of multiple caspases induced by H_2O_2 in human leukemia cells*. Biochemical Pharmacology 2002; 63:1325-1335

Guo Z, Sadler PJ. *Metals in medicine*. Angew Chem Int Ed Engl 1999; 38: 1512–31

Heffeter P, Jungwirth U, Jakupec M, Hartinger C, Galanski M, Elbling L, Micksche M, Keppler B, Berger W. *Resistance against novel anticancer metal compounds: Differences and similarities.* Drug Resistance Updates 2008; 11: 1–16

Hegemann L, Toso SM, Lahijani KI, Webster GF, Uitto J. *Direct interaction of antifungal azole-derivatives with calmodulin: a possible mechanism for their therapeutic activity*. J. Invest. Dermatol 1993; 100: 343-346

Hengartner MO. *The biochemistry of apoptosis.* Nature 2000; 407: 770–776

Highley MS, Calvert AH, edited by Kelland L, Farrel N. P*latinum Based Drugs in Cancer Therapy: Clinical experience with cisplatin and carboplatin*. Humana Press, Totowa, New Jersey, 2000: 171–194

Hill MM, Adrain C, Martin SJ. *Portrait of a killer: the mitochondrial apoptosome emerges from the shadows.* Mol. Interv. 2003; 3: 19

Hoke GD, Macia RA, Meunier PC, Bugelski PJ, Mirabelli CK, Rush GF, Matthews WD. *In vivo and In vitro Cardiotoxicity of a gold-containing antineoplastic drug candidate in the rabbit*. Toxicol Appl Pharmacol 1989; 100(2): 293-306

Hoke GD, Rush GF, Bossard GE, McArdle JV, Jensen BD, Mirabelli CK. *Mechanism of Alterations in Isolated Rat Liver Mitochondrial Function Induced by Gold Complexes of Bidentate Phosphines*.J. Biol. Chem 1988; 263(23): 11203-11210

Huppertz B, Frank HG, Kaufmann P. *The apoptosis cascade – morphological and immunohistochemical methods for its visualization.* Anat Embryol 1999; 200: 1-18

Ichiro N, Takeshi U, Hiroto I, Takayuki TOE, Tetsuro W, Tomonori I, Naoya M, Takamitsu O, Masaki S, Ryuichi S, Kazuo C, Kimitoshi K. *DNA topoisomerase inhibitor, etoposide, enhances GC-box-dependent promoter activity via Sp1 phosphorylation*. Cancer science 2007; 98 (6): 858-863

Ishibasi T, Lippard SJ. *Telomere loss in cells treated with cisplatin*. Proceedings of the National Academy of Sciences of the United States of America 95: 4219-4223

Kashiyama E, Hutchinson I, Chua MS, Stinson SF, Phillips LR, Kaur G, Sausville EA, Bradshaw TD, Westwell AD, Stevens MFG. *Antitumor benzothiazoles. 8. Synthesis, metabolic formation and biological properties of the C- and N-oxidation products of antitumor2-(4-aminophenyl)benzothiazoles*. J Med Chem 1999; 42: 4172–4184

Kerr JFR, Searle J, Harmon BV, Bishop CJ, Potten CS. *Apoptosis in*: *Perspectives on Mammalian Cell Death.* Oxford University Press, New York 1987; 93–128

Kiechle FL, Zhang X. *Apoptosis: biochemical aspects and clinical implications.* Clinica Chimica Acta 2002; 326: 27–45

Kiechle FL, Zhang X. *Apoptosis: a brief review*. J Clin Ligand Assay 1998; 21: 58 – 61

Kim S, Cho M, Lee T, Lee S, Minb H, Leeb SK. *Design, synthesis, and preliminary biological evaluation of a novel triazole analogue of ceramide.* Bioorganic & Medicinal Chemistry Letters 2007; 17: 4584–4587

Kopf-Maier P. *Complexes of metals other than platinum as anti-tumour agents*. European Journal of Clinical Pharmacology 1994; 47(1): 1-16

Kruskall WH, Wilkins WA. *Use of ranks in one-criterion variance analysis.* Journal of the American Statistical Association 1952; 47(260): 583 - 621

Lee S, Schmitt CA. *Chemotherapy response and resistance*. Curr Opin Genet Dev. 2003; 13(1): 90–96

Lewin B. *Genes V*. Oxford University Press, New York, 1995

Maertens JA. *History of the development of azole derivatives.* Clin Microbiol Infect 2004; 10 (Suppl. 1): 1–10

Magedov IV, Manpadi M, Van Slambrouck S, Steelant WFA, Rozhkova E, Przheval'skii NM, Rogelj S, Kornienko A. *Discovery and Investigation of Antiproliferative and Apoptosis- Inducing Properties of New Heterocyclic Podophyllotoxin Analogues Accessible by a One-Step Multicomponent Synthesis.* J. Med. Chem. 2007; 5: 5183-5192

Mahepal S, Bowen R, Mamo MA, Layh M, Jansen van Rensburg CE. *The In Vitro Antitumour Activity of Novel, Mitochondrial-Interactive, Gold-Based Lipophilic Cations*. Metal-Based Drugs 2008:1-5

McKeage MJ, Berners-Price SJ, Galettis P, Bowen RJ, Brouwer W, Ding L, Zhuang L, Baguley BC. *Role of Lipophilicity in determining cellular uptake and ant-tumour activity of gold phosphine complexes.* Cancer Chemotherapy and Pharmacology 2000; 46(5): 343-350

McKeage MJ, Maharaj L, Berners-Price SJ. *Mechanisms of Cytotoxicity and Antitumor Activity of Gold(I) Phosphine Complexes: the Possible Role of Mitochondria*. Coordination Chemistry Reviews 2002; 232: 127-135

Meeks RG, Harrison SD, Bull RJ. *Hepatotoxicology*. CRC Press 1991:254

Meira DD, Marinho-Carvalho MM, Teixeira CA, Veiga VF, Da Poian AT, Holandino C, De Freitas MS, Sola-Penna M. *Clotrimazole decreases human breast cancer cells viability through alterations in cytoskeleton-associated glycolytic enzymes*. Molecular genetics and Metabolism 2005; 84: 354-362

Michie J, Akudugu J, Binder A, Van Rensburg CEJ, Böhm L. *Flow cytometric evaluation of apoptosis and cell viability as a criterion of anti-tumour drug toxicity*. Anticancer Research 2003; 23: 2675-2680

Mignen O, Brink C, Enfissi A, Nadkarni A, Shuttleworth TJ, Giovannucci DR, Capiod T. *Carboxyamidotriazole-induced inhibition of mitochondrial calcium import blocks capacitative calcium entry and cell proliferation in HEK-293 cells*. Journal of Cell Science 2005; 118, 5615-5623

Mirabelli CK, Johnson RK, Hill DT, Faucette LF, Girard GR, Kuo GY, Sung CM, Crooke ST. *Correlation of the in vitro cytotoxic and in vivo anti-tumour activities of gold(I) coordination complexes.* J Med Chem 1986; 29(2): 218 - 223

Modica-Napolitano JS, Singh K. *Mitochondria as targets for detection and treatment of cancer*. Expert Reviews in Molecular Medicine 2002; (4)9:1-19

Mullauer L, Gruber P, Sebinger D, Buch J, Wohlfart S, Chott A. *Mutations in apoptosis genes: a pathogenetic factor for human disease.* Mutat Res 2001; 488: 211– 231

Ohwada J, Murasaki C, Yamazaki T, Ichihara S, Umeda I, Shimma N. *Synthesis of novel water soluble benzylazolium prodrugs of lipophilic azole antifungals*. Bioorganic & Medicinal Chemistry Letters 2002; 12, 19: 2775-2780

Olson M, Kornbluth S. *Mitochondria in Apoptosis and Human Disease*. Cuurent molecular medicine 2001; 1: 91-122

Pagana KD, Pagana TJ. *Mosby's Manual of Diagnostic and Laboratory Tests.* St. Louis: Mosby, Inc., 1998

Pandit NK . *Introduction to the Pharmaceutical Sciences.* Lippincot Williams & Wilkins. 2006:35-36

Penso J, Beitner R. *Clotrimazole decreases glycolysis and the viability of lung carcinoma and colon adenocarcinoma cells*. European Journal of Pharmacology, 2002; 451: 227-235

Perchellet EM, Perchellet J, Baures PW. *Imidazole-4,5-dicarboxamide Derivatives with Antiproliferative Activity against HL-60 Cells*. J. Med. Chem. 2005; *48*(19): 5955–5965

Rang HP, Dale MM, Ritter JM, Flower RJ. *Rand and Dale's Pharmacology, sixth edition.* Churchill Livingstone 2007:74, 282

Reed JC. *Mechanisms of apoptosis*. Am J Pathol 2000; 157:1415– 30

Rideout DC, Calogeropoulou T, Jaworski JS, Dougino R, McCarthy MR. *Phosphoniumsalts exhibiting selective adenocarcinoma activity in vitro*. Anticancer drug design 1989; 4: 265-280

Rodriguez RJ, Acosta Jr D. *Comparison of ketoconazole- and fluconazole-induced hepatotoxicity in a primary culture system of rat hepatocytes*. Toxicology 1995; 96: 83-92

Rush GF, Smith PF, Alberts DW, Mirabelli CK, Snyder RM, Crooke ST, Sowinski J, Jones HB, Bugelski PJ. *The mechanism of acute cytotoxicity of triethylphosphine gold(I) complexes : I. Characterization of triethylphosphine gold chloride-induced biochemical and morphological changes in isolated hepatocytes.* Toxicology and Applied Pharmacology 1987; 90(3): 377-390

Sadler PJ. *The biological chemistry of gold: a metallo-drug and heavy-atom label with variable valency*. Struct Bond 1976; 29: 171–214.

Sadler PJ, Guo Z. *Metal complexes in medicine: design and mechanism of action*. Pure & applied chemistry 1998; 70(4): 863-871

Salido M, Gonzalez JL, Vilches J**.** *Loss of mitochondrial membrane potential is inhibited by bombesin in etoposide-induced apoptosis in PC-3 prostate carcinoma cells*. Molecular Cancer Therapeutics 2007; 6: 1292-1299

Salih NA, Turk J. *Synthesis and Characterization of Novel Azole Heterocycles Based on 2,5-Disubstituted Thiadiazole.* Chem 2008; 32: 229 – 235

Samuels ML, Witmer JA. *Statistics for the life sciences. 2nd Ed*. Prentice Hall, Upper Saddle River, New Jersey 1999: 455-459

Schiff ER, Sorrel MF, Madrey WC. *Schiff's Diseases of the Liver, Volume 2. 10th Ed.* Lippincott Williams & Wilkins, 2006: 1129

Schoonen WGEJ, De Roos JADM, Westerink ED. *Cytotoxic effects of 110 reference compounds on HepG2 cells and for 60 compounds on HeLa, ECC-1 and CHO cells. II Mechanistic assays on NAD(P)H, ATP and DNA contents.* Toxicology *in vitro* 2005; 19: 491-503

Schmidt M, Bastians H. *Mitotic drug targets and the development of novel anti-mitotic anticancer drugs*. Drug resistance updates 2007; 10: 162-181

Scott SL, Gumerlock PH, Beckett L, Li Y, Goldberg Z. *Survival and cell cycle kinetics of human prostate cancer cell lines after single-and multi-fraction exposures to ionizing radiation.* Int. J Radiation Oncology Biol. Phys 2004; 1: 219-227

Searle J, Kerr JFR, Bishop CJ. *Necrosis and apoptosis: distinct modes of cell death with fundamentally different significance.* Pathol. Annu 1982; 17: 229–259

Sengupta TK, Leclerc GM, Hsieh-Kinser TT, Leclerc GJ, Singh I, Barredo JC. *Cytotoxic effect of 5-aminoimidazole-4-carboxamide-1-β-4-ribofuranoside (AICAR) on childhood acute lymphoblastic leukemia (ALL) cells: implication for targeted therapy.* Molecular Cancer 2007, 6:46

Shi DF, Bradshaw TD, Wrigley S, McCall C, Lelieveld P, Fichtner I, Stevens MFG. *Antitumor benzothiazoles. 3. Synthesis of 2-(4-aminophenyl) benzothiazoles and evaluation of their activities against breast cancer cell lines in vitro and in vivo*. J Med Chem 1996; 39: 3375–3384

Schiff ER, Sorrell MF, Maddrey WC. *Schiff's Diseases of the liver.* Lippincott Williams & Wilkins 2006: 47

Shirasaka T, Murakami K, Ford, jr H, Kelley JA, Yosoika H, Kojima E, Aoki S, Broder S, Mitsuya H. *Lipophilic halogenated congeners of 2',3'-dideoxypurine nucleosides*

active against human immunodeficiency virus in vitro. Proc. Nati. Acad. Sci. USA 1990; 87: 9426-9430

Siegel S. *Nonparametric statistics for behavioural sciences.* New York. McGraw-Hill. 1956

Sinha M, Manna P, Sil PC. *Arjunolic acid attenuates arsenic-induced nephrotoxicity.* Pathophysiology 2008; 15(3): 147-156

Smiley ST, Reers M, Mottola-Hartshorn C, Lin M, Chen A, Smith TW, Steele GD, Chen LB. *Intracellular heterogeneity in mitochondrial membrane potential revealed by a J-aggregate-forming lipophilic cation JC-1*. Proc. Natl. Acad. Sci. USA 1991; 88: 3671-3675

Smith PF, Hoke GD, Alberts DW, Bugelski PJ, Lupo S, Mirabelli CK, Rush GF. *Mechanism of Toxicity of an Experimental Bidentate Phosphine Gold Complexed Antineoplastic Agent in Isolated Rat Hepatocytes*. J. Pharmacol. Exp. Therap 1989; 249 (3): 944-950

Solary E, Bettaieb A, Dubrez-Daloz L, Corcos L. *Mitochondria as a target for inducing death of malignant hematopoietic cell*. Leuk Lymphoma 2003; 44: 563–574

Somosy Z. *Radiation response of cell organelles*. Micron 2000; 31: 165-181

Sorenson CM, Eastman A. *Influence of cisdiamminedichloroplatinum(II) on DNA synthesis and cell cycle progression in excision repair proficient and deficient Chinese hamster ovary cells*. Cancer Reasearch 1988; 48(23):6703-6707

Spiegel K, Magistrato A, Carloni P, Reedijk J, Klein ML. *Azole-Bridged Diplatinum Anticancer Compounds. Modulating DNA Flexibility to Escape Repair Mechanism and Avoid Cross-resistance.* J. Phys. Chem. B, 2007; 111: 41

Spearman C.*The proof and measurement of association between two things*. Amer. J. Psychol. , 1904; 15: 72-101

Thurston DE. *Chemistry and Pharmacology of anticancer drugs*. CRC press 2007: 37-84

Tiekink ERT, *Gold derivatives for the treatment of cancer.* Critical reviews in oncology/hematology 2002; 42: 225-248

Trapani V, Patel V, Leong CO, Ciolino HP, Yehz GC, Hose C, Trepel JB, Stevens MFG, Sausville EA, Loaiza-Perez AI. *DNA damage and cell cycle arrest induced by 2-(4-amino-3 methylphenyl)-5-fluorobenzothiazole (5F 203, NSC 703786) is attenuated in aryl hydrocarbon receptor deficient MCF-7.* British journal of cancer 2003; 88: 559-605

Van Rompay AR, Johansson M, Karlsson A. *Substrate specificity and phosphorylation of antiviral and anticancer nucleoside analogues by human deoxyribonucleoside kinases and ribonucleoside kinases*. Pharmacology & Therapeutics 2003; 100:119-139

Walker GA. *Common Statistical Methods for Clinical Research with SAS example*. SAS publishing 2002: 227

Wang D, Lippard SJ. *Cellular processing of platinum anticancer drugs*. Nature reviews drug discovery 2005; 4: 307-320

Wilkins DE, Ng CE, Raaphorst GP. *Cell cycle perturbations in cisplatin-sensitive and resistant human ovarian carcinoma cells following treatment with cisplatin and low dose rate irradiation*. Cancer chemotherapy and pharmacology 1997; 40(2): 159 - 166

WHO (World health organization). Available from: www.who.int/cancer. Accessed: 01/03/2008

Yalowitz JA, Pankiewiczb K, Pattersonb SE, Jayarama HN. *Cytotoxicity and cellular differentiation activity of methylenebis(phosphonate) analogs of tiazofurin and mycophenolic acid adenine dinucleotide in human cancer cell lines.* Cancer Letters 2002; 181: 31–38

Yu F, Megyesi JK, Price PM. *Cytoplasmic Initiation Of Cisplatin Cytotoxicity*. Am J Physiol Renal Physiol 2008; ahead of print

Zemlicka J. *Enantioselectivity of the antiviral effects of nucleoside analogues*. Pharmacology & Therapeutics 2000; 85: 251-266

Zhang CX, Lippard SJ. *New metal complexes as potential theraputics*. Current Opinion in Chemical Biology 2003; 7: 481-489

Zhu C, Johansson M, Karlsson A. *Differential incorporation of 1-H-D arabinofuranosylcytosine and 9-H-D-arabinofuranosylguanine into nuclear and mitochondrial DNA*. FEBS Lett 2000; 474: 129–132

Zimmerman KC, Bonzon C, Green DR. *The machinery of programmed cell death*. Pharmacol Ther 2002; 92: 57– 70

APPENDIX A

1. STATISTICS FOR CHAPTER 2

1.1 Kruskall-Wallis one-way analysis of variance test (synonymous for *H* test)

a) Motivation for use of test

The Kruskall-Wallis test is used when comparing more than two groups in terms of a continuous variable that appears to be non-normally distributed (DeCaprio 2005; Siegel 1956; Kruskall and Wallis 1952). In this case, the aim was to determine whether there was a statistical difference between the group medians pertaining to the octanol/water partition coefficient (PC) values. The different groups are i) $[Au(dppe)_2]Cl$, ii) cisplatin, iii) azole-containing compounds and iv) purine containing compounds. The present data is non-normally distributed, therefore, the non-parametric Kruskall-Wallis test is suitable (Samuels and Witmer 2003).

b) Equation

$$H = (12/N(N+1))\sum_{i=1}^{C}(R_i^2/n_i - 3(N+1))$$

C =the number of samples, n_i = the number of observations in the ith sample, $N = \sum n_i$, the number of observations in all samples combined, R_i = the sum of the ranks in the ith sample (Kruskall and Wallis 1952).

c) Calculations and software

Raw data was analysed for statistical significane by BMDP Statistical Software©. All calculations were done via BMDP Statistical Software©. BMDP Statistical Software, Inc. 12121 Wilshire Blvd, Suite 300, Los Angeles, CA 90025 USA.

An indicator of statistical significance is the p value. The P value is a probability, with a value ranging from zero to one. If a p value is 0.05, random sampling from identical populations would lead to a difference smaller than you observed in 95% of experiments and larger than you observed in 5% of experiments. The standard error of the mean

(SEM) quantifies the precision of the mean. It is a measure of how far a sample mean is likely to be from the true population mean.

2. STATISTICS FOR CHAPTER 3

2.1 Wilcoxon signed-rank test

a) Motivation for use of test

The Wilcoxon Signed-rank test is a non-parametric test, which is analogous to the student's *t*-test for paired values. This test is applicable when the data is non-normally distributed and when one of the nominal variables has only two values, such as "pre-test" and "post-test," and the other nominal variable often represents individuals (Walker 2002). In this study, the aim was to determine whether there was a statistical difference between the untreated control cells and the drug treated cells pertaining to the percentage of viable cells at specified concentrations. It can be assumed that the data is non-normally (Samuels and Witmer 2003). In this study the one nominal variable (percentage cell viability) had two values, i) untreated control cells (can be seen as "pre-test") and ii) drug treated cells (can be seen as "post-test"). The cells came from the exact same population.

b) Equation

A sample is given: $y_1, y_2, \ldots\ldots\ldots\ldots y_n$

Ri represents the rank of $|y_i|$ (when ranked lowest to highest)

R(+) represents the sum of ranks associated with positive values of y_i's

R(-) represents the sum of ranks associated with negative values of y_i's

The test statistic is based on the smaller of the R(+) and R(-) (Walker 2002).

A table has been standardized to extrapolate values to statistical significance (Allan 1982).

If the sum of the ranks of the smaller sign is equal to, or less than the tabular value, there is a significant difference between the two groups of data (Allan 1982).

c) Calculations and software

Raw data was analyzed for statistical significance by GRAPHPAD Prism 4 Software©. Calculations were done via GRAPHPAD Prism 4 Software©. GraphPad Software, Inc. 2236 Avenida de la Playa La Jolla, CA 92037 USA.

An indicator of statistical significance is the p value. The P value is a probability, with a value ranging from zero to one. If a p value is 0.05, random sampling from identical populations would lead to a difference smaller than you observed in 95% of experiments and larger than you observed in 5% of experiments. The standard error of the mean (SEM) quantifies the precision of the mean. It is a measure of how far a sample mean is likely to be from the true population mean.

2.2 Spearman rank correlation coefficient

a) Motivation for use of test

The Spearman rank correlation coefficient is a non-parametric test, which determines the strength of association between two variables. This test is applicable when the data is non-normally distributed, as in this study. The aim was to determine whether there is a correlation between the octanol/water partition coefficients and cytotoxic effects of the tested compounds against cancer cell lines and normal cells, i.e. what is the strength of association between the lipophilicity and IC_{50} values? Significance of the correlation is determined with a Student's *t*-distribution with degrees of freedom n –2 (Allan 1982).

b) Equation

Spearman correlation coefficient to determine correlation

$$r_s = 1 - 6 \sum [d_i^2 / n(n^2 - 1)]$$

where:

$d_i = x_i - y_i$ = the difference between the ranks of corresponding values X_i and Y_i, and

n = the number of values in each data set (same for both sets) (Spearman 1904).

Student's *t*-distribution to determine statistical significance

$$t = r_s \sqrt{(n-2) / 1 - r_s^2}$$

If the calculated value of t is greater than the standardized tabular value at the 5% probability value (p value ≤ 0.05), the correlation is significant (Allan 1982).

c) Calculations and software

Raw data was analysed for statistical significane by GRAPHPAD Prism 4 Software©. Calculations were done via GRAPHPAD Prism 4 Software©. GraphPad Software, Inc. 2236 Avenida de la Playa La Jolla, CA 92037 USA.

An indicator of statistical significance is the p value. The P value is a probability, with a value ranging from zero to one. If a p value is 0.05, random sampling from identical populations would lead to a difference smaller than you observed in 95% of experiments and larger than you observed in 5% of experiments. The standard error of the mean (SEM) quantifies the precision of the mean. It is a measure of how far a sample mean is likely to be from the true population mean.

3. STATISTICS FOR CHAPTER 4

3.1 Mann-Whitney U test

a) Motivation for use of test

The Mann-Whitney U test is a non-parametric test, which is analogous to the student's *t*-test for unpaired values. This test is applicable when the data is non-normally distributed and when the two variables are independent (Allan 1982). In this study, the aim was to determine whether there was a statistical difference between the outcomes of the untreated control cells and the outcomes of the drug treated cells. Each compound at each tested concentration was seen as a single variable. For example, the percentage of non-viable cells detected in the "initial apoptosis" phase after 24 hours was compared to the percentage of non-viable cells detected in the "initial apoptosis" phase after 24 hours for each concentration of each compound separately. The data was non-normally distributed (Samuels and Witmer 2003).

b) Equation

$T = \sum$ ranks of smaller group of variables

$$U_1 = [(n_x \text{ x } n_y) + n_x(n_x + 1) / 2 - T]$$

where

n_x =the number of items in the smaller group,

n_y = the number of items in the larger group

$$U_2 = n_x n_y - U_1$$

If the calculated value of the smaller of the U_1 and U_2 values is equal to or less than the standardized tabular value (Alan 1982), at $p = 0.05$, there is a significant difference between the sets of data.

c) Calculations and software

Raw data was analysed for statistical significane by GRAPHPAD Prism 4 Software©. Calculations were done via GRAPHPAD Prism 4 Software©. GraphPad Software, Inc. 2236 Avenida de la Playa La Jolla, CA 92037 USA.

An indicator of statistical significance is the p value. The P value is a probability, with a value ranging from zero to one. If a p value is 0.05, random sampling from identical populations would lead to a difference smaller than you observed in 95% of experiments and larger than you observed in 5% of experiments. The standard error of the mean (SEM) quantifies the precision of the mean. It is a measure of how far a sample mean is likely to be from the true population mean.

4. STATISTICS FOR CHAPTER 5

4.1 Mann-Whitney U test

a) Motivation for use of test

The Mann-Whitney U test is a non-parametric test, which is analogous to the student's *t*-test for unpaired values. This test is applicable when the data is non-normally distributed and when the two variables are independent (Allan 1982). In this study, the aim was to determine whether there was a statistical difference between the obtained ratio of the untreated control cells and obtained ratio of the drug treated cells. Each compound at each tested concentration for each tested cell culture was seen as a single variable. For example, the ratio that was obtained for untreated control cells was compared to the ratio that was obtained for each compound at each concentration seperately. The data was non-normally distributed (Samuels and Witmer 2003).

b) Equation

Refer to section 3.1 (b) of Appendix A, page 134.

c) Calculations and software

Raw data was analysed for statistical significane by GRAPHPAD Prism 4 Software©. Calculations were done via GRAPHPAD Prism 4 Software©. GraphPad Software, Inc. 2236 Avenida de la Playa La Jolla, CA 92037 USA.

An indicator of statistical significance is the p value. The P value is a probability, with a value ranging from zero to one. If a p value is 0.05, random sampling from identical populations would lead to a difference smaller than you observed in 95% of experiments and larger than you observed in 5% of experiments. The standard error of the mean (SEM) quantifies the precision of the mean. It is a measure of how far a sample mean is likely to be from the true population mean.

5. STATISTICS FOR CHAPTER 6

5.1 Mann-Whitney U test

a) Motivation for use of test

The Mann-Whitney U test is a non-parametric test, which is analogous to the student's *t*-test for unpaired values. This test is applicable when the data is non-normally distributed and when the two variables are independent (Allan 1982). In this study, the aim was to determine whether there was a statistical difference between percentage of cells that accumulated in each phase of the cell cycle due to the addition of different compounds at different concentrations and for different time periods vs. the corresponding untreated control cells. Each compound at each tested concentration for each time period of incubation was seen as a single variable. For example, the ratio that was obtained for untreated control cells was compared to the ratio that was obtained for each compound at each concentration seperately. The data was non-normally distributed (Samuels and Witmer 2003).

b) Equation

Refer to section 3.1 (b) of Appendix A, page 134.

c) Calculations and software

Raw data was analysed for statistical significane by GRAPHPAD Prism 4 Software©. Calculations were done via GRAPHPAD Prism 4 Software©. GraphPad Software, Inc. 2236 Avenida de la Playa La Jolla, CA 92037 USA.

An indicator of statistical significance is the p value. The P value is a probability, with a value ranging from zero to one. If a p value is 0.05, random sampling from identical populations would lead to a difference smaller than you observed in 95% of experiments and larger than you observed in 5% of experiments. The standard error of the mean (SEM) quantifies the precision of the mean. It is a measure of how far a sample mean is likely to be from the true population mean.

6. STATISTICS FOR CHAPTER 7

6.1 Wilcoxon signed-rank test

a) Motivation for use of test

The Wilcoxon Signed-rank test is a non-parametric test, which is analogous to the student's *t*-test for paired values. This test is applicable when the data is non-normally distributed and when one of the nominal variables has only two values, such as "pre-test" and "post-test," and the other nominal variable often represents individuals (2002). In this study, the aim was to determine whether there was a statistical difference between the body weight of a group of mice, as measured at different time intervals (can be seen as "post-test"), when compared to the initial body weight of that same group (can be seen as "pre-test"). The data was non-normally distributed (Samuels and Witmer 2003).

b) Equation

Refer to section 2.1 (b) of Appendix A, page 134.

c) Calculations and software

Raw data was analysed for statistical significane by GRAPHPAD Prism 4 Software©. Calculations were done via GRAPHPAD Prism 4 Software©. GraphPad Software, Inc. 2236 Avenida de la Playa La Jolla, CA 92037 USA

An indicator of statistical significance is the p value. The P value is a probability, with a value ranging from zero to one. If a p value is 0.05, random sampling from identical populations would lead to a difference smaller than you observed in 95% of experiments and larger than you observed in 5% of experiments. The standard error of the mean (SEM) quantifies the precision of the mean. It is a measure of how far a sample mean is likely to be from the true population mean.

6.2 Kruskall-Wallis one-way analysis of variance test (synonymous for H test)

a) Motivation for use of test

The Kruskall-Wallis test is used when comparing more than two groups in terms of a continuous variable that appears to be non-normally distributed (DeCaprio 2006 ; Siegel 1956; Kruskall and Wallis 1952). In this case, the aim was to determine whether a

statistically significant variation existed between the measured values of the untreated control groups for a specific parameter at different phases of the study. It can be assumed that the data is non-normally distributed (Samuels and Witmer 2003).

b) Equation

Refer to section 1.1 (b) of Appendix A, page 130.

c) Calculations and software

Raw data was analysed for statistical significane by GRAPHPAD Prism 4 Software©. Calculations were done via GRAPHPAD Prism 4 Software©. GraphPad Software, Inc. 2236 Avenida de la Playa La Jolla, CA 92037 USA

An indicator of statistical significance is the p value. The P value is a probability, with a value ranging from zero to one. If a p value is 0.05, random sampling from identical populations would lead to a difference smaller than you observed in 95% of experiments and larger than you observed in 5% of experiments. The standard error of the mean (SEM) quantifies the precision of the mean. It is a measure of how far a sample mean is likely to be from the true population mean.

6.3 Mann-Whitney U test

a) Motivation for use of test

The Mann-Whitney U test is a non-parametric test, which is analogous to the student's *t*-test for unpaired values. This test is applicable when the data is non-normally distributed and when the two variables are independent (Allan 1982). In this study, the aim was to determine whether there was a statistical difference between the measured values obtained for the various drug treated groups vs. the measured values obtained for the untreated control groups (pertaining to different parameters) The data was non-normally distributed (Samuels and Witmer 2003).

b) Equation

Refer to section 3.1 (b) of Appendix A, page 134.

c) Calculations and software

Raw data was analysed for statistical significane by GRAPHPAD Prism 4 Software©. Calculations were done via GRAPHPAD Prism 4 Software©. GraphPad Software, Inc. 2236 Avenida de la Playa La Jolla, CA 92037 USA.

An indicator of statistical significance is the p value. The P value is a probability, with a value ranging from zero to one. If a p value is 0.05, random sampling from identical populations would lead to a difference smaller than you observed in 95% of experiments and larger than you observed in 5% of experiments. The standard error of the mean (SEM) quantifies the precision of the mean. It is a measure of how far a sample mean is likely to be from the true population mean.

APPENDIX B

1. Preparation of chicken embryo fibroblasts

Chicken embryo fibroblasts were prepared according to the method by Freshney (2000).

(i) Eggs were incubated at 38.5°C in a humid atmosphere for 6 days. Eggs were kept in an egg incubator and turned over once in 24 hours.

(ii) All procedures were carried out under sterile conditions.

(iii) Eggs were swabbed with 70% alcohol and placed with the blunt end facing up in a small beaker.

(iv) The top of the shell was cracked and the shell peeled off to the edge of the air sac. Sterile forceps were used for this purpose.

(v) The forceps were re-sterilized and used to peel off the white shell membrane to reveal the chorioallantoic membrane (CAM) below, with its blood vessels.

(vi) The CAM was pierced with sterile curved forceps and the embryos lifted out by grasping it gently under the head.

(vii) Embryos were transferred to a new sterile petri dish.

(viii) Embryos were then decapitated to kill them instantly.

(ix) Fat and necrotic material was removed from the embryos.

(x) Embryos were transferred to a new sterile petri dish.

(xi) Embryos were cut with crossed scalpels into very small pieces.

(xii) Tissue was transferred to a sterile 50ml centrifuge tube and washed three times with RPMI medium supplemented with 10% bovine FCS.

(xiii) Pieces were allowed to settle and the medium discarded. This step was repeated twice.

(xiv) Tissue was transferred to a sterile 100ml Schott bottle.

(xv) 45ml phosphate buffered saline with albumin (PBSA) (filter sterilized) and 5 ml 2.5% trypsin was added together with a magnetic stirrer and the flask will be closed.

(xvi) Tissue and trypsin mixture was stirred at 100 rpm for 30 min at 37°C.

(xvii) Pieces were allowed to settle, and the supernatant was poured (with disaggregated cells in suspension) into a sterile 50ml centrifuge tube and placed on ice.

Steps 15-17 were repeated until the disaggregation was complete (3-4hours).

(xviii) The disaggregated cell suspension that was stored on ice was decanted into new sterile tubes (leave debris behind) and then centrifuged at 200g for 5 minutes.

(xix) The supernatant was discarded and the cell pellet was re-suspended in medium supplemented with 10% bovine FCS.

(xx) The cell suspension was transferred to cell culture flasks and incubated at 37°C in 5% CO_2.

(xxi) The medium was changed at regular intervals (2-4days) as the pH decreased.

2. Preparation of human lymphocytes

(i) Venous blood was collected in heparin vacutubes (Sigma- Aldrich, Johannesburg, South Africa) from healthy volunteers.

(ii) 35ml of heparinized blood was loaded carefully onto 15ml Histopaque 1077, (Sigma-Aldrich, Johannesburg, SA).

(iii) The lymphocyte monolayer was removed and transferred to sterile 50 centrifuge tubes.

(iv) The tubes were filled with sterile RPMI 1640 medium (without bovine FCS) and then centrifuged at 1000 rpm's for 15 minutes.

(v) After discarding the supernatant, the pellet was gently mixed and the tube filled with 10% RPMI medium.

(vi) The suspension was centrifuged for a further 10 minutes at 1000 rpm's after which the supernatant was discarded.

(vii) The pellet was manually mixed and the tube was then filled with ice-cold ammonium chloride (NH_4Cl) in order to induce cell lysis.

(viii) The cell suspension was left on ice for about 10 minutes, for any remaining red blood cells to be lysed.

(ix) The suspension was centrifuged at 1000 rpm's for 10 minutes, and the supernatant was then discarded.

(x) Tubes were filled with RPMI 1640 medium containing 10% bovine FCS.

(xi) The suspension was centrifuged for a further 10 minutes at 1000 rpm.

(xii) The supernatant was discarded and the pellet was resuspended in 1ml of 10% RPMI medium containing 10% bovine FCS.

(xiii) Lymphocytes were then counted and diluted to the appropriate concentration used in the experimental procedure.

Resting and PHA (Phyto-haemagglutenin, Remel, USA) – stimulated lymphocytes were used in cytotoxicity tests.

APPENDIX C

Figures 1 - 26 are graphic presentations of results, which determined the cell death pathway that was induced by the experimental compounds UH 126.1, UH 127.1, Au, and cisplatin, at different concentrations and time intervals respectively (**refer to Chapter 4, section 4.6).**

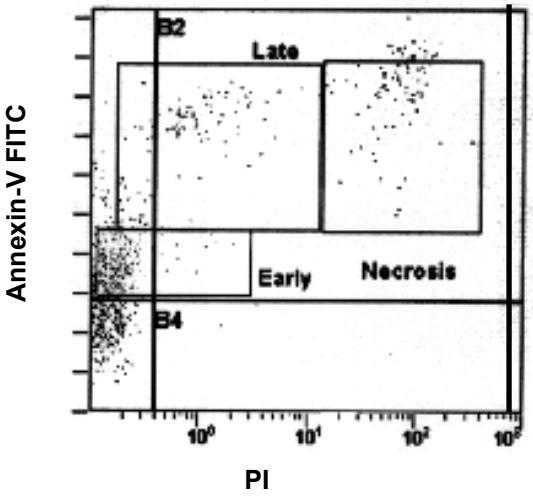

Figure 1. Histogram of untreated Jurkat cells after 24 hours incubation

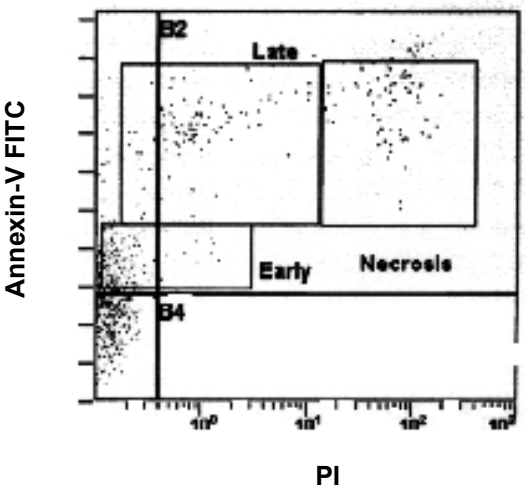

Figure 2. Histogram of Jurkat cells after 24 hours incubation with UH 126.1 at a concentration equal to the previously determined IC_{50}

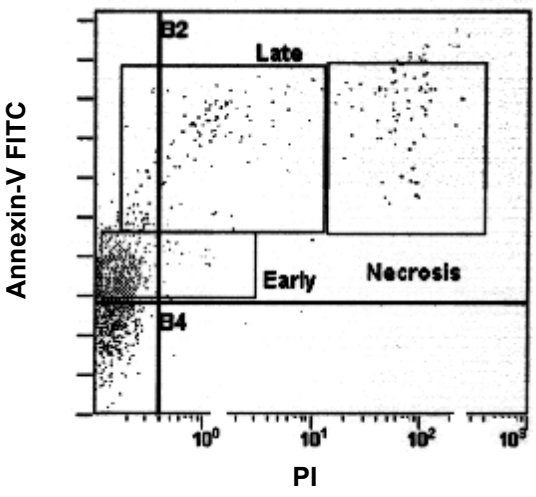

Figure 3. Histogram of Jurkat cells after 24 hours incubation with UH 126.1 at a concentration equal to the previously determined $IC_{50} \times 2$

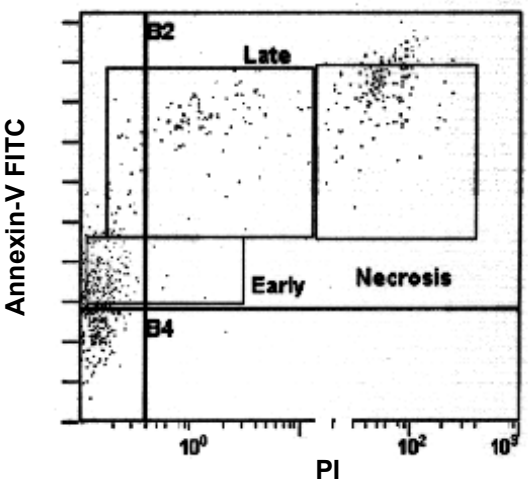

Figure 4. Histogram of Jurkat cells after 24 hours incubation with UH 126.1 at a concentration equal to the previously determined $IC_{50} \times 5$

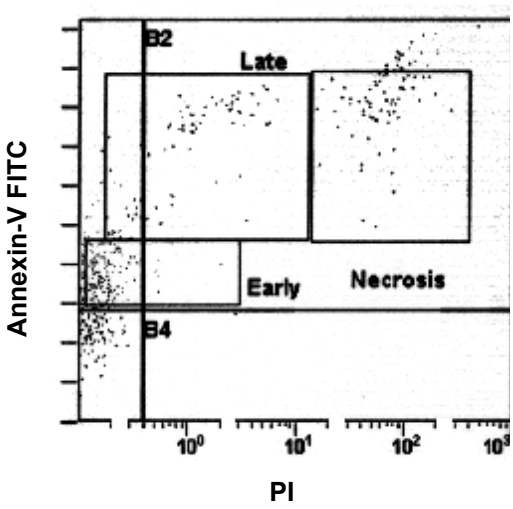

Figure 5. Histogram of Jurkat cells after 24 hours incubation with UH 127.1 at a concentration equal to the previously determined IC_{50}

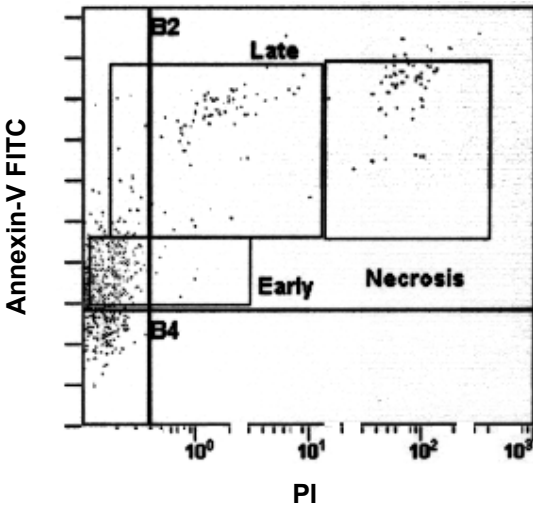

Figure 6. Histogram of Jurkat cells after 24 hours incubation with UH 127.1 at a concentration equal to the previously determined $IC_{50} \times 2$

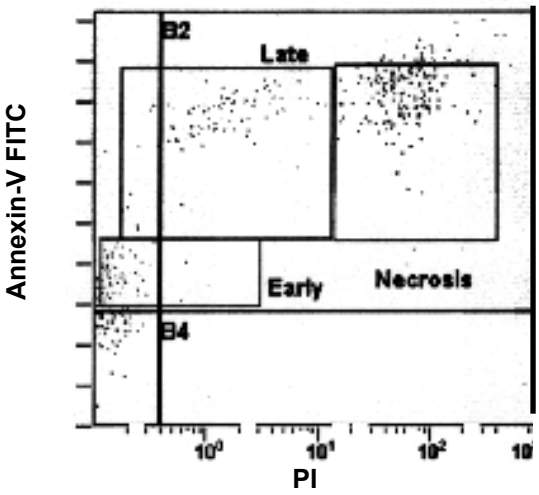

Figure 7. Histogram of Jurkat cells after 24 hours incubation with UH 127.1 at a concentration equal to the previously determined $IC_{50} \times 5$

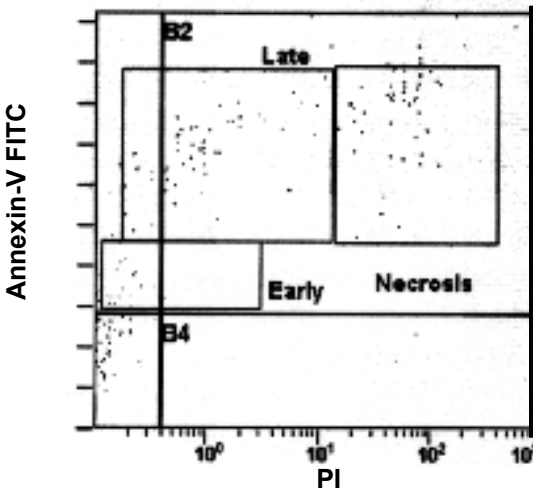

Figure 8. Histogram of Jurkat cells after 24 hours incubation with $[Au(dppe)_2]Cl$ at a concentration equal to the previously determined IC_{50}

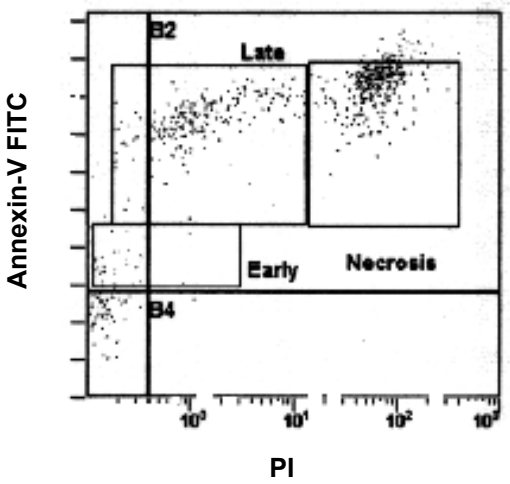

Figure 9. Histogram of Jurkat cells after 24 hours incubation with $[Au(dppe)_2]Cl$ at a concentration equal to the previously determined $IC_{50} \times 2$

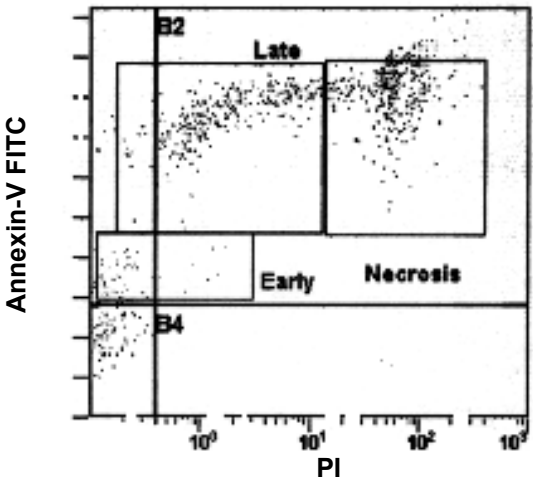

Figure 10. Histogram of Jurkat cells after 24 hours incubation with $[Au(dppe)_2]Cl$ at a concentration equal to the previously determined $IC_{50} \times 5$

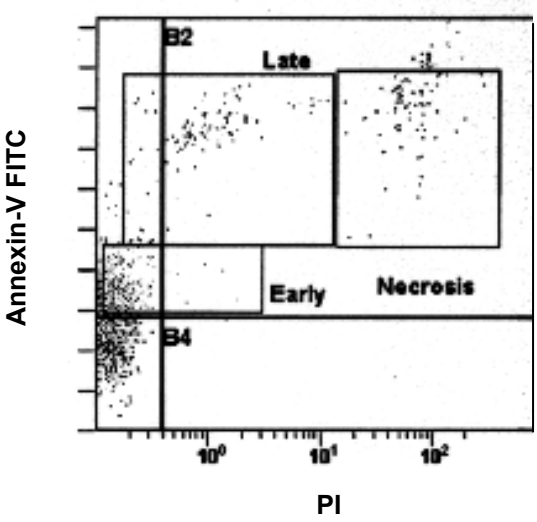

Figure 11. Histogram of Jurkat cells after 24 hours incubation with cisplatin at a concentration equal to the previously determined IC_{50}

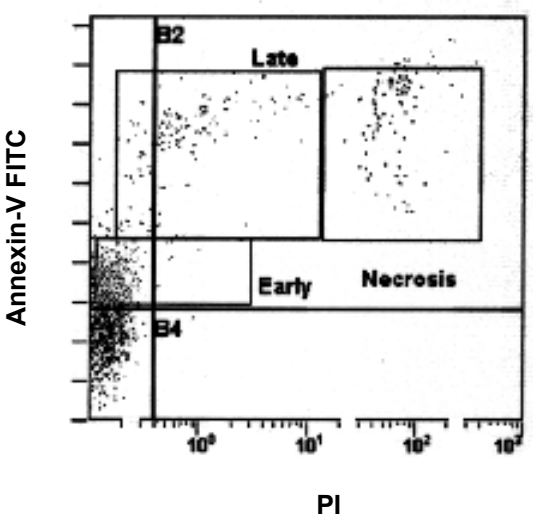

Figure 12. Histogram of Jurkat cells after 24 hours incubation with cisplatin at a concentration equal the previously determined $IC_{50} \times 2$

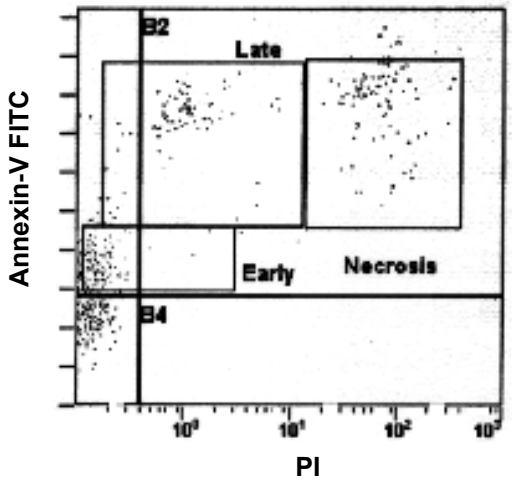

Figure 13. Histogram of Jurkat cells after 24 hours incubation with cisplatin a concentration equal the previously determined $IC_{50} \times 5$

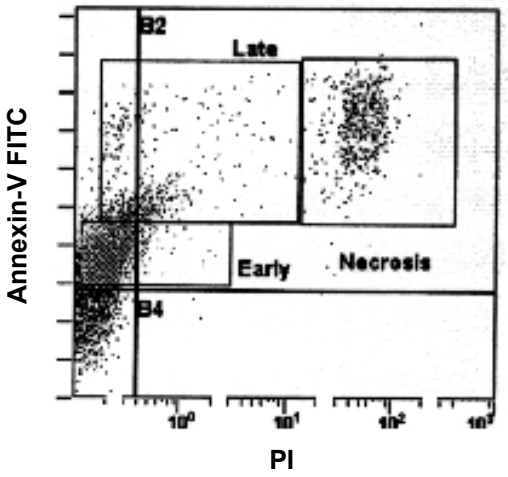

Figure 14. Histogram of untreated Jurkat cells after 48 hours

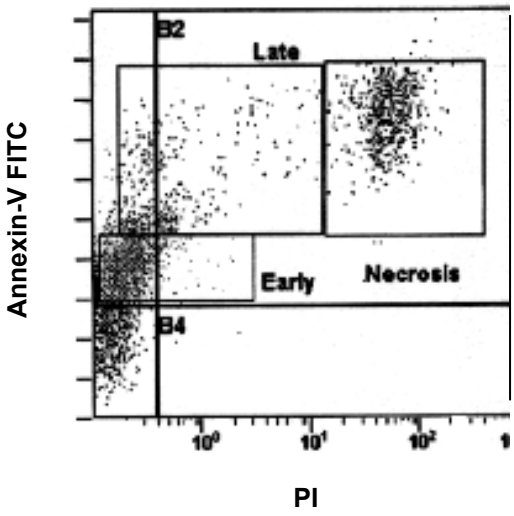

Figure 15. Histogram of Jurkat cells after 48 hours incubation with UH 126.1 at a concentration equal to the previously determined IC_{50}

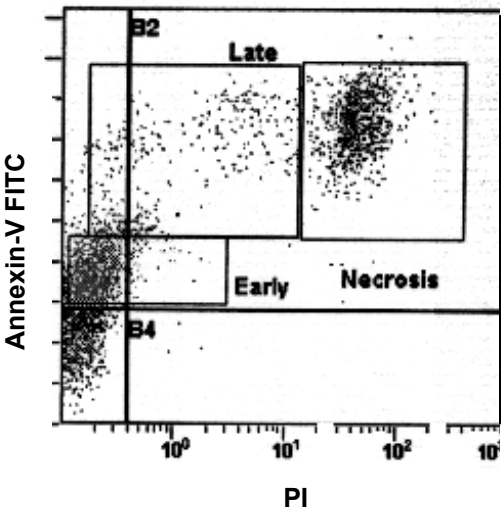

Figure 16. Histogram of Jurkat cells after 48 hours incubation with UH 126.1 at a concentration equal the previously determined $IC_{50} \times 2$

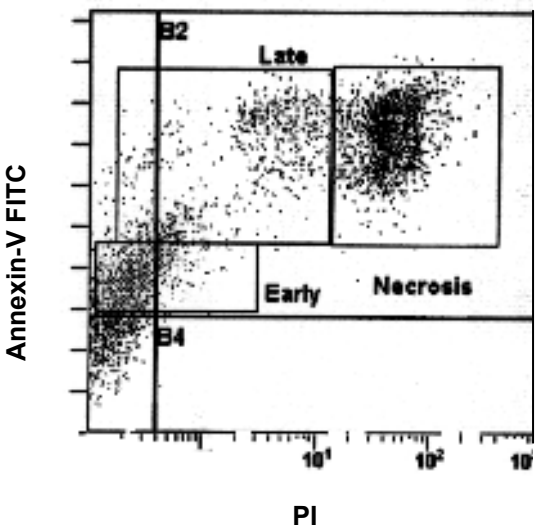

Figure 17. Histogram of Jurkat cells after 48 hours incubation with UH 126.1 at a concentration equal to the previously determined $IC_{50} \times 5$

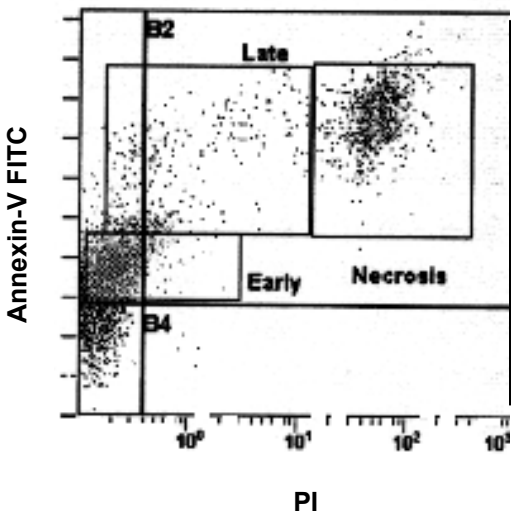

Figure 18. Histogram of Jurkat cells after 48 hours incubation with UH 127.1 at a concentration equal the previously determined IC_{50}

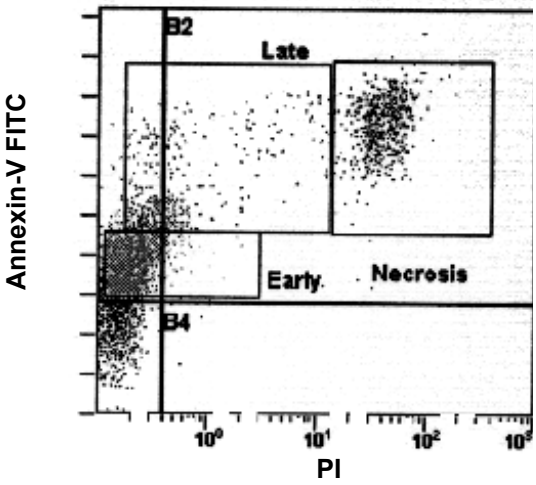

Figure 19. Histogram of Jurkat cells after 48 hours incubation with UH 127.1 at a concentration equal to the previously determined $IC_{50} \times 2$

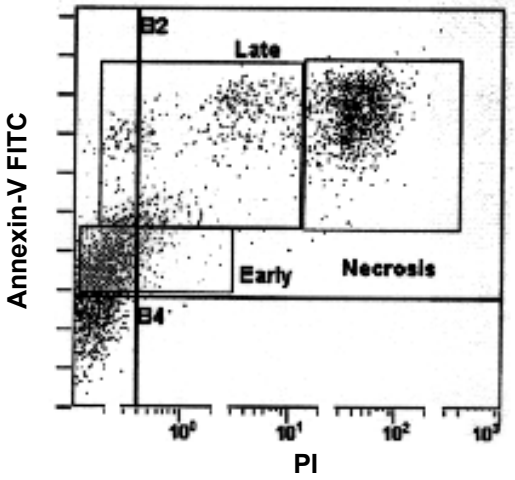

Figure 20. Histogram of Jurkat cells after 48 hours incubation with UH 127.1 at a concentration equal to the previously determined $IC_{50} \times 5$

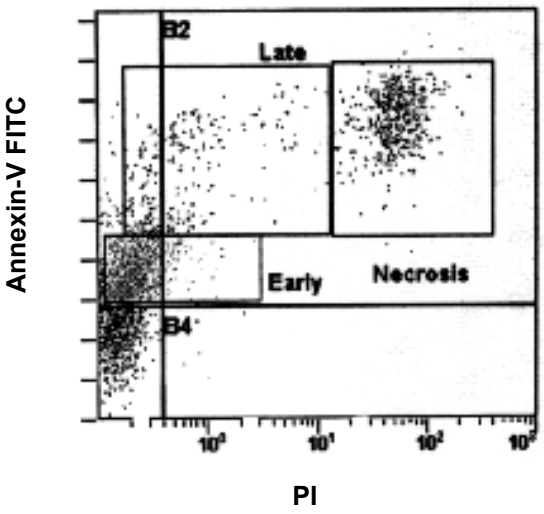

Figure 21. Histogram of Jurkat cells after 48 hours incubation with $[Au(dppe)_2]Cl$ at a concentration equal to the previously determined IC_{50}

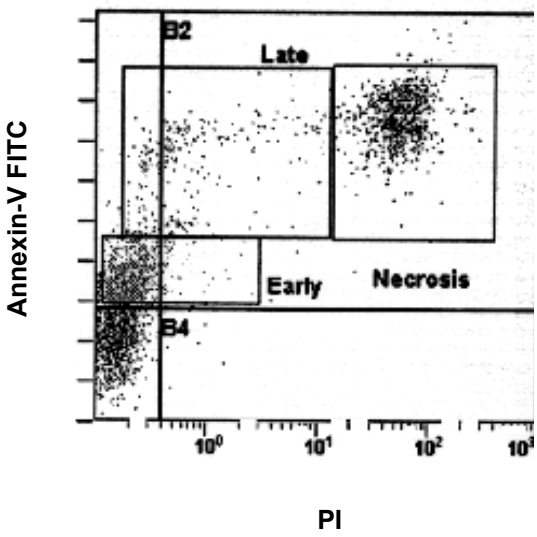

Figure 22. Histogram of Jurkat cells after 48 hours incubation with $[Au(dppe)_2]Cl$ at a concentration equal to the previously determined $IC_{50} \times 2$

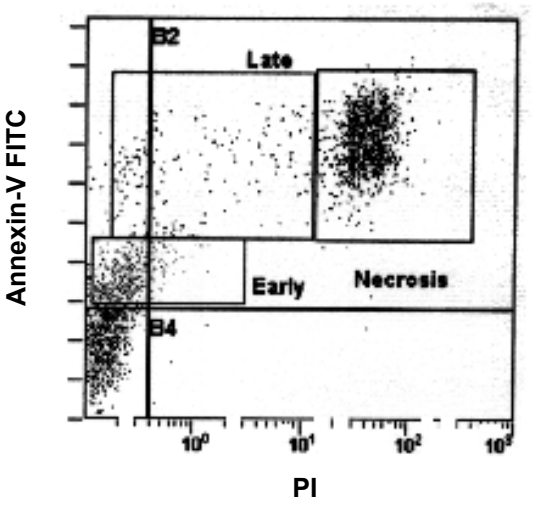

Figure 23. Histogram of Jurkat cells after 48 hours incubation with $[Au(dppe)_2]Cl$ at a concentration equal to the previously determined $IC_{50} \times 5$

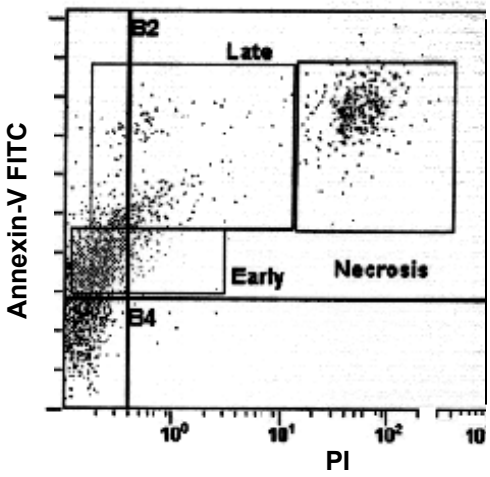

Figure 24. Histogram of Jurkat cells after 48 hours incubation with cisplatin at a concentration equal to the previously determined IC_{50}

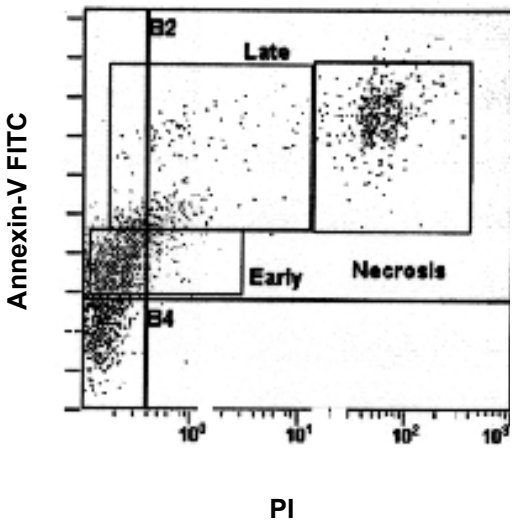

Figure 25. Histogram of Jurkat cells after 48 hours incubation with cisplatin at a concentration equal to the previously determined $IC_{50} \times 2$

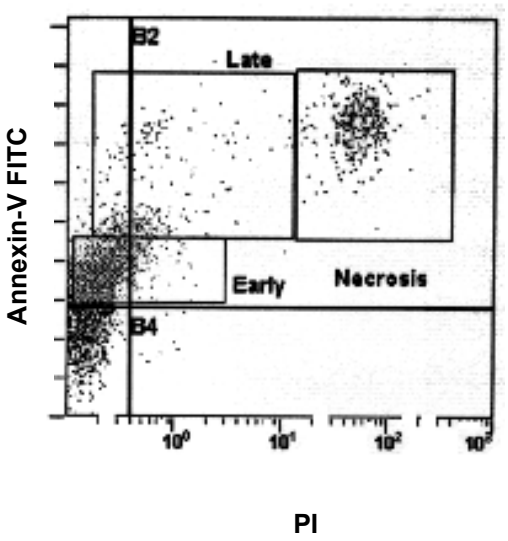

Figure 26. Histogram of Jurkat cells after 24 hours incubation with cisplatin at a concentration equal to the previously determined $IC_{50} \times 5$